University of Southern Queensland
Faculty of Engineering and Surveying

Autonomous Unmanned Aerial Surveillance Vehicle – Autonomous Control and Flight Dynamics

A dissertation submitted by

Craig Andrew LITTLETON

In fulfilment of the requirements of

Courses ENG4111 and 4112 – Research Project

Towards the degree of

Bachelor of Engineering Electrical and Electronic
Bachelor of Business Operations and Logistics Management

Submitted: October 2005

Abstract

The field of autonomous UAV research and development is a rapidly expanding sector of engineering. Technological advances in aircraft design, solid state devices, communications and battery technology have allowed for a shift in UAV technology from purely militarised applications towards lower cost general aviation purposes. In short, it appears that autonomous UAV technology is the future for aviation as we know it.

The overall project (when combined with "Navigation and User Interface", Knox 2005) seeked to develop a low cost, fixed wing UAV system to conduct specific flight path surveillance over a pre-determined waypoint path. This particular section of the project focussed on the task of controlling the stability of the aircraft during its mission. The basis for the autonomous control of the UAV system lies within the analysis of aircraft flight dynamics. From the dynamics of flight, it is possible to design a control system based on either conventional control techniques, or more simply an "observe and correct" system.

Whilst it is recommended for future work that a more conventional approach be taken to this AFCS design, an "observe and correct" approach was adopted for the purposes of this project. This system automatically corrected for heading errors via an outer loop function, and maintained aircraft stability, by monitoring the pitch and roll characteristics of the aircraft, via an inner loop function. This process was achieved through the use of a MC912D60A HC12 microcontroller for all embedded computing requirements and a single ADXL213 accelerometer module for pitch and roll measurement. Heading information was passed to the AFCS from "Navigation and User Interface" (Knox, 2005).

Whilst a prototype UAV system was unable to be developed and therefore final flight testing was unable to be conducted, this project has provided a strong base for future work in this area. The flight dynamics analysis and simulation methods outlined in this dissertation will provide a useful starting point for any future AFCS design. Also, program development such as Rx/Tx remote signal routing

through the HC12, accelerometer signal decoding, and servo motor control, are fundamental to any control method utilising similar components and were all tested and verified, hence providing a solid programming base for any future work.

This project encountered numerous limitations such as budgetary constraints and unavailability of crucial information (in the form of stability data for a model aircraft). If these limitations can be overcome in the future, this project has provided sound guidance and a solid foundation towards the development of a fully functioning prototype autonomous UAV system.

University of Southern Queensland

Faculty of Engineering and Surveying

ENG4111 & ENG4112 *Research Project*

Limitations of Use

The Council of the University of Southern Queensland, its Faculty of Engineering and Surveying, and the staff of the University of Southern Queensland, do not accept any responsibility for the truth, accuracy or completeness of material contained within or associated with this dissertation.

Persons using all or any part of this material do so at their own risk, and not at the risk of the Council of the University of Southern Queensland, its Faculty of Engineering and Surveying or the staff of the University of Southern Queensland.

This dissertation reports an educational exercise and has no purpose or validity beyond this exercise. The sole purpose of the course pair entitled "Research Project" is to contribute to the overall education within the student's chosen degree programme. This document, the associated hardware, software, drawings, and other material set out in the associated appendices should not be used for any other purpose: if they are so used, it is entirely at the risk of the user.

Prof G Baker
Dean
Faculty of Engineering and Surveying

Certification

I certify that the ideas, designs and experimental work, results, analyses and conclusions set out in this dissertation are entirely my own effort, except where otherwise indicated and acknowledged.

I further certify that the work is original and has not been previously submitted for assessment in any other course or institution, except where specifically stated.

Craig Andrew LITTLETON

Student Number: Q1221674

……
Signature

……
Date

Acknowledgements

The initial concept for this project came from Mr Terry Byrne from the Faculty of Engineering and Surveying, and if it wasn't for his vision this project would not have been undertaken. So thanks must first go to Terry for the idea as well as his continued technical support and suggestions throughout the year. Thankyou also to my supervisor Mr Mark Phythian for the guidance and expertise he has provided throughout the course of this project, without his input this project would have been significantly more difficult.

Also to my colleague Ms Soz Knox who undertook the other half of this very large (and very technically demanding!) project. Even though we didn't make it to a final prototyping stage (an aircraft would have been helpful here!), and therefore never actually got to see our creation fly, I have enjoyed working on this project with you and I know that you have enjoyed the challenge also. I hope that the end result of the combined project will provide a solid foundation for future research.

The concept of the UAV is both exciting and challenging. I suggest to anyone considering a final year project to take up the challenge and to continue development. Hopefully in future years someone will be able to develop a working prototype UAV and hopefully that student/students will take pride in their achievements and exhibit the same enthusiasm that I have felt for this project.

Table of Contents

List of Figures

List of Equations

List of Tables

Nomenclature

UAV	Unmanned Aerial Vehicle
MAV	Micro Aerial Vehicle
Tx	Transmit
Rx	Receive
GPS	Global Positioning System
X_E	X-axis of the earth axis system
Y_E	Y-axis of the earth axis system
Z_E	Z-axis of the earth axis system
X_B	X-axis of the aircraft (Body-fixed axis system)
Y_B	Y-axis of the aircraft (Body-fixed axis system)
Z_B	Z-axis of the aircraft (Body-fixed axis system)
U	Forward velocity
V	Side velocity
R	Yawing velocity
L	Rolling moment
M	Pitching moment
N	Yawing moment
P	Roll angular velocity
Q	Pitch angular velocity
R	Yaw angular velocity
Φ	Roll angle
Θ	Pitch angle
Ψ	Yaw angle
α	Angle of attack
β	Side slip angle of attack
g	Acceleration due to gravity – 9.81 $m.s^{-2}$
m	Mass of an object
V_T	Total velocity vector
δ_e	Elevator deflection angle
δ_a	Aileron deflection angle
δ_r	Rudder deflection angle
AFCS	Automatic Flight Control System

A	State matrix
B	Driving matrix
C	Output matrix
D	Feed-forward matrix
K	State feedback matrix
x	State vector
u	Control vector
y	Output vector
SISO	Single-input, Single-output system
MIMO	Multiple-input, Multiple-output system
$\mathbf{C_M}$	Controllability matrix
$\mathbf{O_M}$	Observability matrix
dB	Decibels
Γ	Discrete driving matrix
Φ	Discrete state matrix
ω_o	Highest frequency component in a signal (Nyquist frequency)
ω_s	Sampling frequency
I	Identity matrix
k	Sample instant
ZOH	Zero-order-hold
Ts	Sample time
PWM	Pulse Width Modulation
IC	Input Capture or Integrated circuit
OC	Output Compare
RTI	Real-time interrupt
PCB	Printed circuit board
MSB	Most Significant Bit
CRO	Cathode Ray Oscilloscope
CASA	Civil Aviation Safety Authority
CASR	Civil Aviation Safety Regulations act
AGL	Above Ground Level

Chapter 1 Introduction

1.1 Project Background

The concept of the Unmanned Aerial Vehicle (UAV) is not a new concept. These aircraft systems, capable of autonomous or semi-autonomous flight (or a combination of the two), have been in operation since World War II. These unpiloted aircraft (or 'drones' as they were known at the time) were originally developed as targets for anti-aircraft gunnery training (Goebel, 2005). Since then recent advances in communications, solid state devices and battery technology (Beard et al, 2003) have allowed small, low-cost, fixed wing UAV systems to be implemented for applications such as:

- Natural disaster monitoring and remediation
- Traffic and environmental monitoring
- Surveillance
- Security and law enforcement
- Terrain mapping (Innovations Report, 2004)

Whilst many of these applications are based on high cost systems, as indicated by Beard et al (2003), there has been a recent shift towards research into more low cost, Micro Aerial Vehicle (MAV) solutions. In recent years this research has been common at a University level and a number of these low cost MAV systems have been developed and refined throughout the world.

A recent undergraduate project conducted at the University of Southern Queensland attempted to develop a low cost autonomous aircraft system (Keeffe, 2003). Straight level flight was achieved; however the ability to fly a predetermined flight path and gather useful information at predetermined points (in the form of digital photographs) was not convincingly achieved. Keeffe (2003) will provide the basis for this continuing project. Some aspects such as the flight dynamics of the aircraft (which are universal) may be re-usable, whilst other aspects such as control system design, sensor implementation and the overall scope of the project will be built upon in an attempt to create a fully functioning, low cost autonomous UAV system.

1.2 Project Aims and Objectives

The ultimate goal of this project, (when integrated with "Navigation and User Interface" (Knox, 2005), was to develop a low cost, fully functional prototype autonomous unmanned aerial vehicle (UAV) to conduct specific flight path surveillance. This particular project focuses on the autonomous flight control aspect of the UAV system based on the dynamics of flight.

The objectives for this project have been defined as follows:

1. Research into various control methods currently employed in similar UAV systems including relevant components (eg Sensing equipment, microcontroller/s), advantages / disadvantages of each system, relevant legal requirements of UAV systems.
2. Select, interface and test hardware components required for autonomous capability.
3. Design and simulate control system algorithms required for autonomous flight.
4. Construct prototype UAV (using a model aircraft) and integrate flight control system with "Navigation and User Interface" being carried out by Soz Knox.

As time permits:

1. Examine the viability of developing control algorithms for autonomous take-off and landing sequences.

See appendix A for a more detailed Project Specification.

1.3 Project Methodology

The basis for this project was to provide stable, autonomous flight between pre-determined waypoints. The determination of the waypoint's themselves are out of the scope of this project and are considered in "Navigation and User Interface" (Knox, 2005). When the two projects are integrated the general form of the system using a block representation is shown in figure 1.1.

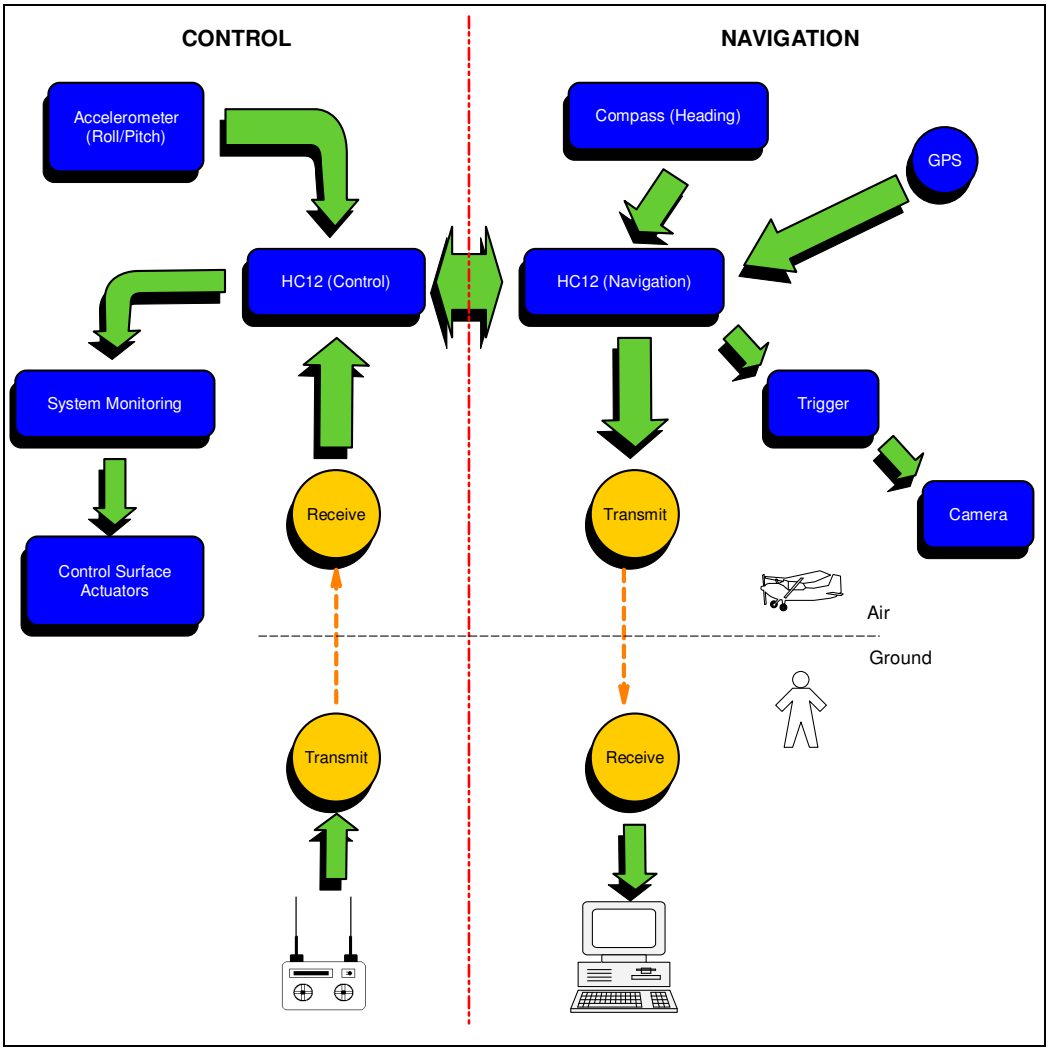

Figure 1.1: Overall System Block Diagram

The “Control” side of figure 1.1 is the primary focus of this project. In its final form it is intended that the UAV will operate as summarised by the flow diagram in figure 1.2.

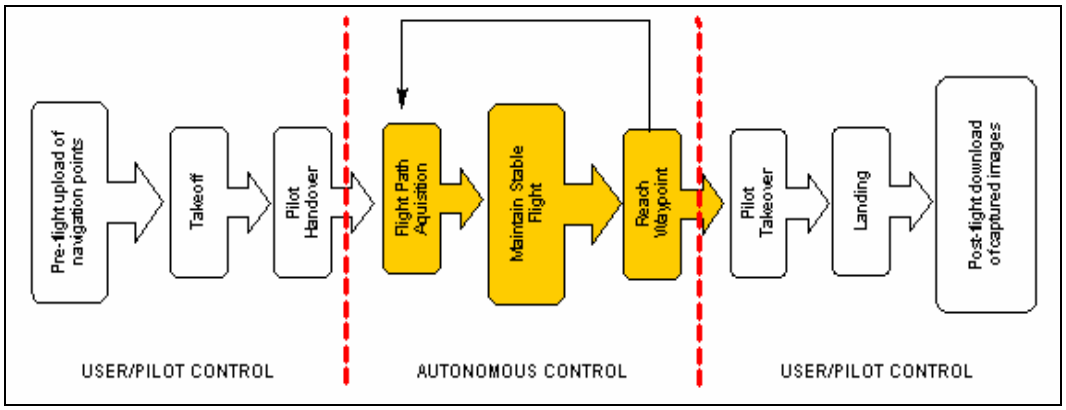

Figure 1.2: System Flow Diagram

Figure 1.2 shows that some user control is still required for both take-off and landing cycles. If time permits the viability of introducing automatic take-off and landing systems will be investigated, however in terms of implementation for this project, based on initial research this issue appears to be quite complex and therefore no attempts will be made to physically implement such a system.

There may also be room for possible expansion in the form of an “aided” flight mode, whereby the user can control parameters such as thrust and/or altitude (pitch) while the controller maintains the desired heading and maintains roll stability. Exploration into this possibility will again only be conducted if all other objectives are met.

1.4 Legal Requirements of UAV systems

Many of the legal aspects of UAV systems stem from common sense ethical responsibilities. The following two aspects of ethical responsibility are exerts from those set out by the Institution of Engineers Australia in *2000 Code of Ethics* (IEAUST, 2000). These ethical responsibilities are directed towards the undertaking of any engineering practice.

- *Members shall place their responsibility for the welfare, health and safety of the community before their responsibility to sectional or private interests, or to other members.*

- *Members shall act with honour, integrity and dignity in order to merit the trust of the community and the profession.*

Basically these two formal responsibilities are directly applicable to the goal of this project. The '*welfare, health and safety of the community'* is of primary importance to consider before any flight tests can be carried out. All systems must be thoroughly tested by a combination of software simulation and on-ground testing where possible. Flight tests should not be conducted until all testing is passed. Aside from physical safety issues, acting with *'honour, integrity and dignity'* is an important constraint of the final objective. The intended applications for these types of UAV systems are listed in section 1.1 of this dissertation. With any surveillance application the issue of privacy becomes important, and it must be made clear that it is not the goal of this project to invade the privacy of the community by conducting surveillance of any private property or unauthorized locations. For any future flight testing stage, the test site needs to be chosen accordingly so as not to impose a threat to the community's right to privacy.

Issues such as these form the basis for legal requirements of UAV systems. These requirements are extensively set out by the Civil Aviation Safety Authority in the Civil Aviation Safety Regulations (CASR) act of 1998 (CASA, 2004), an exert of which appears in appendix B. This act covers all forms of UAV platforms including; tethered balloons and kites, unmanned free balloons, and UAV systems. The initial classification of a UAV system is broken into large, small or micro, where:

UAV means unmanned aircraft, other than a balloon or a kite;

A large UAV means any of the following:

(a) An unmanned airship with an envelope capacity greater than 100 cubic metres;

(b) An unmanned powered parachute with a launch mass greater than 150 kilograms;

(c) An unmanned aeroplane with a launch mass greater than 150 kilograms;

(d) An unmanned rotorcraft with a launch mass greater than 100 kilograms;

(e) An unmanned powered lift device with a launch mass greater than 100 kilograms.

A micro UAV means a UAV with a gross weight of 100 grams or less.

And a small UAV means a UAV that is neither a large UAV nor a micro UAV.

Figure 1.3: Classification of UAV Systems
(Adapted from Civil Aviation Safety Regulations act of 1998 (CASA, 2004))

Figure 1.3 indicates that for the purposes of this project the UAV system in question will be under the "small" category. Operational regulations differ slightly between the three system classes, a summary of the operating regulations for a "small" UAV system are summarized in figure 1.4.

Operation near people

(1) A person must not operate a UAV within 30 metres of a person who is not directly associated with the operation of the UAV.

(2) Subregulation (1) does not apply in relation to a person who stands behind the UAV while it is taking off.

(3) Subregulation (1) also does not prevent the operation of a UAV airship within 30 metres of a person if the airship approaches no closer to the person than 10 metres horizontally and 30 feet vertically.

Where small UAVs may be operated

(1) A person may operate a small UAV outside an approved area only if:

(a) Where the UAV is operated above 400 feet AGL, the operator has CASA's approval to do so; and

(b) The UAV stays clear of populous areas.

Figure 1.4: Operating Regulations of "Small" UAV Systems
(Adapted from Civil Aviation Safety Regulations act of 1998 (CASA, 2004))

The "approved area" mentioned in the act is further defined as follows in figure 1.5.

Approval of areas for operation of unmanned aircraft or rockets

(1) A person may apply to CASA for the approval of an area as an area for the operation of:
(a) Unmanned aircraft generally, or a particular class of unmanned aircraft; or
(b) Rockets.

(2) For paragraph (1) (a), the classes of unmanned aircraft are:
(a) Tethered balloons and kites;
(b) Unmanned free balloons;
(c) UAVs;
(d) Model aircraft.

(3) In considering whether to approve an area for any of those purposes, CASA must take into account the likely effect on the safety of air navigation of the operation of unmanned aircraft in, or the launching of rockets in or over, the area.

(4) An approval has effect from the time written notice of it is given to the applicant, or a later day or day and time stated in the approval.

(5) An approval may be expressed to have effect for a particular period (including a period of less than 1 day), or indefinitely.

(6) CASA may impose conditions on the approval in the interests of the safety of air navigation.

(7) If CASA approves an area under subregulation (1), it must publish details of the approval (including any condition) in NOTAM or on an aeronautical chart.

(8) CASA may revoke the approval of an area, or change the conditions that apply to such an approval, in the interests of the safety of air navigation

Figure 1.5: Approved Areas for UAV Systems
(Adapted from Civil Aviation Safety Regulations act of 1998 (CASA, 2004))

The CASR act also indicates guidelines for the operation of UAV systems in populated areas. These are summarized in figure 1.6.

UAVs not to be operated over populous areas

(1) In this regulation: ***certificated UAV*** means a UAV for which a certificate of airworthiness has been issued.

(2) A person must not operate a UAV that is not a certificated or does not have approval of CASA over a populous area at a height less than the height from which, if any of its components fails, it would be able to clear the area.

(3) In considering whether to give an approval under subregulation (2), CASA must take into account:
(a) The degree of redundancy in the UAV's critical systems; and
(b) Any fail-safe design characteristics of the UAV; and
(c) The security of its communications and navigation systems.

(4) Before giving an approval CASA must be satisfied that the UAV operator will take proper precautions to prevent the proposed flight being dangerous to people and property.

Figure 1.6: Operating UAV Systems over Populated Areas
(Adapted from Civil Aviation Safety Regulations act of 1998 (CASA, 2004))

Figure 1.7 summarises further legal information relating to issues such as airspace restrictions, maximum operating heights, dropping or discharging of objects and weather and day limitations.

Maximum operating height

(1) A person may operate an unmanned aircraft at above 400 feet AGL only:
(a) In an area approved under regulation 101.030 as an area for the operation of unmanned aircraft of the same class as the aircraft concerned, and in accordance with any conditions of the approval; or
(b) As otherwise permitted by this Part.

Dropping or discharging of things

(1) A person must not cause a thing to be dropped or discharged from an unmanned aircraft in a way that creates a hazard to another aircraft, a person, or property.

Weather and day limitations

(1) A person may operate an unmanned aircraft:
(a) In or into cloud; or
(b) At night; or
(c) In conditions other than VMC;
Only if permitted by another provision of this Part, or in accordance with an air traffic control direction.

Figure 1.7: Summary of Further Legalities of UAV Operation
(Adapted from Civil Aviation Safety Regulations act of 1998 (CASA, 2004))

All of these legal requirements are written specifically for Australian airspace and may vary depending on global location. If a prototype design were to be taken offshore, further research would be needed to examine legal requirements of non-Australian airspace. A more comprehensive copy of the relevant sections of the CASR can be found in appendix B.

1.5 Dissertation Overview

This dissertation will be structured in a way that outlines the basic timeline of processes and events that led to the design and implementation of the overall system. This chapter (chapter one) has focussed on providing the reader with an introduction to the project itself as well as a brief history into the concept of the Unmanned Aerial Vehicle. This analysis is necessary to provide insight into information such as why the project was commissioned, what aspects this project

was to focus on, and how the overall system was expected to be designed and integrated. Once this information is known to the reader, a detailed description of the design and implementation stages can be delivered.

Chapter two was an essential starting point for any fixed wing aeroplane based control system design. This chapter focuses on detailing the dynamic characteristics of the aircraft, and more specifically the derivation of longitudinal and lateral equations of motion. Chapter two forms the theoretical foundations for the design of the automatic flight control system.
The development of the aircraft control theory itself is detailed in chapter three. Chapter three links directly with the previous chapter and as mentioned, the controller design depends primarily on the analysis of the dynamic characteristics of the aircraft. Chapter three allows the reader to appreciate the theoretical complexity behind aircraft flight control system development. However, a flight controller itself is of course not sufficient for autonomous capability, this can only be achieved through the integration of all systems of hardware and software alike.

Chapters four and five take a detailed analysis into the expected responses of the aircraft based on the development of the theory from chapter three. Chapter four examines the dynamic responses of the aircraft in the continuous-time domain, whereas chapter five focuses on system discretization and discrete-time simulations. These two chapters are essential in developing an understanding of expected aircraft responses as well as ensuring both the safety of the general public and the safety of onboard equipment

Chapter six outlines the hardware requirements that must be met in order to achieve autonomous capability. The focus of this chapter progresses from aircraft selection down to custom built hardware components. Selection of the microcontroller, together with the integration of various sensing elements, is of course fundamental to any control based application and are all dealt with in chapter six.

Chapter seven focuses on the development of the intuitive control system to be used as the primary automatic flight control system for this project. Chapter seven is essentially the culmination of chapters three through six, utilising the system response analysis together with the hardware features and limitations.

Chapter eight is entitled “Discussion and Conclusions” and is aimed at revisiting the successes or failures encountered throughout the course of the project. This chapter will also deal with all final conclusions that have been drawn from the performance of the system/s. These conclusions include comments on systems/components that operated adequately and as expected, as well as comments on those systems/components that did not meet the designated requirements or could be improved on. The ultimate aim of chapter eight is to outline all success and failure, discuss any limitations encountered, and give an insight into areas that may need future redevelopment, or indeed areas that may be valuable to explore for a future project.

Chapter 2 Dynamics of Flight

2.1 Axis Referencing

Initially, as with any computer control based application it is essential to analyse the physical characteristics of the system and to mathematically describe that system to allow for the development of the required control algorithms. For this particular flight control application the physical characteristics of the system are based around the flight dynamics of the aircraft.

The first step in analysing the flight dynamics of any aircraft is to develop an initial reference axis system to describe the position and attitude of the aircraft in relation to the Earth. The most convenient inertial reference frame to use is known as the tropocentric coordinate system or 'Earth axis system' (McLean, 1990); where the origin of this axis is regarded as being fixed at the centre of the Earth. Figure 2.1 diagrammatically summarises this system.

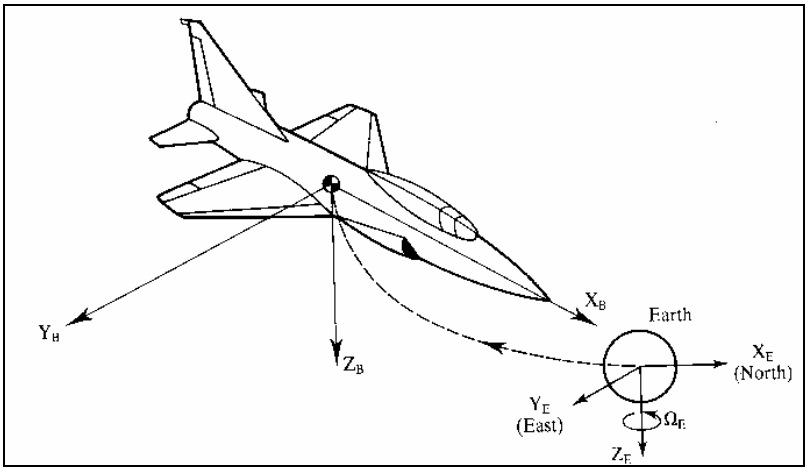

Figure 2.1: Aircraft Earth Axis System (McLean, 1990)

To supplement the Earth axis system and to characterise the aircraft in relation to this initial Earth reference frame, the aircraft itself must also be referenced by a suitable axis system. The system chosen for this project is the 'body-fixed axis system' (McLean, 1990). The components of this system are summarised in figure 2.2.

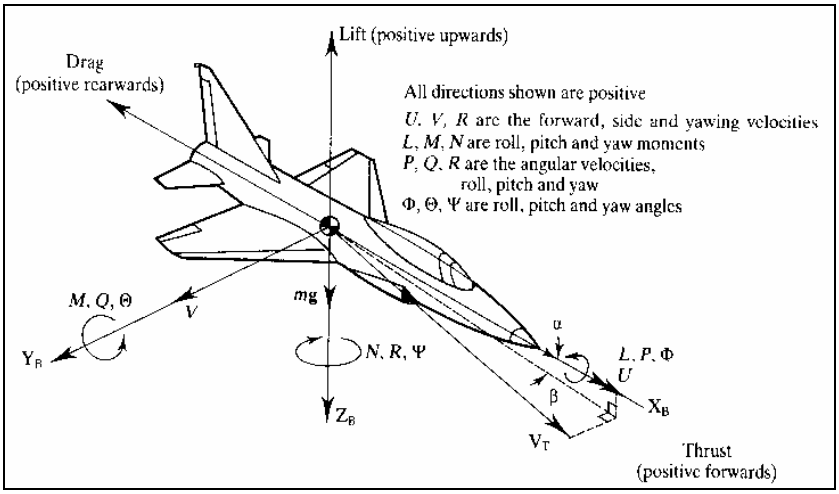

Figure 2.2: Aircraft Body-fixed Axis System (McLean, 1990)

The selection of both of the above axis systems' is critical in determining the equations of motion that will describe the attitude of the aircraft at any point in time. As shown in figure 2, there exist six degrees of freedom in any aircraft system. These elements consist of longitudinal ('X'), lateral ('Y') and vertical ('Z') translational motions, and roll ('L'), pitch ('M') and yaw ('N') motions about the aircraft's centre of gravity (Keeffe, 2003).

2.2 Euler's Equations of Motion

To characterise the six degrees of freedom the following equations, known as Euler's Equations of Motion, have been derived from Newton's Second Law and become fundamental in developing any flight control system using the previously described axis systems.

$$
\begin{aligned}
\Delta X &= m\left[\dot{U} + QW - RV\right] \\
\Delta Y &= m\left[\dot{V} + RU - PW\right] \\
\Delta Z &= m\left[\dot{W} + PV - QU\right] \\
L &= \dot{P} I_{xx} - I_{xz}\left(\dot{R} + PQ\right) + \left(I_{zz} - I_{yy}\right)QR \\
M &= \dot{Q} I_{yy} - I_{xz}\left(P^2 - R^2\right) + \left(I_{xx} - I_{zz}\right)PR \\
N &= \dot{R} I_{zz} - I_{xz}\dot{P} + PQ\left(I_{yy} - I_{xx}\right) + I_{xz}QR
\end{aligned}
$$

Equation 2.1: Euler's Equations of Motion

The equations listed in equation 2.1 represent the inertial forces acting on the aircraft. For completeness it then becomes necessary to characterise the contribution of the forces due to gravity. These contributions (only inherent in the translational dynamics of the aircraft) are summarised in equation 2.2.

$$
\begin{aligned}
\delta X &= -mg\sin\Theta \\
\delta Y &= mg\cos\Theta\sin\Phi \\
\delta Z &= mg\cos\Theta\cos\Phi
\end{aligned}
$$

Equation 2.2: Gravitational Contributions to Euler's Equations of Motion

Now that both the inertial forces of the aircraft and the contributions made by gravity have been quantified, the equations can be combined to produce the complete equations of motion of the aircraft for its six degrees of freedom (equation 2.3).

$$
\begin{aligned}
X &= \Delta X + \delta X \\
&= m\left[\dot{U} + QW - RV + g\sin\Theta\right] \\
Y &= \Delta Y + \delta Y \\
&= m\left[\dot{V} + RU - PW - g\cos\Theta\sin\Phi\right] \\
Z &= \Delta Z + \delta Z \\
&= m\left[\dot{W} + PV - QU - g\cos\Theta\cos\Phi\right] \\
\\
L &= \dot{P}I_{xx} - I_{xz}\left(\dot{R} + PQ\right) + \left(I_{zz} - I_{yy}\right)QR \\
M &= \dot{Q}I_{yy} - I_{xz}\left(P^2 - R^2\right) + \left(I_{xx} - I_{zz}\right)PR \\
N &= \dot{R}I_{zz} - I_{xz}\dot{P} + PQ\left(I_{yy} - I_{xx}\right) + I_{xz}QR
\end{aligned}
$$

Equation 2.3: Equations of Motion for all Six Degrees of Freedom

To supplement these base equations, it is also important to note the equations which relate the Euler angles (Ψ, Φ, and Θ) to the angular velocities (P, R and Q). These equations are defined as follows in equation 2.4.

$$
\begin{aligned}
P &= \dot{\Phi} - \dot{\Psi}\sin\Theta \\
Q &= \dot{\Theta}\cos\Phi + \dot{\Psi}\cos\Theta\sin\Phi \\
R &= -\dot{\Theta}\sin\Phi + \dot{\Psi}\cos\Theta\cos\Phi \\
\\
\dot{\Phi} &= P + \dot{\Psi}\sin\Theta \\
\dot{\Theta} &= Q\cos\Phi - R\sin\Phi \\
\dot{\Psi} &= \frac{R\cos\Phi}{\cos\Theta} + \frac{Q\sin\Phi}{\cos\Theta}
\end{aligned}
$$

Equation 2.4: Auxiliary Relationships

2.3 Small-Disturbance Theory

From these base equations it is then possible to characterise aircraft motion by using Small-Disturbance Theory (Keeffe, 2003) which describes motion in two

parts, an equilibrium condition and a dynamic condition which accounts for small perturbations from the mean motion. This theory essentially describes all of the motion variables in the equations of motion as having two components, a reference (or equilibrium) component and a dynamic (or perturbation) component as shown in equation 2.5.

$$\begin{aligned} U &= U_0 + u & Y &= Y_0 + y \\ V &= V_0 + v & Z &= Z_0 + z \\ W &= W_0 + w & M &= M_0 + m \\ P &= P_0 + p & N &= N_0 + n \\ Q &= Q_0 + q & L &= L_0 + l \\ R &= R_0 + r & \delta &= \delta_0 + \delta_1 \\ X &= X_0 + x \end{aligned}$$

Equation 2.5: Small Disturbance Theory

In equation 2.5, the trim, or equilibrium values are denoted by the subscript 0, whilst the perturbation values about this equilibrium condition are denoted by the lower case letter.

It then becomes necessary to define both equilibrium and perturbation equations. In equilibrium conditions there can be no translational or rotational acceleration (McLean, 1990), and as such the equilibrium equations can be expressed as shown in equation 2.6.

$$\begin{aligned} X_0 &= m\left[Q_0 W_0 - R_0 V_0 + g \sin \Theta_0 \right] \\ Y_0 &= m\left[R_0 U_0 - P_0 W_0 - g \cos \Theta_0 \sin \Phi_0 \right] \\ Z_0 &= m\left[\dot{W} + PV - QU \right] \\ L_0 &= -I_{xz} P_0 Q_0 + \left(I_{zz} - I_{yy} \right) Q_0 R_0 \\ M_0 &= I_{xz}\left(P_0^{\,2} - R_0^{\,2} \right) + \left(I_{xx} - I_{zz} \right) P_0 R_0 \\ N_0 &= P_0 Q_0 \left(I_{yy} - I_{xx} \right) + I_{xz} Q_0 R_0 \end{aligned}$$

Equation 2.6: Equations Representing Equilibrium Conditions

The auxiliary equations of angular velocity representing the rotation of the body-fixed axis system to the Earth axis system are also applicable and should be defined in the equilibrium state.

$$
\begin{aligned}
P_0 &= \dot{\Phi}_0 - \dot{\Psi}_0 \sin\Theta_0 \\
Q_0 &= \dot{\Theta}_0 \cos\Phi_0 + \dot{\Psi}_0 \cos\Theta_0 \sin\Phi_0 \\
R_0 &= -\dot{\Theta}_0 \sin\Phi_0 + \dot{\Psi}_0 \cos\Theta_0 \cos\Phi_0 \\
\\
\dot{\Phi}_0 &= P_0 + \dot{\Psi}_0 \sin\Theta_0 \\
\dot{\Theta}_0 &= Q_0 \cos\Phi_0 - R_0 \sin\Phi_0 \\
\dot{\Psi}_0 &= \frac{R_0 \cos\Phi_0}{\cos\Theta_0} + \frac{Q_0 \sin\Phi_0}{\cos\Theta_0}
\end{aligned}
$$

Equation 2.7: Auxiliary Equations Representing Equilibrium Conditions

The perturbation equations describing the small disturbances from the equilibrium condition are represented as shown in equations 2.8 and 2.9.

$$
\begin{aligned}
dX &= m\left[\dot{u} + W_0 q + Q_0 w - V_0 r - R_0 v + g\cos\Theta_0\theta\right] \\
dY &= m\left[\dot{v} + U_0 r + R_0 u - W_0 p - P_0 w - (g\cos\Theta_0\cos\Phi_0)\phi + (g\sin\Theta_0\sin\Phi_0)\theta\right] \\
dZ &= m\left[\dot{w} + V_0 p + P_0 v - U_0 q - Q_0 u + (g\cos\Theta_0\sin\Phi_0)\phi + (g\sin\Theta_0\cos\Phi_0)\theta\right] \\
\\
dL &= \dot{p} I_{xx} - I_{xz}\dot{r} + \left(I_{zz} - I_{yy}\right)\left(Q_0 r + R_0 q\right) - I_{xz}\left(P_0 q + Q_0 p\right) \\
dM &= \dot{q} I_{yy} + \left(I_{xx} - I_{zz}\right)\left(P_0 r + R_0 p\right) - I_{xz}\left(2R_0 r - 2P_0 p\right) \\
dN &= \dot{r} I_{zz} - I_{xz}\dot{p} + \left(I_{yy} - I_{xx}\right)\left(P_0 q + Q_0 p\right) + I_{xz}\left(Q_0 r + R_0 q\right)
\end{aligned}
$$

Equation 2.8: Equations Representing Perturbation Conditions

$$
\begin{aligned}
p &= \dot{\phi} - \dot{\Psi}_0 \sin\Theta_0 - \theta\left(\dot{\Psi}_0 \cos\Theta_0\right) \\
q &= \dot{\phi}\cos\Phi_0 - \theta\left(\dot{\Psi}_0 \sin\Phi \sin\Theta_0\right) + \dot{\Psi}\cos\Theta\sin\Psi_0 \\
&\quad + \phi\left(\dot{\Psi}_0 \cos\Theta_0 \cos\Phi_0 - \Theta_0 \sin\Phi_0\right) \\
r &= \dot{\Psi}\cos\Theta_0\cos\Phi_0 - \phi\left(\dot{\Psi}_0 \cos\Theta_0 \sin\Phi_0 + \dot{\Psi}_0 \cos\Phi_0\right) - \dot{\theta}\sin\Phi_0 \\
&\quad - \theta\left(\dot{\Psi}_0 \sin\Theta_0 \cos\Phi_0\right)
\end{aligned}
$$

Equation 2.9: Auxiliary Equations Representing Perturbation Conditions

2.4 Simplification

After applying Small-Disturbance Theory, simplification is needed to adapt the equations into a form that will be easier to analyse and implement in a computerised control system. It becomes necessary to analyse the motion variables for a given flight condition. Essentially, the requirements of this project indicate that the aircraft is needed to fly straight in steady, symmetric flight, with its wings level. Given these conditions the following assumptions can be made (McLean, 1990):

- Straight flight implies $\dot{\Psi}_0 = \Theta_0 = 0$
- Symmetric flight implies $\Psi_0 = V_0 = 0$
- Flying with wings level implies $\Phi_0 = 0$
- Also $Q_0 = P_0 = R_0 = 0$

Therefore it now becomes possible to rewrite the equations in this new form with reference to the above flight condition. Note that in equation 2.10, the equations for ‘x’, ‘z’ and ‘m’ are referred to as equations of longitudinal motion as they deal with all motion in the X-Z plane. Equations for ‘y’, ‘l’ and ‘n’ are referred to as equations of lateral motion as they deal with all motion in the X-Y plane. These distinctions will become important when designing a controller to represent the motion of the aircraft in all six degrees of freedom.

$$
\begin{aligned}
x &= m\left[\dot{u} + W_0 q - g\cos\Theta_0\theta\right] \\
y &= m\left[\dot{v} + U_0 r - W_0 p - g\cos\Theta_0\phi\right] \\
z &= m\left[\dot{w} - U_0 q + g\sin\Theta_0\theta\right] \\
\\
l &= \dot{p} I_{xx} - I_{xz}\dot{r} \\
m &= \dot{q} I_{yy} \\
n &= \dot{r} I_{zz} - I_{xz}\dot{p} \\
\\
p &= \dot{\phi} - \dot{\Psi}_0 \sin\Theta_0 \\
q &= \dot{\theta} \\
r &= \dot{\Psi}\cos\Theta_0
\end{aligned}
$$

Equation 2.10: Simplified Equations for Specific Flight Condition

2.5 Equations of Longitudinal Motion

The final step in the simplification process is to use Taylor Series approximations to expand the left hand side of the equations of motion (McLean, 1990). With Taylor Series expansion, the desired equations of longitudinal motion are yielded.

$$
\begin{aligned}
\frac{dX}{du}u + \frac{dX}{d\dot{u}}\dot{u} + \frac{dX}{dw}w + \frac{dX}{d\dot{w}}\dot{w} + \frac{dX}{dq}q + \frac{dX}{d\dot{q}}\dot{q} + \frac{dX}{d\delta_E}\delta_E + \frac{dX}{d\dot{\delta}_E}\dot{\delta}_E &= m\left[\dot{u} + W_0 q - g\cos\Theta_0\theta\right] \\
\\
\frac{dZ}{du}u + \frac{dZ}{d\dot{u}}\dot{u} + \frac{dZ}{dw}w + \frac{dZ}{d\dot{w}}\dot{w} + \frac{dZ}{dq}q + \frac{dZ}{d\dot{q}}\dot{q} + \frac{dZ}{d\delta_E}\delta_E + \frac{dZ}{d\dot{\delta}_E}\dot{\delta}_E &= m\left[\dot{w} - U_0 q + g\sin\Theta_0\theta\right] \\
\\
\frac{dM}{du}u + \frac{dM}{d\dot{u}}\dot{u} + \frac{dM}{dw}w + \frac{dM}{d\dot{w}}\dot{w} + \frac{dM}{dq}q + \frac{dM}{d\dot{q}}\dot{q} + \frac{dM}{d\delta_E}\delta_E + \frac{dM}{d\dot{\delta}_E}\dot{\delta}_E &= \dot{q} I_{yy}
\end{aligned}
$$

Equation 2.11: Taylor Series Expansion for Longitudinal Equations of Motion

By simplifying the Taylor series shown in equation 2.11, the following equations of longitudinal motion can be derived.

$$
\begin{aligned}
\dot{u} &= X_u u + X_{\dot{u}}\dot{u} + X_w w + X_{\dot{w}}\dot{w} + X_q q + X_{\dot{q}}\dot{q} - W_0 q - g\cos\Theta_0\theta + X_{\delta_E}\delta_E + X_{\dot{\delta}_E}\dot{\delta}_E \\
\dot{w} &= Z_u u + Z_{\dot{u}}\dot{u} + Z_w w + Z_{\dot{w}}\dot{w} + Z_q q + Z_{\dot{q}} + U_0 q - g\sin\Theta_0\theta + Z_{\delta_E}\delta_E + Z_{\dot{\delta}_E}\dot{\delta}_E \\
\dot{q} &= M_u u + M_{\dot{u}}\dot{u} + M_w w + M_{\dot{w}}\dot{w} + M_q q + M_{\dot{q}} + M_{\delta_E}\delta_E + M_{\dot{\delta}_E}\dot{\delta}_E \\
\dot{\theta} &= q
\end{aligned}
$$

Equation 2.12: Full, Complete, Expanded Equations of Longitudinal Motion

The constant terms: X_u, M_u, Z_u etc, are known as stability derivatives, and are specific to both the aircraft and the flight conditions. From studying the aerodynamic data of a large number of aircraft it becomes evident that not every stability derivative is significant, and in many cases, a number can be neglected (McLean, 1990). After neglecting the insignificant derivatives the final form of the equations of longitudinal motion are found.

$$
\begin{aligned}
\dot{u} &= X_u u + X_w w + W_0 q - g\cos\Theta_0\theta \\
\dot{w} &= Z_u u + Z_w w + U_0 q - g\sin\Theta_0\theta + Z_{\delta_E}\delta_E \\
\dot{q} &= M_u u + M_w w + M_{\dot{w}}\dot{w} + M_q q + M_{\delta_E}\delta_E \\
\dot{\theta} &= q
\end{aligned}
$$

Equation 2.13: Final Equations of Longitudinal Motion

2.6 Equations of Lateral Motion

To formulate the equations of lateral motion to accompany the longitudinal equations described above, the same process is followed, using Taylor Series expansion, simplification and exclusion of insignificant stability derivatives.

$$\begin{aligned}
\frac{dY}{dv}v+\frac{dY}{d\dot{v}}\dot{v}+\frac{dY}{dr}r+\frac{dY}{d\dot{r}}\dot{r}+\frac{dY}{dp}p+\frac{dY}{d\dot{p}}\dot{p}+\frac{dY}{d\delta_A}\delta_A+\frac{dY}{d\delta_R}\delta_R &= m\left[\dot{v}+U_0 r-W_0 p-g\cos\Theta_0\phi\right] \\
\frac{dL}{dv}v+\frac{dL}{d\dot{v}}\dot{v}+\frac{dL}{dr}r+\frac{dL}{d\dot{r}}\dot{r}+\frac{dL}{dp}p+\frac{dL}{d\dot{p}}\dot{p}+\frac{dL}{d\delta_A}\delta_A+\frac{dL}{d\delta_R}\delta_R &= I_{xx}\dot{p}-I_{xz}\dot{r} \\
\frac{dN}{dv}v+\frac{dN}{d\dot{v}}\dot{v}+\frac{dN}{dr}r+\frac{dN}{d\dot{r}}\dot{r}+\frac{dN}{dp}p+\frac{dN}{d\dot{p}}\dot{p}+\frac{dN}{d\delta_A}\delta_A+\frac{dN}{d\delta_R}\delta_R &= I_{zz}\dot{r}-I_{xz}\dot{p}
\end{aligned}$$

Equation 2.14: Taylor Series Expansion for Lateral Equations of Motion

$$\begin{aligned}
\dot{v} &= Y_v v+Y_{\dot{v}}\dot{v}+Y_r r+Y_{\dot{r}}\dot{r}+Y_p p+Y_{\dot{p}}\dot{p}+Y_{\delta_A}\delta_A+Y_{\delta_R}\delta_R+U_0 r-W_0 p-g\cos\Theta_0\phi \\
\dot{p} &= \frac{I_{xz}}{I_{xx}}\dot{r}+L_v v+L_{\dot{v}}\dot{v}+L_r r+L_{\dot{r}}\dot{r}+L_p p+L_{\dot{p}}\dot{p}+L_{\delta_A}\delta_A+L_{\delta_R}\delta_R \\
\dot{r} &= \frac{I_{xz}}{I_{zz}}\dot{p}+N_v v+N_{\dot{v}}\dot{v}+N_r r+N_{\dot{r}}\dot{r}+N_p p+N_{\dot{p}}\dot{p}+N_{\delta_A}\delta_A+N_{\delta_R}\delta_R \\
p &= \dot{\phi}-\dot{\Psi}\sin\Theta_0 \\
r &= \dot{\Psi}\cos\Theta_0
\end{aligned}$$

Equation 2.15: Full, Complete, Expanded Equations of Lateral Motion

$$\begin{aligned}
\dot{v} &= Y_v v+U_0 r-W_0 p-g\cos\Theta_0\phi+Y_{\delta_R}\delta_R \\
\dot{p} &= \frac{I_{xz}}{I_{xx}}\dot{r}+L_v v+L_P p+L_R r+L_{\delta_A}\delta_A+L_{\delta_R}\delta_R \\
\dot{r} &= \frac{I_{xz}}{I_{zz}}\dot{p}+N_v v+N_P p+N_R r+N_{\delta_A}\delta_A+N_{\delta_R}\delta_R \\
p &= \dot{\phi}-\dot{\Psi}\sin\Theta_0 \\
r &= \dot{\Psi}\cos\Theta_0
\end{aligned}$$

Equation 2.16: Final Equations of Lateral Motion

Equations 2.13 and 2.16 form the basis for conventional control system design.

Chapter 3 Flight Controller Development

3.1 Flight Control Theory

McLean (1990) states that the primary purpose of any flight control system is to 'compare commanded motion with measured motion and, if a discrepancy exists, generate in accordance with the required control law, the command signals to the actuator to produce the control surface deflections which will result in the correct control force or moment being applied'. Essentially a control system is used to automatically correct for disturbances without any input from the pilot or user. The general structure of the AFCS is shown in figure 3.1 below.

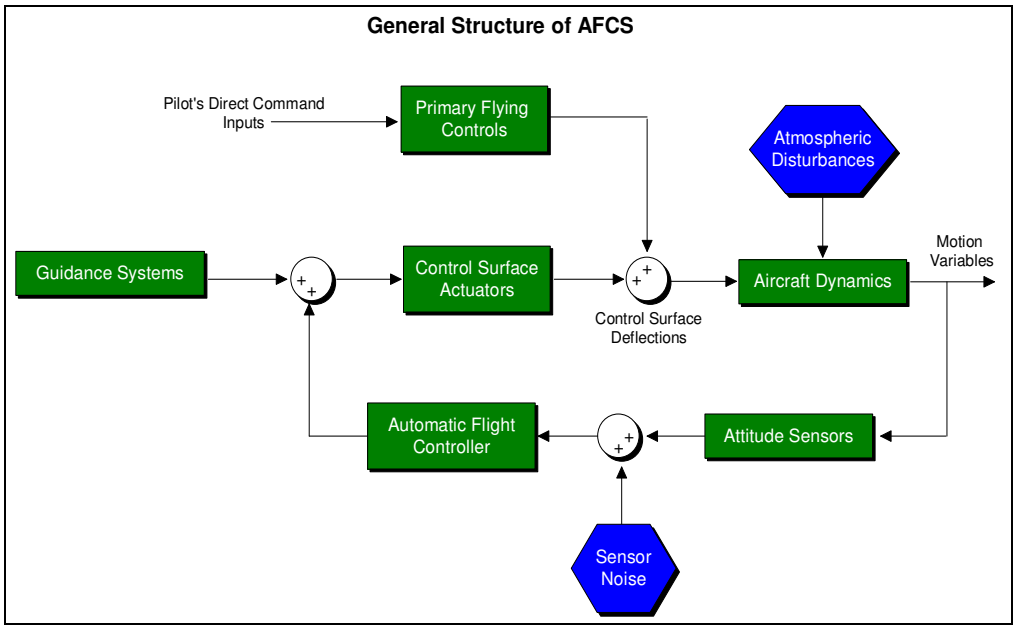

Figure 3.1: General AFCS Structure

The design of the AFCS will form the bulk of the content for this project. The ability to achieve straight, level flight is crucial for success. There are many various methods of designing automatic flight controllers and this project aims at implementing probably the simplest form of these. A simple error correction controller should be sufficient to achieve stable flight and basic waypoint navigation.

The AFCS theory for this project is ultimately based upon the equations shown in chapter two, essentially with separate control for both longitudinal and lateral control. These equations, based on the flight dynamics of the aircraft, will provide a reasonable starting point from which to predict the behaviour of the system. It should be noted at this point that the AFCS for a UAV of this scale (a small, inherently stable model aircraft travelling at relatively low speed) can essentially be designed in two ways. The dynamics investigated in chapter two are critical for stability in large scale aircraft, however in the case of this project; this analysis is simply used to give a representation of the system dynamics without the need for actual stability testing of the aircraft. The mathematical control theory itself can be built upon to design a more conventional control system that would no doubt be adequate for this project. However due to the small scale of the system in question and the fact that stability data relating to a model aircraft was difficult to obtain, a more intuitive approach was taken in regards to controlling the stability of the aircraft. Figure 3.2 shows how the control of the aircraft will be achieved, and where the mathematical system dynamics analysis conducted in chapter two will feature, particularly in the simulation stages of development.

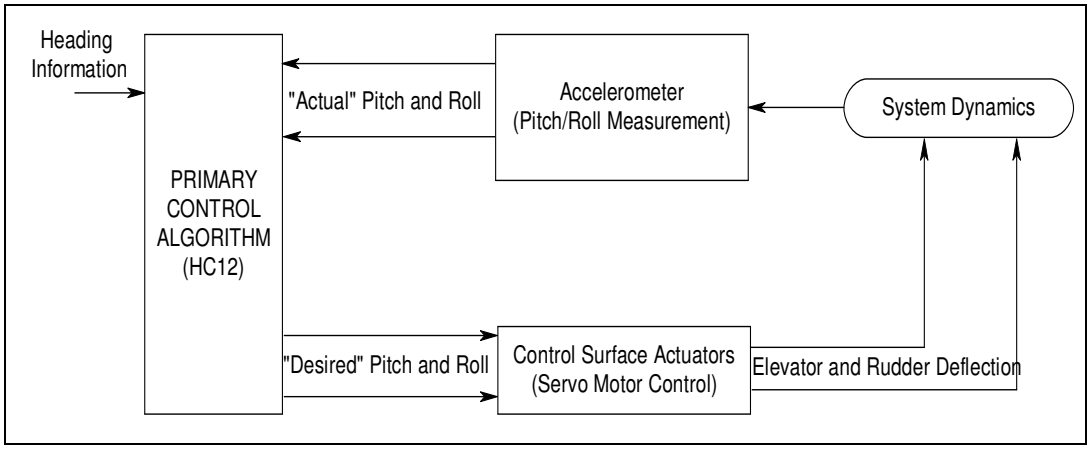

Figure 3.2: Primary closed loop system

An intuitive approach to stability control (essentially pitch and roll control) will simply need to record attitude measurements, examine heading information, and apply constraints to desired attitudes based upon the required heading. This essentially means that if the aircraft is flying at the desired heading, then pitch and roll simply need to be maintained at zero level (stable, level flight). If however there is a heading error, pitch and roll constraints must be relaxed to allow the required heading correction to take place. The system dynamics analysed in chapter two will be important in developing timing requirements and constraints in the primary control algorithm. The need to simulate how the aircraft will respond to various control inputs is necessary to ensure that the primary control algorithm does not deliver system commands that dramatically alter the aircraft attitudes and force instability.

3.2 State Space Representation

Both the longitudinal and lateral systems described by the equations in chapter 2 can be represented in the following state space form for control system design and simulation purposes. Not that these systems are initially characterised in the continuous-time domain. For any computer control application it is necessary to operate in the discrete-time domain. This will be dealt with later.

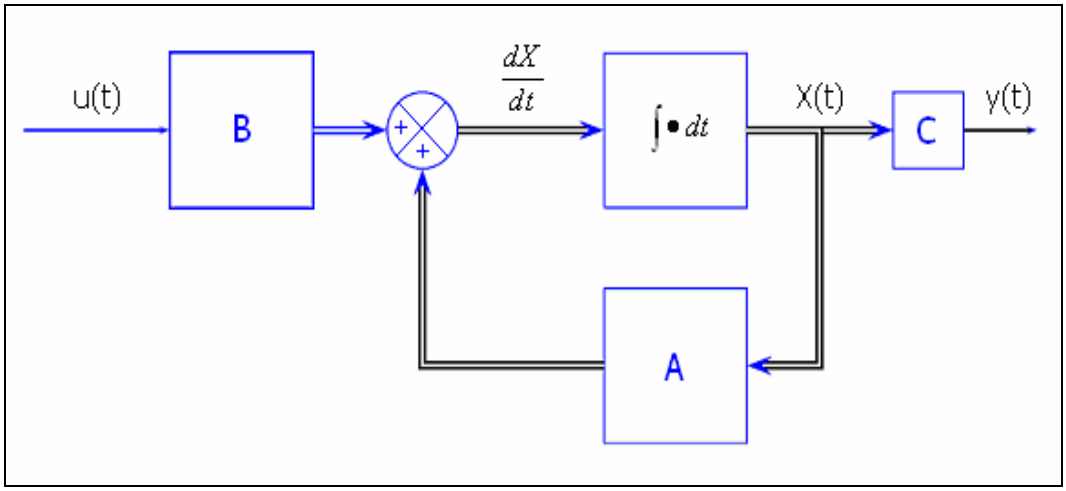

Figure 3.3: Continuous-time State Space Block Diagram Representation

Mathematically the block diagram in figure 3.3 can be represented as the following state space equations shown in equation 3.1.

$$\dot{x}(t) = Ax(t) + Bu(t)$$
$$y(t) = Cx(t) + Du(t)$$

Where : 'x' represents the state vector
'u' represents the input or control vector
'A' represents the state coefficient matrix
'B' represents the driving matrix
'C' represents the output matrix
'D' represents the feed - forward matrix

Equation 3.1: General Form of State Equations

3.2.1 Longitudinal System

The longitudinal equations shown in equation 2.13 in the previous chapter can be represented in state space matrix form as shown in equation 3.2.

$$\begin{bmatrix} \dot{\Delta U} \\ \dot{\Delta W} \\ \dot{\Delta Q} \\ \dot{\Delta \Theta} \\ \dot{\Delta h} \end{bmatrix} = \begin{bmatrix} X_u & X_w & 0 & -g\cos\gamma_0 & 0 \\ Z_u & Z_w & U_0 & -g\sin\gamma_0 & 0 \\ M_u & M_w & M_q & M_\theta & 0 \\ 0 & 0 & 1 & 0 & 0 \\ 0 & -1 & 0 & U_0 & 0 \end{bmatrix} \begin{bmatrix} \Delta U \\ \Delta W \\ \Delta Q \\ \Delta \Theta \\ \Delta h \end{bmatrix} + \begin{bmatrix} X_{\delta E} \\ Z_{\delta E} \\ M_{\delta E} \\ 0 \\ 0 \end{bmatrix} [\Delta \delta_E]$$

$$y = \begin{bmatrix} 0 & 0 & 0 & 0 & 1 \end{bmatrix} \begin{bmatrix} \Delta U \\ \Delta W \\ \Delta Q \\ \Delta \Theta \\ \Delta h \end{bmatrix} + [0][\Delta \delta_E]$$

Equation 3.2: Longitudinal State Space Representation

The 'C' matrix is essentially the required parameters that are of value from a longitudinal control perspective. In a simulation situation this matrix can be altered to examine the effect of changes on different parameters, for example the height of the aircraft and the pitch angle of the aircraft. The 'C' matrix presented in equation 3.2 is focussed on examining the response of the height of the aircraft.

The constants shown in the 'A' and 'B' matrix are the stability derivatives specific to the aircraft being modelled. It is at this point that adequate estimations need to be made as stability data for the exact aircraft chosen for this project is unavailable. This data essentially needs to be obtained through testing of the aircraft in a wind tunnel. Wind tunnel tests are often carried out as a simulation technique, to examine the effect of both atmospheric and control surface disturbances on the physical dynamics of the aircraft. The stability derivatives shown in equation 3.3 have been taken from an undergraduate project conducted at the Queensland University of Technology that modelled the longitudinal characteristics of a similar model aircraft in a wind tunnel (Abdullah, Fookes, Kumar-Mills, 1998). These figures should provide the necessary accuracy for the simulation purposes of this project.

$$\begin{bmatrix} \dot{\Delta U} \\ \dot{\Delta W} \\ \dot{\Delta Q} \\ \dot{\Delta \Theta} \\ \dot{\Delta h} \end{bmatrix} = \begin{bmatrix} -0.6284 & -2.6762 & 0 & -9.81 & 0 \\ -0.2232 & -2.6764 & 16 & 0 & 0 \\ 0.0102 & -0.1384 & -0.1575 & 0 & 0 \\ 0 & 0 & 1 & 0 & 0 \\ 0 & -1 & 0 & 16 & 0 \end{bmatrix} \begin{bmatrix} \Delta U \\ \Delta W \\ \Delta Q \\ \Delta \Theta \\ \Delta h \end{bmatrix} + \begin{bmatrix} -0.0610 \\ 0.1543 \\ 0.9686 \\ 0 \\ 0 \end{bmatrix} \begin{bmatrix} \Delta \delta_E \end{bmatrix}$$

$$y = \begin{bmatrix} 0 & 0 & 0 & 0 & 1 \end{bmatrix} \begin{bmatrix} \Delta U \\ \Delta W \\ \Delta Q \\ \Delta \Theta \\ \Delta h \end{bmatrix}$$

Equation 3.3: Longitudinal Representation with Stability Derivatives

3.2.2 Lateral System

The lateral system can be represented similarly to the longitudinal system described above. The primary difference in the lateral plane is the existence of two control inputs. Longitudinally it is only necessary to consider the control of the elevators, whereas in a lateral sense it is necessary to consider both rudder and aileron control. Despite the fact that the aircraft chosen for this project does not require aileron control, it is still important to consider this aspect during the simulation phase, that way if the aircraft was changed at some point in the future, simulation results would not be significantly affected. The lateral state space description is shown in equation 3.4.

$$\begin{bmatrix} \dot{\Delta V} \\ \dot{\Delta P} \\ \dot{\Delta R} \\ \dot{\Delta \Phi} \\ \dot{\Delta \Psi} \end{bmatrix} = \begin{bmatrix} Y_v & 0 & -1 & \frac{-g}{U_0}\cos\gamma_0 & 0 \\ L_v & L_p & L_r & 0 & 0 \\ N_v & N_p & N_r & 0 & 0 \\ 0 & 1 & \tan\gamma_0 & 0 & 0 \\ 0 & 0 & \sec\gamma_0 & 0 & 0 \end{bmatrix} \begin{bmatrix} \Delta V \\ \Delta P \\ \Delta R \\ \Delta \Phi \\ \Delta \Psi \end{bmatrix} + \begin{bmatrix} 0 & Y_{\delta R} \\ L_{\delta A} & L_{\delta R} \\ N_{\delta A} & N_{\delta R} \\ 0 & 0 \\ 0 & 0 \end{bmatrix} \begin{bmatrix} \Delta\delta_A \\ \Delta\delta_R \end{bmatrix}$$

$$y = \begin{bmatrix} 0 & 0 & 0 & 1 & 0 \\ 0 & 0 & 0 & 0 & 1 \end{bmatrix} \begin{bmatrix} \Delta V \\ \Delta P \\ \Delta R \\ \Delta \Phi \\ \Delta \Psi \end{bmatrix} + \begin{bmatrix} 0 & 0 \end{bmatrix} \begin{bmatrix} \Delta\delta_A \\ \Delta\delta_R \end{bmatrix}$$

Equation 3.4: Lateral State Space Representation

Again the focus of the 'C' matrix can be altered to focus on different aspects of the aircraft. At present (as shown in equation 3.4) the focus is placed on the roll and yaw angles. The lateral stability derivatives shown in equation 3.5 are again simply an estimate of the actual derivatives that could be expected from the aircraft chosen for this project. The figures displayed are stability derivative estimates from a twin-piston engined general aviation aircraft (McLean, 1990). Whilst these figures will not be entirely accurate, they will be a suitable estimation for the purposes of this analysis. Substitution of these constants is shown in equation 3.5.

$$\begin{bmatrix} \dot{\Delta V} \\ \dot{\Delta P} \\ \dot{\Delta R} \\ \dot{\Delta \Phi} \\ \dot{\Delta \Psi} \end{bmatrix} = \begin{bmatrix} -0.17 & 0 & -1 & -0.61 & 0 \\ -3.71 & -2.43 & 0.36 & 0 & 0 \\ 3.71 & -0.27 & -0.33 & 0 & 0 \\ 0 & 1 & 0 & 0 & 0 \\ 0 & 0 & 1 & 0 & 0 \end{bmatrix} \begin{bmatrix} \Delta V \\ \Delta P \\ \Delta R \\ \Delta \Phi \\ \Delta \Psi \end{bmatrix} + \begin{bmatrix} 0 & 0.05 \\ 2.62 & 1.02 \\ -0.06 & -2.1 \\ 0 & 0 \\ 0 & 0 \end{bmatrix} \begin{bmatrix} \Delta\delta_A \\ \Delta\delta_R \end{bmatrix}$$

$$y = \begin{bmatrix} 0 & 0 & 0 & 1 & 0 \\ 0 & 0 & 0 & 0 & 1 \end{bmatrix} \begin{bmatrix} \Delta V \\ \Delta P \\ \Delta R \\ \Delta \Phi \\ \Delta \Psi \end{bmatrix} + \begin{bmatrix} 0 & 0 \end{bmatrix} \begin{bmatrix} \Delta\delta_A \\ \Delta\delta_R \end{bmatrix}$$

Equation 3.5: Lateral Representation with Stability Derivatives

3.3 Transfer Function Representation

Nise (2000) states that a transfer function is a 'viable definition for a function that algebraically relates a system's output to its input'. In simple block diagram form any system can be represented as shown in figure 3.4.

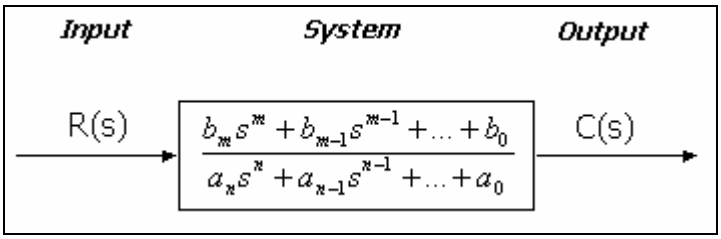

Figure 3.4: Block Diagram of a Transfer Function (Nise, 2000)

The transfer function of the system is defined as shown in equation 3.6.

$$\frac{C(s)}{R(s)} = G(s) = \frac{b_m s^m + b_{m-1} s^{m-1} + \ldots + b_0}{a_n s^n + a_{n-1} s^{n-1} + \ldots + a_0}$$

Equation 3.6: Transfer Function General Form

Note that the above representations are shown in the Laplacian 's' domain, which is directly related to the continuous-time characteristics of the system. Later the system will be explored in the discrete-time domain or the 'z' domain.

3.3.1 Longitudinal Transfer Function and Stability

MATLAB allows for easy conversion from state space form to transfer function form, with the code used for this conversion shown in appendix C(a) and C(b). The transfer function of the single input single output (SISO) longitudinal system is shown in equation 3.7. The significance of this transfer function will become more apparent in the system simulations discussed later in this chapter.

$$\frac{-0.1543s^3 - 0.1349s^2 + 41.12s + 14.33}{s^5 + 3.462s^4 + 3.819s^3 + 2.099s^2 + 0.5706s}$$

Equation 3.7: Longitudinal Transfer Function

As mentioned earlier the output of the system is really determined by the 'C' matrix and can be altered depending on the response in question. The transfer function shown above is for the height of the aircraft as the output focus. If other output variables are to be examined they would have differing, unique transfer functions.

Closely related to the transfer function is the concept of system poles and zeros. The poles of a transfer function are:

- The values of the Laplacian Domain ('s') that cause the transfer function to become infinite.
- Any roots of the denominator that are common to the roots of the numerator (Nise, 2000).

The zeros of a transfer function are:

- The values of the Laplacian Domain ('s') that cause the transfer function to become zero.
- Any roots of the numerator that are common to the roots of the denominator (Nise, 2000).

System poles have a significant connection with the stability of that system. Essentially there are three rules governing the location of system poles and consequent stability.

1) Stable systems have closed-loop transfer functions with poles only in the left half-plane (that is with a negative real part).
2) Unstable systems have closed-loop transfer functions with at least one pole in the right half-plane.
3) Marginally stable systems have closed-loop transfer functions with only imaginary poles of multiplicity one, and poles in the left half-plane (Nise, 2000).

Based on these definitions we can determine the stability of the longitudinal system without even looking at a response. The poles of the system are essentially the eigenvalues of the transfer function and are shown in figure 3.5.

$$\begin{bmatrix} 0 \\ -2.0127 \\ -0.7515 \\ -0.3490 + 0.5054 \\ -0.3490 - 0.5054i \end{bmatrix}$$

Figure 3.5: Eigenvalues (pole locations) of Longitudinal System

Applying the criteria listed above, it can be seen that the longitudinal continuous-time system appears stable.

3.3.2 Lateral Transfer Function and Stability

Because the lateral system is not a SISO model, and actually contains two inputs and two outputs (making the system a multi-input multi-output (MIMO) system), there will essentially be four transfer functions, one for each combination of input and output. These representations are shown in equation 3.8.

As above, if alternate output variables were being analysed, different transfer functions would result.

Input: Aileron, Output: Roll Angle

$$\frac{2.62s^2 + 1.285s + 9.638}{s^4 + 2.929s^3 + 5.076s^2 + 7.897s + 0.07961}$$

Input: Aileron, Output: Yaw Angle

$$\frac{-0.061s^3 - 0.8662s^2 - 0.1489s - 5.821}{s^5 + 2.929s^4 + 5.076s^3 + 7.897s^2 + 0.07961s}$$

Input: Rudder, Output: Roll Angle

$$\frac{1.02s^2 - 0.4288s - 4.074}{s^4 + 2.929s^3 + 5.076s^2 + 7.897s + 0.07961}$$

Input: Rudder, Output: Yaw Angle

$$\frac{-2.1s^3 - 5.562s^2 - 0.445s + 2.457}{s^5 + 2.929s^4 + 5.076s^3 + 7.897s^2 + 0.07961s}$$

Equation 3.8: Lateral Transfer Functions

For the pole locations of the lateral system, the four transfer functions relating each input to each output have the same eigenvalues, and it is therefore only

necessary to examine the values for any of the transfer functions. The pole locations are as follows.

0
- 2.2326
- 0.0101
- 0.3431 + 1.8430i
- 0.3431 - 1.8430i

Figure 3.6: Eigenvalues (pole locations) of Lateral System

Again, after applying the stability criteria related to pole locations, the lateral systems appear stable for each input/output combination.

3.4 Controllability and Observability

Whilst not critical to the development of the control method being implemented in this project, the concept of system controllability and observability is essential when designing a control system based on conventional mathematical control techniques and utilising state variable feedback.

A control system is said to be completely controllable if it is possible to transfer the system from any arbitrary initial state to any desired state in a finite time period (Ogata, 1995). Controllability is important to consider as an optimal control solution may not exist if the system is not controllable. Controllability is determined via a controllability matrix related to the 'A' and 'B' matrices in the continuous-time domain. Nise (2000) states the criteria for controllability as follows:

An n^{th} order plant (system) whose state equation is:

$$\dot{x} = Ax + Bu$$

Is completely controllable if the matrix (controllability matrix),

$$C_M = \begin{bmatrix} B & AB & A^2B & \cdots & A^{n-1}B \end{bmatrix}$$

is of rank n.

Both the longitudinal and lateral systems in the AFCS are of rank 5 (essentially the number of state variables in each system). Using MATLAB to compute the controllability matrix ('C_M'), figure 3.7 shows the rank of this matrix and indicates that both systems are indeed completely controllable.

Longitudinal

$$C_M = \begin{bmatrix} -0.061 & -0.3746 & -49.6725 & 148.3183 & -322.982 \\ 0.1543 & 15.0982 & -43.1178 & 93.4327 & -190.5801 \\ 0.9686 & -0.1745 & -2.0659 & 5.7867 & -12.3311 \\ 0 & 0.9686 & -0.1745 & -2.0659 & 5.7867 \\ 0 & -0.1543 & 0.3994 & 40.3253 & -126.4875 \end{bmatrix}$$

Controlable States = 5
Uncontrollable States = 0

Lateral

$$C_M = \begin{bmatrix} 0 & 0.05 & 0.06 & 2.09 & -0.92 & -1.57 & 1.90 & -6.12 & -1.34 & 9.42 \\ 2.62 & 1.02 & -6.38 & -3.41 & 15.05 & 0.75 & -32.3 & 7.07 & 68.5 & 2.33 \\ -0.06 & -2.10 & -0.68 & 0.58 & 2.17 & 8.49 & -8.21 & -8.81 & 18.4 & -21.7 \\ 0 & 0 & 2.62 & 1.02 & -6.38 & -3.41 & 15.0 & 0.75 & -32.3 & 7.07 \\ 0 & 0 & -0.06 & -2.10 & -0.68 & 0.58 & 2.17 & 8.49 & -8.21 & -8.81 \end{bmatrix}$$

Controlable States = 5
Uncontrollable States = 0

Figure 3.7: Longitudinal and Lateral Controllability

Similar to controllability, a system is said to be completely observable if every initial state x(0) can be determined from the observation of y(t) over a finite time period (Ogata, 1995). In a state feedback approach to control, it is a requirement to have the feedback of all state variables. In a practical system however, some of these state variables may not be accessible (directly measurable). It therefore becomes necessary to estimate the value of these unknown state variables based on the system output y(t) and an initial state x(0). If a conventional control method was being utilised for this project a state observer system may well be

required. Therefore it is useful to examine the observability of both longitudinal and lateral systems. Nise (2000) states the criteria for observability as follows:

An n^{th} order plant (system) whose state and output equations are:

$$\begin{aligned} \dot{x} &= Ax + Bu \\ y &= Cx \end{aligned}$$

Is completely observable if the matrix (controllability matrix),

$$O_M = \begin{bmatrix} C & CA & CA^2 & \cdots & CA^{n-1} \end{bmatrix}$$

is of rank n.

As mentioned the longitudinal and lateral systems in the AFCS are of rank 5. Using MATLAB to compute the observability matrix ('O_M'), figure 3.8 shows the rank of this matrix and indicates that both systems are indeed completely observable.

Longitudinal

$$O_M = \begin{bmatrix} 0 & 0 & 0 & 0 & 1 \\ 0 & -1 & 0 & 16 & 0 \\ 0.2232 & 2.6764 & 0 & 0 & 0 \\ -0.7376 & -7.7604 & 42.8224 & -2.1896 & 0 \\ 2.6320 & 16.8175 & -133.1012 & 7.2362 & 0 \end{bmatrix}$$

$$\text{Observable States} = 5$$
$$\text{Unobservable States} = 0$$

Lateral

$$O_M = \begin{bmatrix} 0 & 0 & 0 & 1 & 0 \\ 0 & 0 & 0 & 0 & 1 \\ 0 & 1 & 0 & 0 & 0 \\ 0 & 0 & 1 & 0 & 0 \\ -3.71 & -2.43 & 0.36 & 0 & 0 \\ 3.71 & -0.27 & -0.3250 & 0 & 0 \\ 10.99 & 5.807 & 2.718 & 2.274 & 0 \\ -0.849 & 0.744 & -3.701 & -2.274 & 0 \\ -13.37 & -12.57 & -9.789 & -6.742 & 0 \\ -16.34 & -3.082 & 2.32 & 0.502 & 0 \end{bmatrix}$$

$$\text{Observable States} = 5$$
$$\text{Unobservable States} = 0$$

Figure 3.8: Longitudinal and Lateral Observability

Chapter 4 Continuous-Time System Simulations

4.1 Root Locus

4.1.1 Longitudinal

Root locus techniques are a powerful graphical representation of the closed loop poles of the system as a parameter is varied (system gain etc). MATLAB allows for easy calculation of the root locus and also gives the user the power to examine system response parameters such as damping and percentage overshoot. The root locus of the continuous-time longitudinal system is shown in figure 4.1.

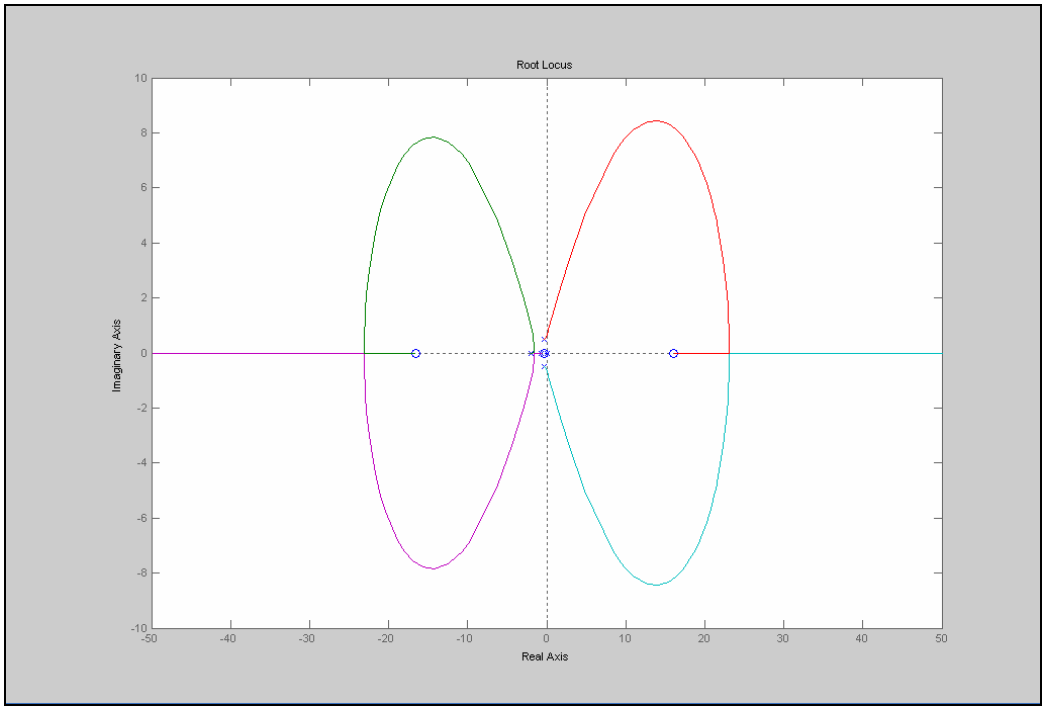

Figure 4.1: Root Locus of Longitudinal System

Figure 4.1 essentially reinforces the stability analysis conducted in section 3.3.1. It can be seen from the figure that all poles are located in the left half-plane, thus stabilizing the system. The root locus lines give an indication of the possible pole locations as system gain is varied. When designing a system it is important to restrict gain to values that will prevent the system poles from entering into the unstable right half-plane.

MATLAB indicates that the gain value for marginal stability is approximately 0.0211. Therefore it may be necessary to scale the system down by an appropriate gain so as to ensure closed loop stability. This will become evident when conducting Bode Plot analysis.

4.1.2 Lateral

Realistically a root locus diagram for the lateral system does not exist, as root locus techniques are not valid for MIMO systems. It is possible however to simply provide a pole/zero map of the system. As mentioned earlier the pole locations (and indeed the zero locations) of each possible input/output combination in the lateral system are identical. A pole/zero map will not provide

the level of detail that a root locus would, such as the effect of parameter changes. The pole/zero map (as shown in figure 4.2) simply gives a graphical representation of the information shown in section 3.3.2, and is therefore useful in visualising the stability of the system.

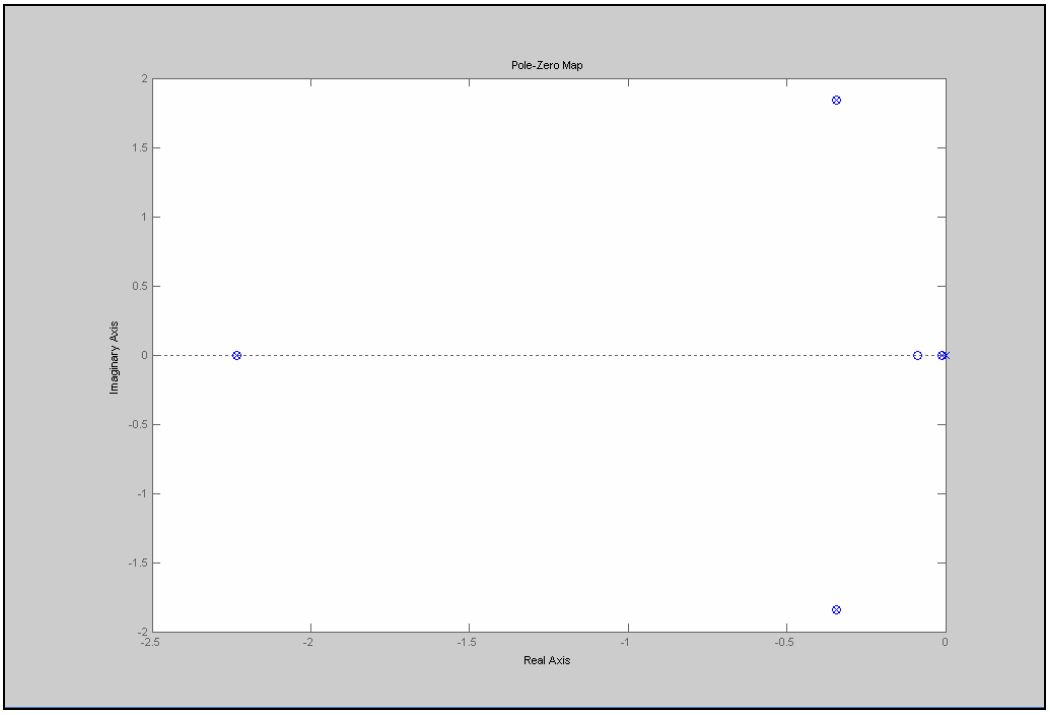

Figure 4.2: Pole/zero Map of Lateral System

As expected, figure 4.2 indicates that all system poles are in the left half-plane and the system (or system combinations) is/are stable.

4.2 Bode Plots

4.2.1 Longitudinal

Bode plot analysis is a frequency response technique that again allows for graphical representation of theoretical concepts (Nise, 2000). Bode plots essentially consist of two plots, magnitude and phase. These plots are used in conjunction with each other to determine closed loop stability, via analysis of gain and phase margins. Gain and phase margin are stability constraints defined as follows:

- Gain margin is the change in open loop gain (in dB) required at 180^{o} of phase shift to make the closed-loop system unstable.
- Phase margin in the change in open-loop phase shift required at unity gain to make the closed-loop system unstable (Nise, 2000).

As mentioned earlier, it has been established from the root locus plot that the system is required to be scaled down by a gain value of less than 0.0211 so as to ensure closed loop stability. MATLAB again allows for easy determination of gain and phase margin via Bode plotting. The Bode plot of the longitudinal system with gain and phase margin is shown in figure 4.3.

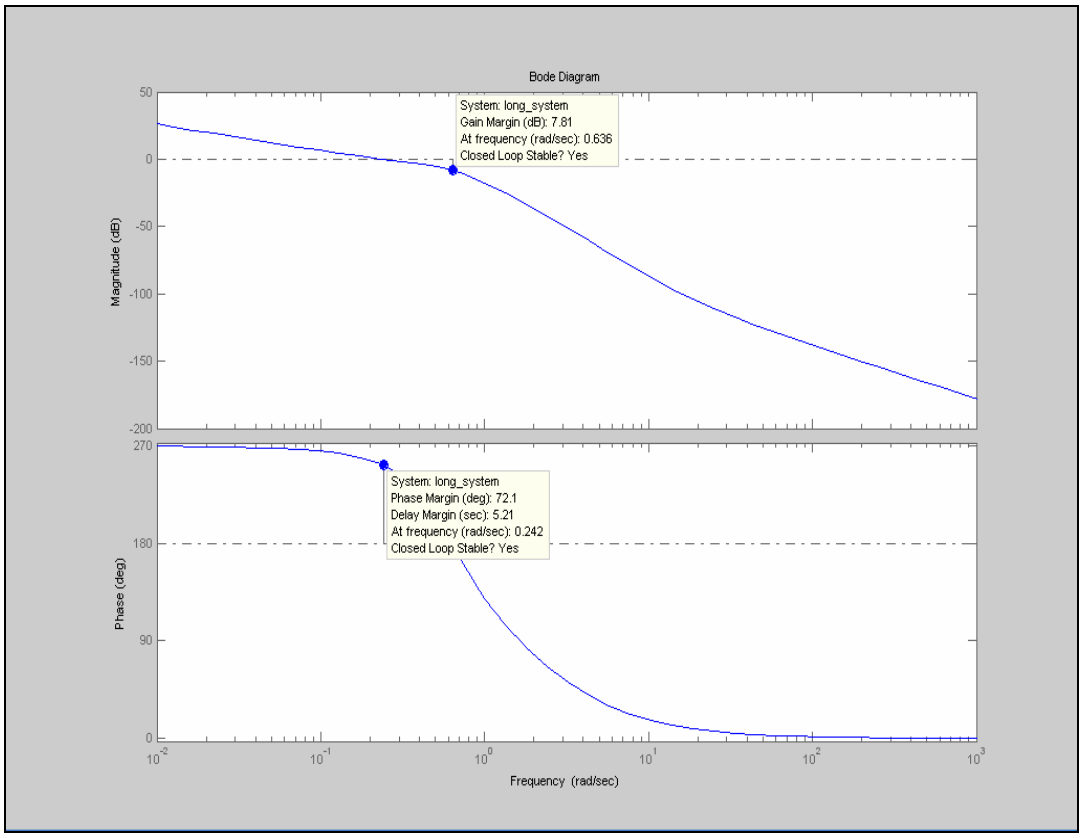

Figure 4.3: Bode Plot of Longitudinal System

Figure 4.3 indicates that the gain margin of the system is 7.81 dB and the corresponding phase margin is 72.1^{o}. MATLAB also indicates closed loop system stability.

4.2.2 Lateral

As with root locus analysis, Bode plots for the lateral system will not be of great use for stability analysis. The concept of gain and phase margin is relevant only for SISO systems and is therefore not valid for the lateral MIMO system. For reference, the Bode plots for each lateral system combination have been shown in figure 4.4.

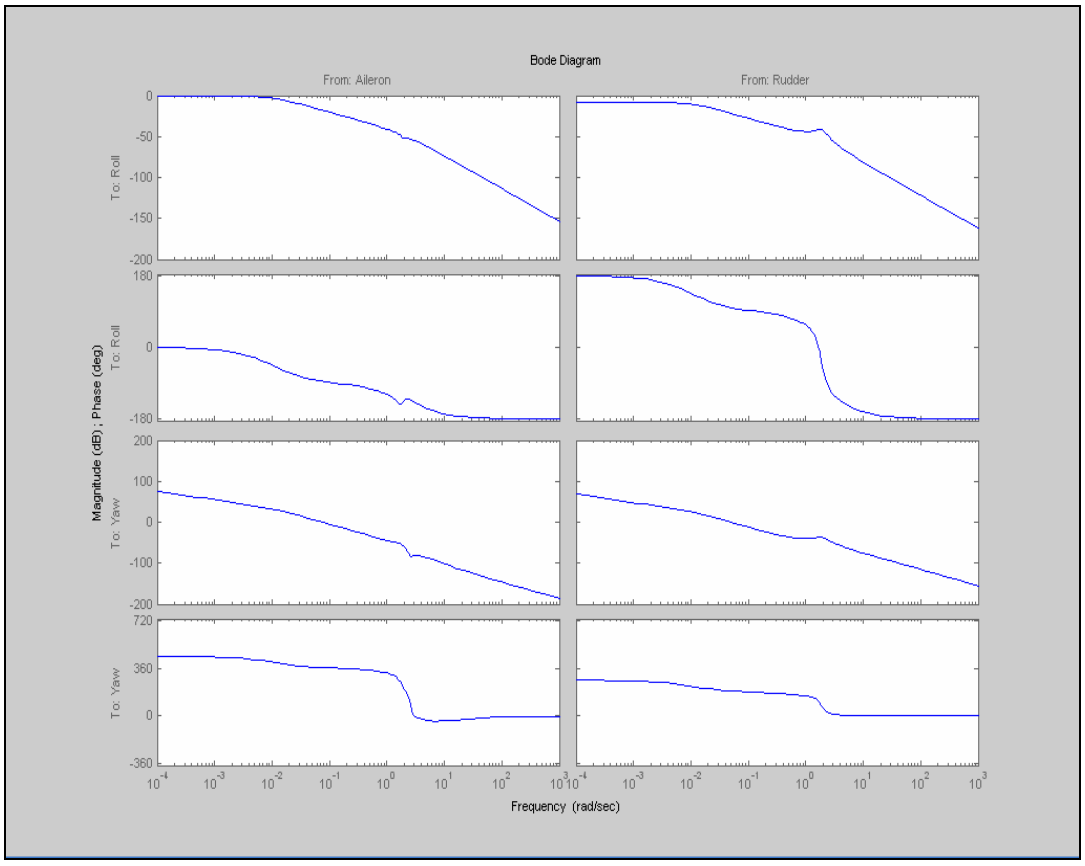

Figure 4.4: Bode Plots of Lateral System

4.3 Longitudinal System Responses

4.3.1 Step Response

A unit step input is essentially a continual unity 'hold' on the system input. Before any actual simulation is carried out, it is possible to predict the response of the system (that is the aircraft itself) to this unit step. Essentially, if a step input was applied to the elevator (as is the case in the longitudinal system) it

would be expected that the aircraft would simply gain altitude at a constant rate. This is indeed the case as figure 4.5 highlights. Note that the output matrix 'C' in this case is set to observe the effect of the control input on the altitude of the aircraft.

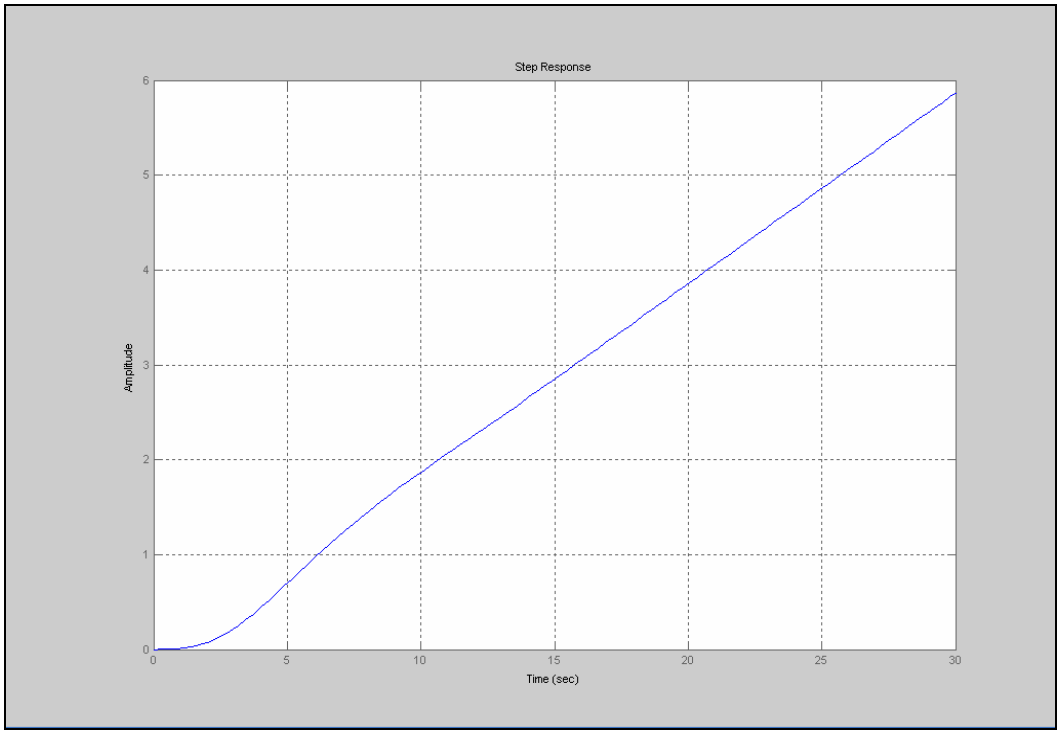

Figure 4.5: Step Response ('C' focus - Altitude) of Longitudinal System

Another important output characteristic to investigate with regards to the longitudinal system is the pitch angle (Θ). Intuitively it can be expected that the pitch angle reaction to a unit step input would be to simply settle on a constant value, as a constant increase aircraft altitude (as shown in figure 4.5) will essentially result in a constant pitch angle. This phenomenon is displayed in figure 4.6.

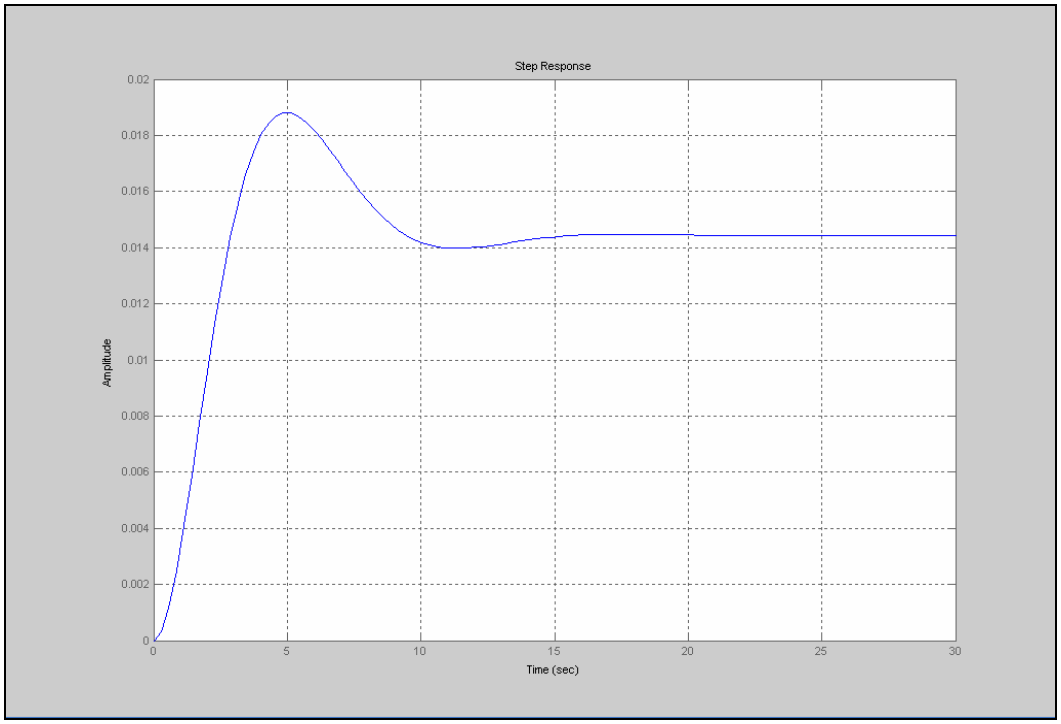

Figure 4.6: Step Response ('C' focus – Pitch Angle) of Longitudinal System

Figures 4.5 and 4.6 indicate that the longitudinal system is responding as expected to a unit step input.

4.3.2 Impulse Response

An impulse input is another form of control input that can be applied to the system. An impulse implies that the input control surface (in the longitudinal case, the elevator) is subject to a 'zero-time' unit pulse. Whilst in practice a true impulse input is impossible (nothing can be 'zero-time'), it is useful to look at the response of the system to a 'short' pulse of its input. Intuitively, a 'short' pulse on the elevator of the aircraft should result in a slight gain in altitude before settling at the new altitude. This is confirmed by the impulse response of the aircraft (altitude as the focus) shown in figure 4.7.

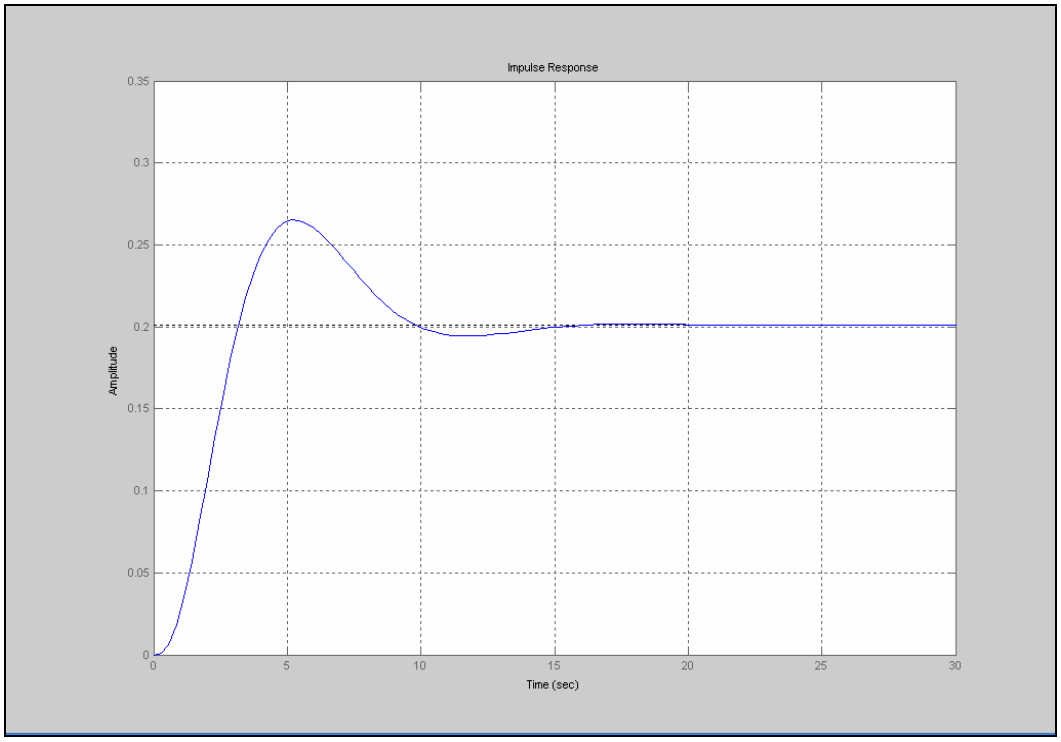

Figure 4.7: Impulse Response ('C' focus – Altitude) of Longitudinal System

The pitch angle reaction to an impulse response can again be predicted. With an impulse input to the elevator it is expected (and confirmed by figure 4.7) that the aircraft will gain altitude momentarily then settle at a new level. Therefore the response of the pitch angle should be to momentarily increase, as the aircraft gains altitude, before settling back to zero as the aircraft levels. Again, figure 4.8 confirms this theory.

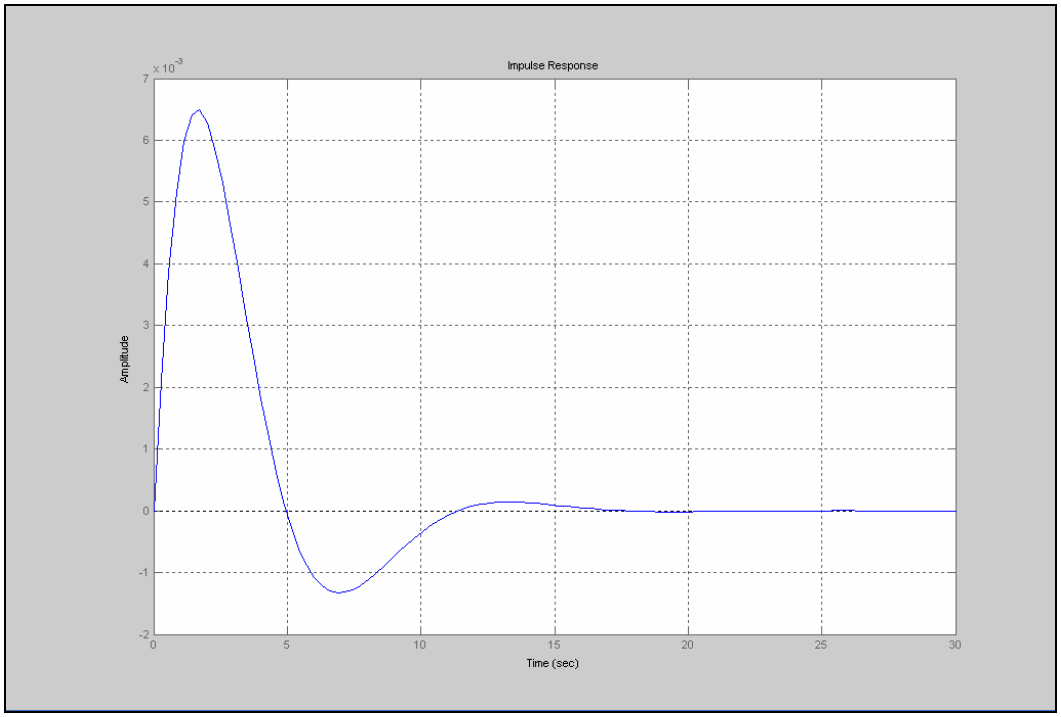

Figure 4.8: Impulse Response ('C' focus – Pitch Angle) of Longitudinal System

Figures 4.7 and 4.8 again confirm that the longitudinal system is responding as predicted and expected.

4.4 Lateral System Responses

4.4.1 Step Response

As previously discovered, the MIMO lateral system will have four combinations of input/output. The primary responses that require further analysis essentially depend on the type of aeroplane chosen as the prototyping platform. For example, some model aircraft do not utilise aileron control at all and simply rely on the combination of rudder deflections and wing structure to initiate a turn. For aircraft such as these, obviously the analysis of responses to aileron input is not necessary. Figure 4.9 shows the step responses for each of the four combinations.

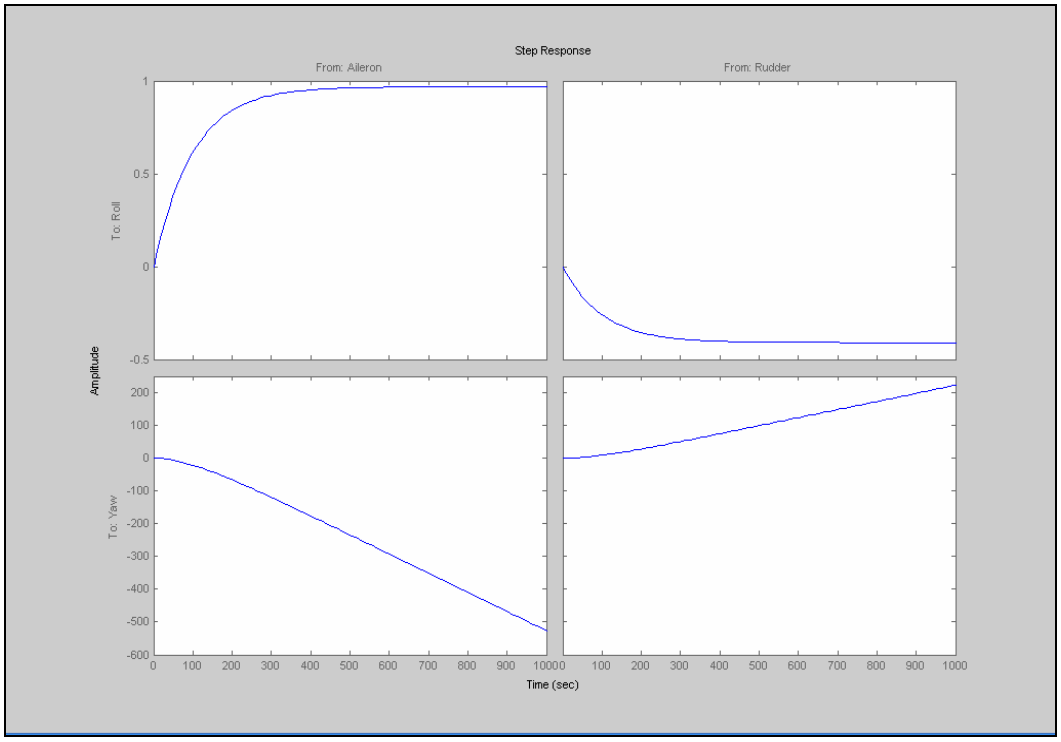

Figure 4.9: Step Responses of Lateral System

The primary response to focus on in figure 4.9 is the response from rudder to yaw (essentially direction). This response is important, because the aircraft chosen for this project does not have aileron control, and also because one of the key design issues is the ability to correct the flight path of the aircraft to fly a pre-determined route. Again, intuitively it can be predicted that a unit step response on the rudder will result in a constant change in direction (yaw) similar to the constant altitude increase with a step input to the elevator. This is indeed reinforced by figure 4.9.

4.4.2 Impulse Response

The primary focus of the impulse response analysis is again on the response of the yaw angle to a rudder impulse. Here it is also interesting to examine the effect of roll angle to an impulse on the aileron. Intuitive conclusions can again be drawn as an impulse input to the rudder of the aircraft will basically alter the yaw angle marginally before settling at a new value. Similar conclusions can be drawn in regards to an impulse on the aileron. Here it is expected that this form of input would result in a momentary increase in roll angle before the aircraft

once again settles at zero roll angle. These two conclusions are validated by figure 4.10.

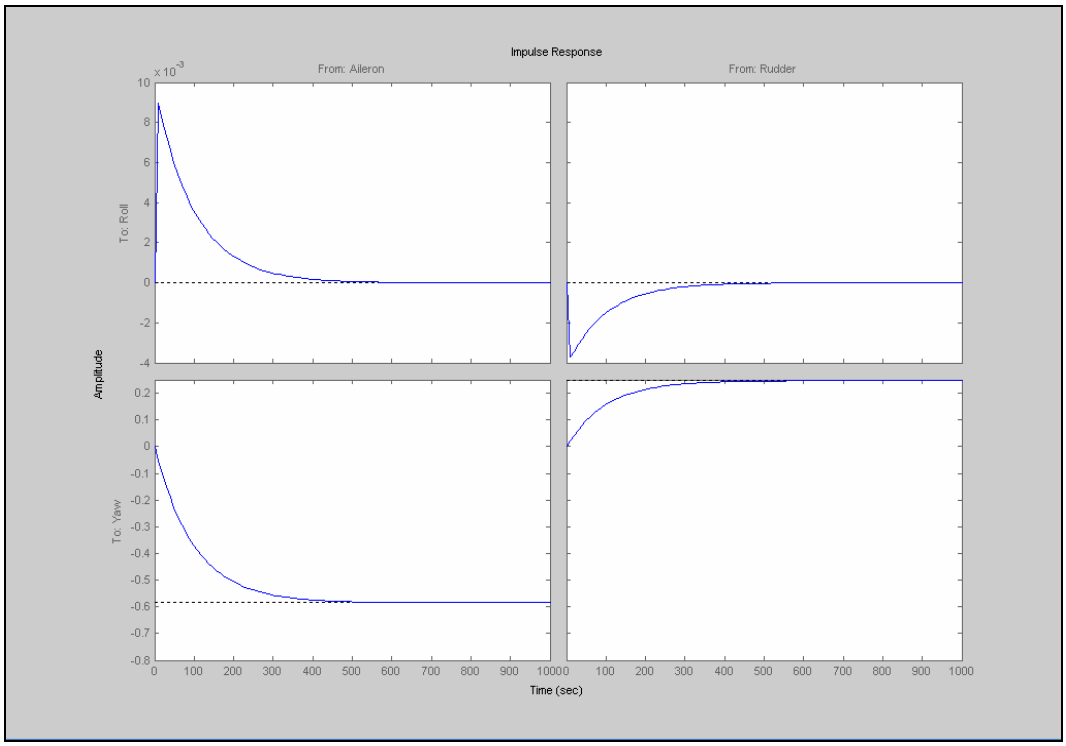

Figure 4.10: Impulse Responses of Lateral System

From these two simple simulations (shown in figures 4.9 and 4.10) it is evident that the lateral system, like the longitudinal system, will respond adequately to control inputs. The time-scale shown for the lateral system is inaccurate for the model aircraft in question. The lateral stability derivatives for a model aircraft could not be found, therefore as mentioned in chapter 3, derivatives from a twin-piston engined general aviation aircraft (McLean, 1990) were used. The time scale appears unnaturally large, as the forward velocity of the simulations was maintained at the same value as the longitudinal system tests. The velocity of a model aircraft would clearly not be feasible for a general aviation aircraft, hence the exceedingly large time scale of the lateral system. For a more detailed analysis of response times the lateral stability data for a model aircraft should be determined (see section 8.3).

Chapter 5 Discrete-Time System Simulations

5.1 System Discretization

So far all analysis that has been undertaken has been done so using a continuous-time representation of the system dynamics. The next important step in any digital control system is to convert from the continuous-time domain to the discrete-time domain. This process is known as discretization. Equation 5.1 shows how the continuous-time state space representation of the system differs from the desired discrete-time representation.

Continuous - Time Domain

$$\dot{x}(t) = Ax(t) + Bu(t)$$
$$y(t) = Cx(t) + Du(t)$$

Discrete - Time Domain

$$X(k+1) = \Phi X(k) + \Gamma u(k)$$
$$y(k) = CX(k) + Du(k)$$

Equation 5.1: Continuous-Time to Discrete-Time State Equations

Discretization of a system is achieved via sampling of the continuous-time system. The *'k'* in equation 5.1 refers to these sample instants. Figure 5.1 represents the discretized system in block diagram form.

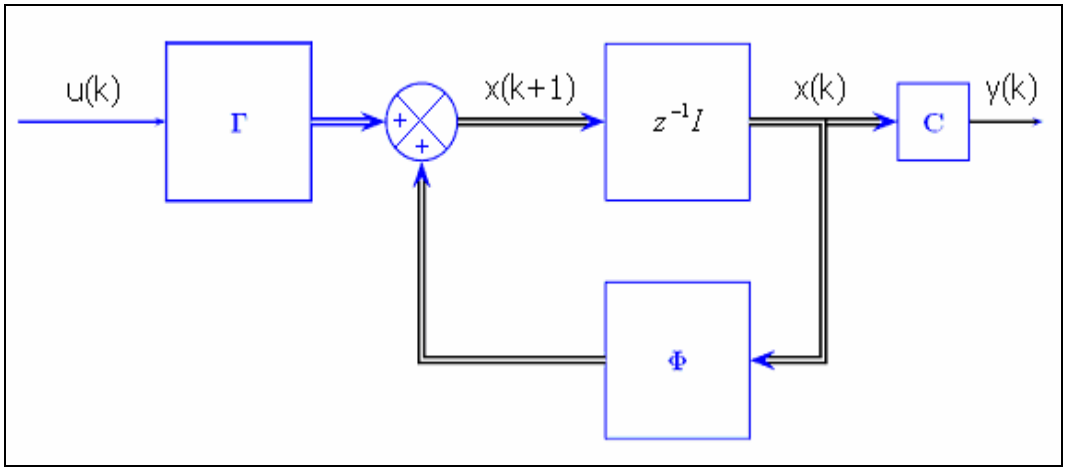

Figure 5.1: Discrete-time State Space Block Diagram Representation

One of the fundamental parameters of a computer controlled system is the rate at which the continuous-time signals are sampled. Shannon's sampling theorem states that a continuous time signal $f(t)$ with a finite bandwidth ω_0 (the highest frequency component in the signal, or the Nyquist frequency) can be uniquely described by the sampled signal $f(kT)\{k = ...,-1,0,1,...\}$, when the sampling frequency ω_s is greater than $2\omega_0$ (Ogata, 1995). Basically if a signal is sampled at a rate that is at least twice the frequency of the highest frequency component present in the original signal, the sampled data can adequately represent all the features of this signal.

To determine a suitable sampling frequency the natural frequencies at each pole location were found. Again MATLAB provides an easy method of achieving this. Figure 5.2 shows the MATLAB output for the *'damp'* command for both the longitudinal and lateral systems.

Longitudinal

Eigenvalue	Damping	Freq. (rad/s)
0.00e+000	-1.00e+000	0.00e+000
-3.49e-001 + 5.05e-001i	5.68e-001	6.14e-001
-3.49e-001 - 5.05e-001i	5.68e-001	6.14e-001
-7.51e-001	1.00e+000	7.51e-001
-2.01e+000	1.00e+000	2.01e+000

Lateral

Eigenvalue	Damping	Freq. (rad/s)
0.00e+000	-1.00e+000	0.00e+000
-1.01e-002	1.00e+000	1.01e-002
-3.43e-001 + 1.84e+000i	1.83e-001	1.87e+000
-3.43e-001 - 1.84e+000i	1.83e-001	1.87e+000
-2.23e+000	1.00e+000	2.23e+000

Figure 5.2: System Poles Damping and Natural Frequency

From figure 5.2 it can be seen that the highest frequency component in the longitudinal system is 2.01 rad/s, and the corresponding lateral high frequency is 2.23 rad/s. Sampling theorem suggests that the sampling rate should be at least twice the highest frequency component, therefore to be safe a factor of five times the highest component will be used. Equation 5.2 shows how to calculate a suitable sampling interval for each system based on this frequency data.

Longitudinal

$$w_n = 2.01\ rad/s$$
$$5w_n = 10.05\ rad/s$$
$$= \frac{10.05}{2\pi}\ Hz$$
$$= 1.6\ Hz$$
$$\therefore T = \frac{1}{5w_n}$$
$$= 0.625\ s$$

Lateral

$$w_n = 2.23\ rad/s$$
$$5w_n = 11.15\ rad/s$$
$$= \frac{11.15}{2\pi}\ Hz$$
$$= 1.77\ Hz$$
$$\therefore T = \frac{1}{5w_n}$$
$$= 0.564\ s$$

Equation 5.2: Determination of Sampling Rate

Now that the sampling rate of each system has been decided upon, MATLAB allows for simple conversion from continuous-time domain to discrete-time domain using the *'c2d'* command. The output of this conversion is shown for both systems in figures 5.3 and 5.4.

Longitudinal

$$X(k+1) = \Phi X(k) + \Gamma u(k)$$

$$\begin{bmatrix} \Delta U \\ \Delta W \\ \Delta Q \\ \Delta \Theta \\ \Delta h \end{bmatrix}(k+1) = \begin{bmatrix} 0.71 & -0.53 & -5.64 & -5.18 & 0 \\ -0.03 & 0.07 & 4.13 & 0.18 & 0 \\ 0.008 & -0.04 & 0.66 & -0.02 & 0 \\ 0.002 & -0.016 & 0.54 & 0.995 & 0 \\ 0.026 & -0.333 & 1.09 & 9.94 & 1 \end{bmatrix} \begin{bmatrix} \Delta U \\ \Delta W \\ \Delta Q \\ \Delta \Theta \\ \Delta h \end{bmatrix} + \begin{bmatrix} -1.40 \\ 1.76 \\ 0.516 \\ 0.173 \\ 0.162 \end{bmatrix} \left[\Delta \delta_E\right]$$

$$y(k) = CX(k) + Du(k)$$

$$y(k) = \begin{bmatrix} 0 & 0 & 0 & 0 & 1 \end{bmatrix} \begin{bmatrix} \Delta U \\ \Delta W \\ \Delta Q \\ \Delta \Theta \\ \Delta h \end{bmatrix}$$

Equation 5.3: Discrete-Time State Space Representation of Longitudinal System

Lateral

$$X(k+1) = \Phi X(k) + \Gamma u(k)$$

$$\begin{bmatrix} \Delta V \\ \Delta P \\ \Delta R \\ \Delta \Phi \\ \Delta \Psi \end{bmatrix}(k+1) = \begin{bmatrix} 0.46 & -0.03 & -0.41 & -0.27 & 0 \\ -0.71 & 0.27 & 0.39 & 0.19 & 0 \\ 1.57 & -0.10 & 0.35 & -0.31 & 0 \\ -0.31 & 0.31 & 0.10 & 1.04 & 0 \\ 0.51 & -0.03 & 0.42 & -0.06 & 1 \end{bmatrix} \begin{bmatrix} \Delta V \\ \Delta P \\ \Delta R \\ \Delta \Phi \\ \Delta \Psi \end{bmatrix} + \begin{bmatrix} -0.01 & 0.29 \\ 0.80 & 0.08 \\ -0.11 & -0.88 \\ 0.28 & 0.07 \\ -0.02 & -0.29 \end{bmatrix} \begin{bmatrix} \Delta \delta_A \\ \Delta \delta_R \end{bmatrix}$$

$$y(k) = CX(k) + Du(k)$$

$$y(k) = \begin{bmatrix} 0 & 0 & 0 & 1 & 0 \\ 0 & 0 & 0 & 0 & 1 \end{bmatrix} \begin{bmatrix} \Delta V \\ \Delta P \\ \Delta R \\ \Delta \Phi \\ \Delta \Psi \end{bmatrix}$$

Equation 5.4: Discrete-Time State Space Representation of Lateral System

After system discretization it is necessary to again examine system responses to ensure that the digital control system will respond as close as possible to the time domain responses.

5.2 Longitudinal System Responses

5.2.1 Step Response

When discretizing any system it should be expected that the responses should not be altered significantly. Output amplitude variations may be expected however this does not affect the response significantly and can easily be corrected by a simple gain constant. Response time should be the same as in the continuous-time domain. The step for the discretized longitudinal system (with a zero-order-hold (ZOH) and output focussed on aircraft altitude) is shown in figure 5.5, and it can be seen that, as expected it is in the same form of the continuous-time response detailed in the chapter 4.

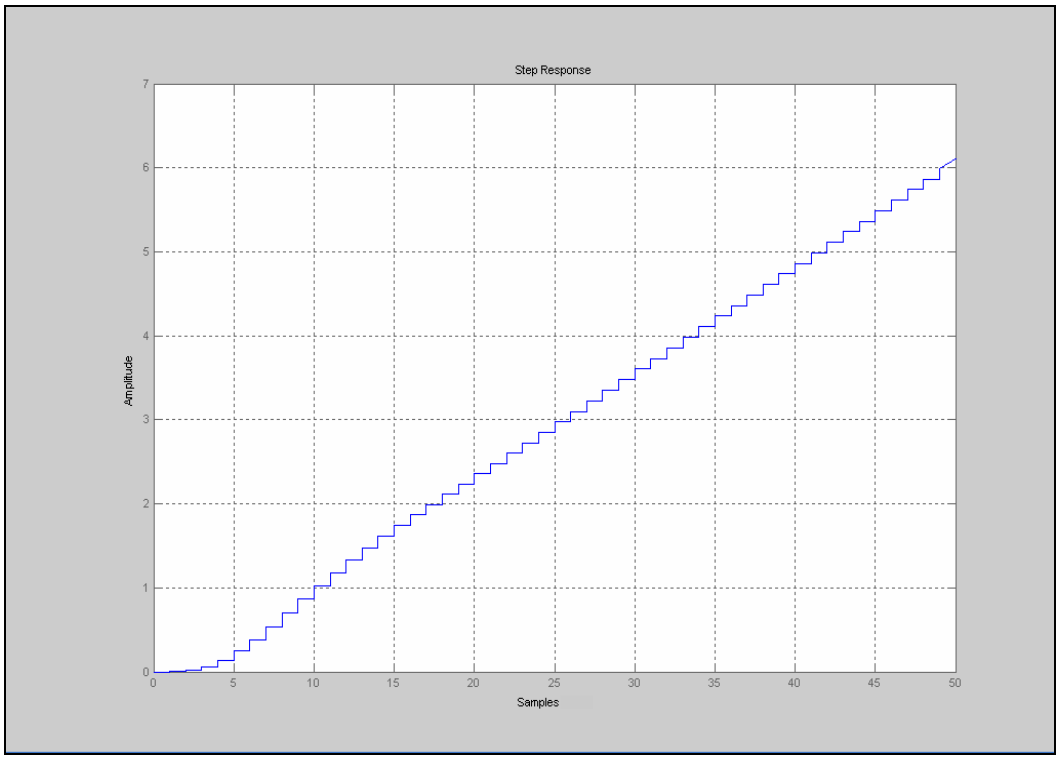

Figure 5.3: Step Response ('C' focus - Altitude) of Discretized Longitudinal System

Similarly, figure 5.6 details the expected step response of the dicretized system with regards to pitch angle.

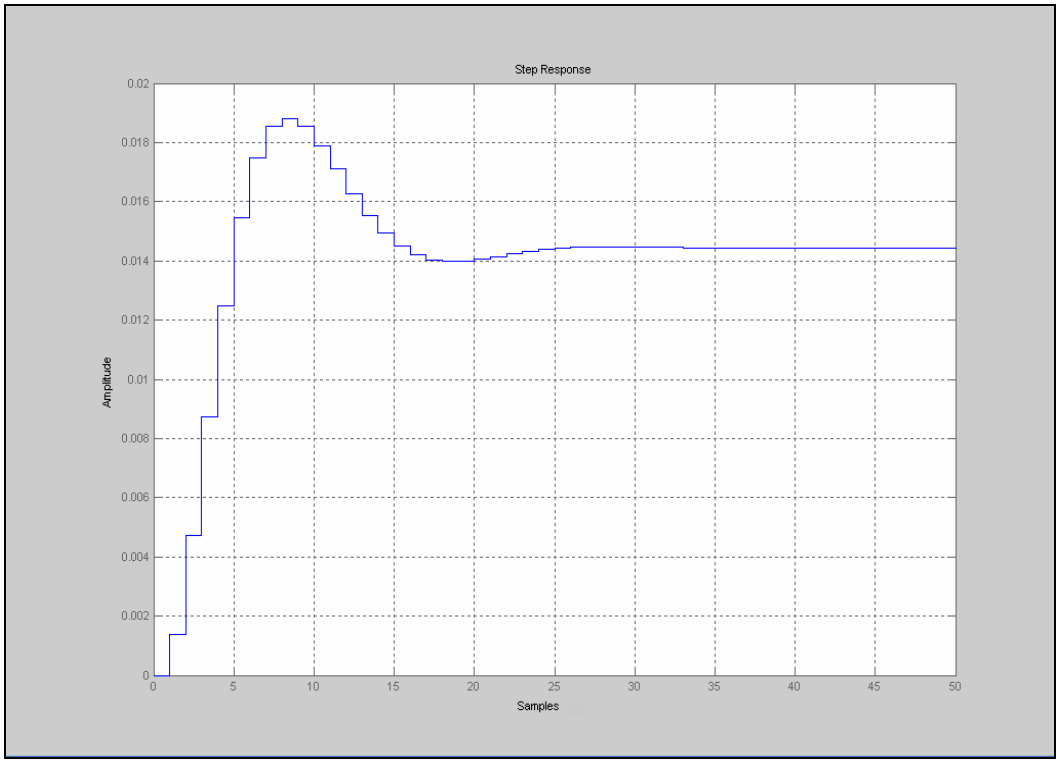

Figure 5.4: Step Response ('C' focus – Pitch Angle) of Discretized Longitudinal System

5.2.2 Impulse Response

Figures 5.7 and 5.8 detail the impulse responses for the altitude and pitch angle of the discretized longitudinal system respectively. Again, these are similar to the continuos-time responses.

All of the longitudinal responses are performing as expected. This indicates that by discretizing the system, the aircraft will continue to respond adequately (in the longitudinal axis) to control inputs. It can also be seen from figures 5.5 to 5.8 that timing issues (such as settling times, rise times etc) are identical to the continuous-time simulations. Conversion is of course required from number of samples to time, however analysis of this conversion (not shown) shows that timing hasn't been altered.

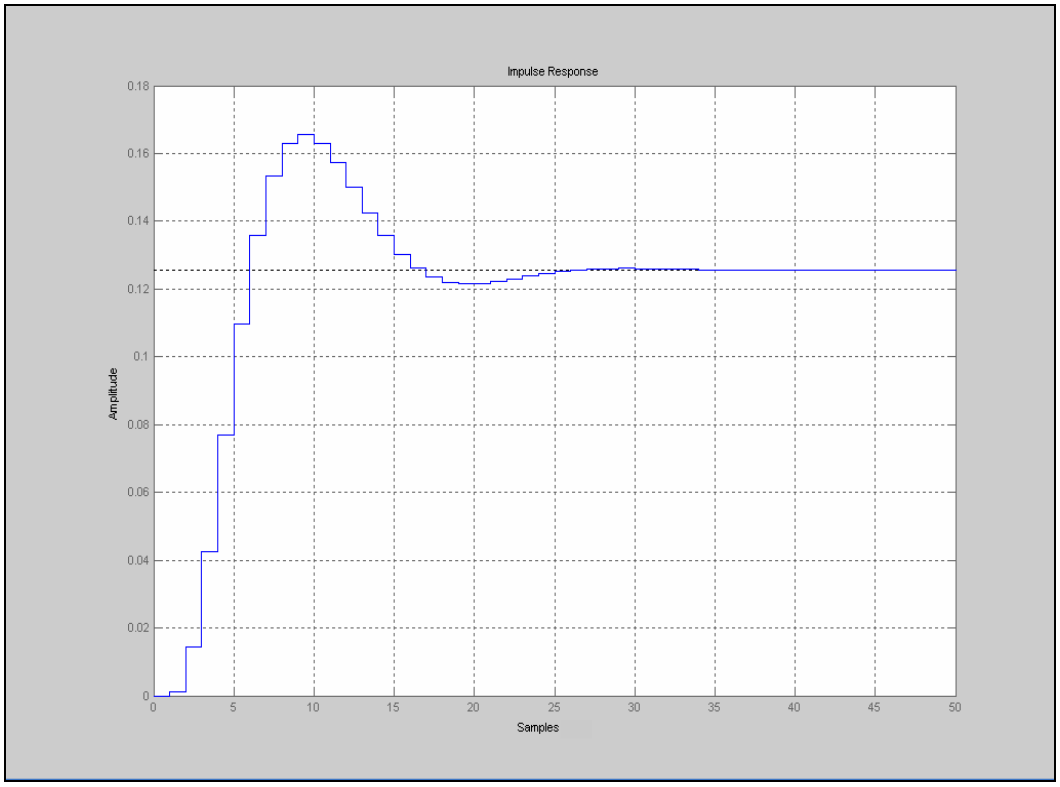

Figure 5.5: Impulse Response ('C' focus - Altitude) of Discretized Longitudinal System

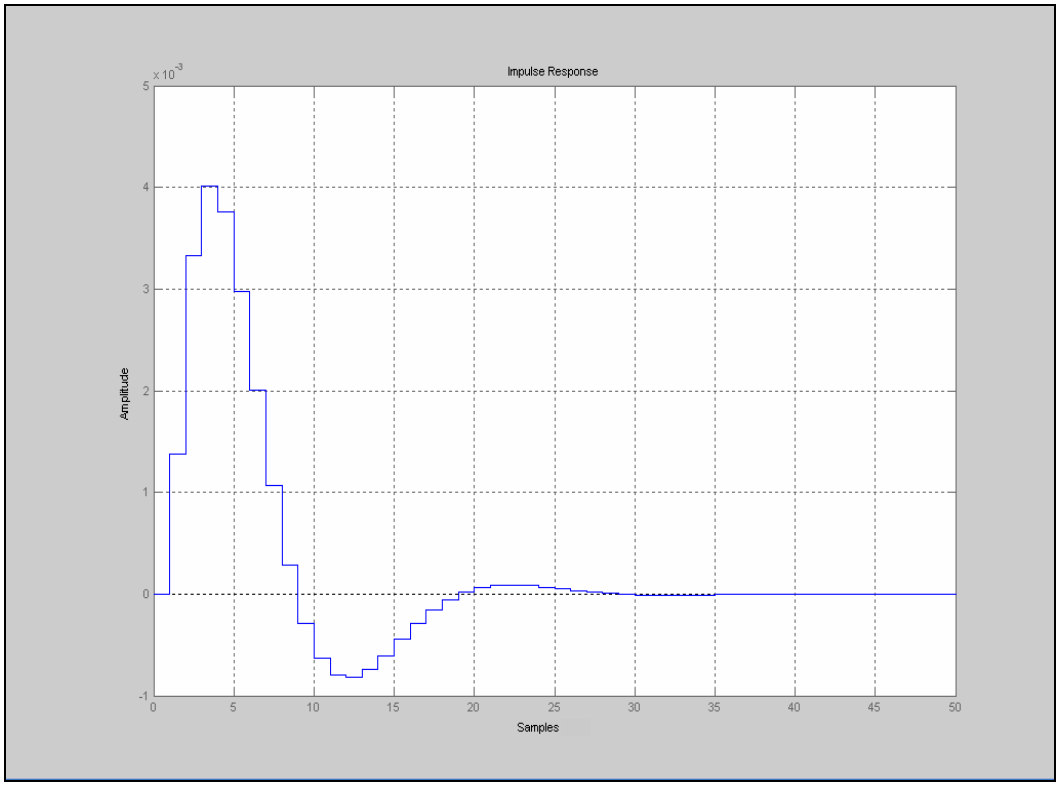

Figure 5.6: Impulse Response ('C' focus – Pitch Angle) of Discretized Longitudinal System

5.3 Lateral System Responses

5.3.1 Step Response

Again there is no expected variation between the discrete-time and continuous-time lateral responses (excluding amplitudes as discussed earlier). The step responses of the discretized lateral system are shown in figures 5.9 and 5.10. These simulations have been divided to allow for expansion of the x-axis in order to display a similar time base to that of the continuous-time simulations.

The sample points in these responses are difficult to distinguish simply because of the number of samples required to achieve a similar time base to that of the continuous-time simulations. These figures indicate that the step responses of the discrete-time lateral system are adequate.

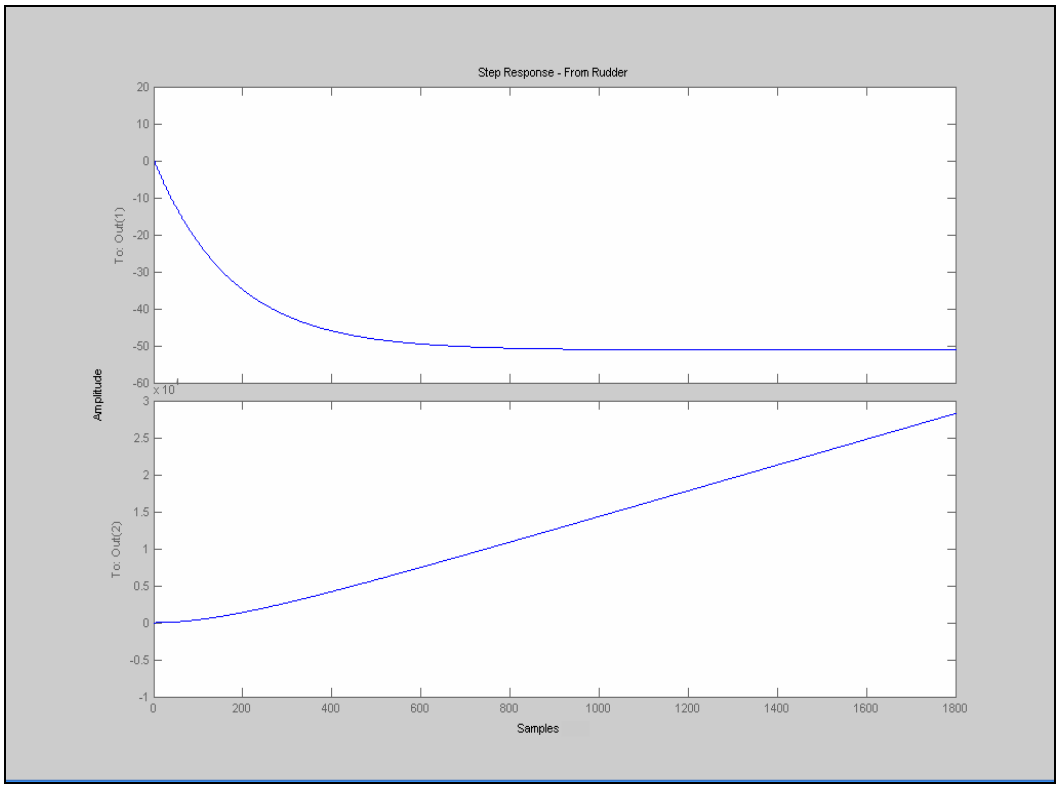

Figure 5.7: Step Response of Lateral System (Input – Rudder)

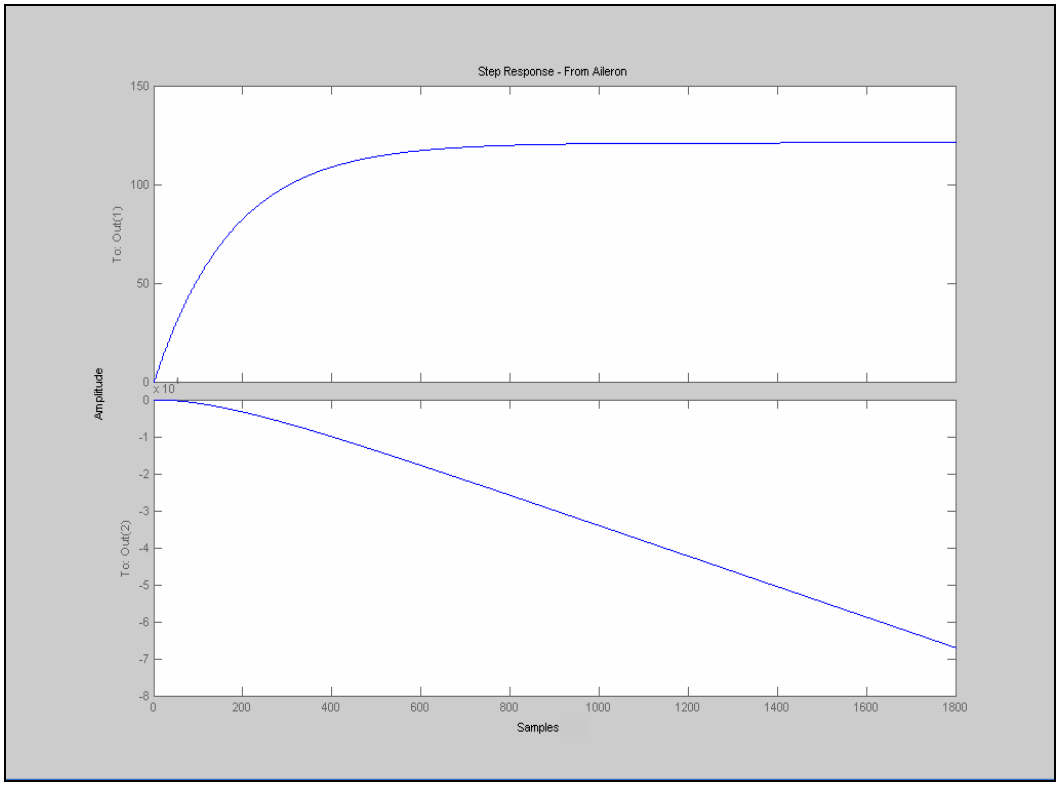

Figure 5.8: Step Response of Lateral System (Input – Aileron)

5.3.2 Impulse Response

Figures 5.11 and 5.12 outline the impulse response characteristics for the discrete-time lateral system.

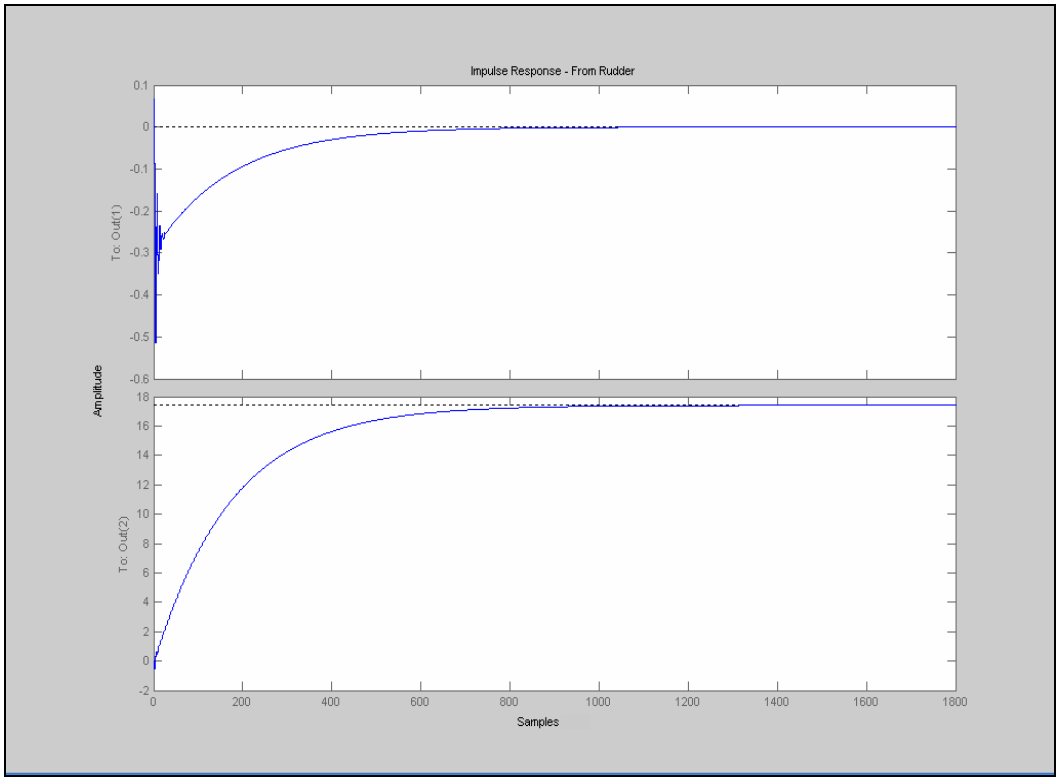

Figure 5.9: Impulse Response of Lateral System (Input –Rudder)

Figure 5.11 indicates some initial oscillations in the early stages of the rudder to roll system. This is not a significant problem for this project due to the inherently stable nature of the aircraft chosen. If a more traditional control method was being employed, the introduction of state feedback and possibly a state observer system would reduce these oscillations. State feedback is basically a manual pole placement technique that allows the designer to choose pole locations for a desired response and force the system to exhibit that response. This process will not be outlined in this dissertation, however should a future project wish to design a more conventional control system; all previous design and simulation information would provide a useful starting point for the implementation of a state feedback regulator and state observer.

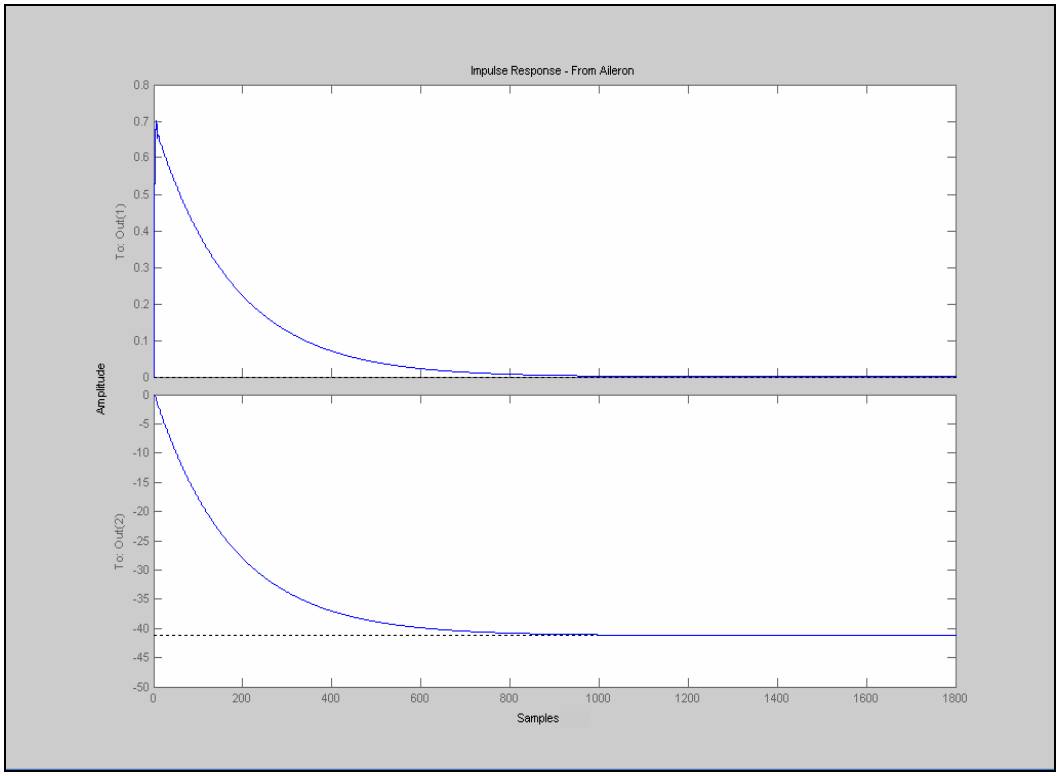

Figure 5.10: Impulse Response of Lateral System (Input – Aileron)

Overall, all responses in the discrete-time domain are sufficiently matched to those in the continuos-time domain. As stated earlier, all of these simulations will provide a good estimation of the system response and will help evaluate the timing needs of the intuitive control method being employed for this project. Future continuing projects may find it useful to take the analysis of chapters 2 to 5 and simply continue with designing a more conventional state feedback controller.

Chapter 6 Hardware Selection and Implementation

6.1 Microcontroller

The microcontroller is the heart of any control application and must provide the necessary computing power to handle complex control algorithms. For this project the Card 12, HC12 controller module with MC912D60A microcontroller has been selected primarily due to availability, ease of programming and input/output features. The ‘D60A is a member of Freescale’s (formerly Motorola’s) HC12 Microcontroller family (Elektronicladen, 2005). This module comes equipped with a version of TwinPEEKs monitor software which allows easy downloading and programming of Flash and EEPROM Memory without the need for additional programming hardware (Elektronikladen, 2005). The features of the HC12 controller module are summarised in table 6.1.

Characteristic	*Specification*
Power Supply	5 V
Typical Power Consumption	50 mA
Processor (CPU12)	16 bit
External Clock	16 MHz
System Clock	8 MHz
Flash EEPROM	60K bytes
EEPROM	1K byte
RAM	2K bytes
Asynchronous Serial Communication (SCI)	2 channels
Serial Peripheral Interface (SPI)	1 channel
Input Capture / Output Compare Timer	8 channels
A/D Converter	16 channel / 10 Bit
Pulse Width Modulator (PWM)	4 channels

Table 6.1: MC912D60A Technical Specifications (Motorola, 2000; Elektronikladen, 2005)

One of the primary features of the HC12 that will be utilised in the software stages of this project is the Enhanced Capture Timer, utilising the input capture/output compare channels. This basic timer consists of a 16-bit, software-programmable counter driven by a prescaler. The timer can be used for many purposes, such as input waveform measurement and generation of output waveforms (Motorola, 2000). These two uses will be critical in sensor decoding and aircraft servo motor control.

6.2 Aircraft

The aircraft initially chosen for this project was the GW/Slow Stick EPS300C Park Flyer. This aircraft is a mass produced electric powered aircraft it has a wingspan of 1.2m (Grand Wing Servo-Tech, 2005). It was initially considered because it was simple inexpensive and robust. Also it is an inherently stable aircraft which means if all control surfaces are trimmed correctly it will continue to fly straight without continual input from the control surfaces (Byrne, 2005). The power system has been upgraded since previous projects to a brushless motor and controller and a 1200mah 11.1 volt lithium polymer battery (Byrne, 2005) to increase power so as to carry heavier payloads. The technical specifications of the aircraft are summarised below in table 6.2.

Parameter	*Specification*
Length	954 mm
Wingspan	1176 mm
Wing Area	32.64 cm^2
Flying Weight	405 - 440 g
Wing Loading	12.4 – 13.5 g/cm^2
Radio	2 – 4 channel

Table 6.2: Aircraft Technical Specifications

Despite the power system upgrade it is still doubtful that the Park Flyer will be able to provide the required payload capacity of control and sensory equipment. Alternatives have been explored, with the simplest solution being the procurement of a larger aeroplane. However due to budgetary constraints this was not a feasible option for this project and therefore a prototyping aircraft could not be procured. Other testing alternatives considered included the use of a remote controlled helicopter; however it should be noted here that helicopter dynamics vary from that of an aeroplane, and therefore the analysis outlined in chapters two to five of this dissertation will not apply to a helicopter based UAV system.

6.2.1 Transmit/Receive Remote Signal Routing

One of the primary design features that incorporates the aircraft into the system is the ability to route the existing transmit (Tx) and receive (Rx) signals from the remote control unit through the HC12. Tx and Rx signals are in the form of pulse width modulated (PWM) outputs for each control surface of the aircraft (elevator, rudder and aileron depending on the aircraft). Essentially, coding for this element of the project was completed after coding was developed for servo motor control and accelerometer PWM decoding (see sections 4.2.1 and 4.3.1 respectively). Tx and Rx routing is basically a combination of these two elements of coding. Basically, the PWM high/low transitions need to be identified and conveyed to the servo outputs. There is no need to record timing information as with the servo control and accelerometer decoding methods as the output required (servo pulses) is identical to the input received (Tx/Rx pulses). Figure 6.1 summarises the process of Tx/Rx signal routing through the HC12, with the actual algorithm shown in appendix D(a).

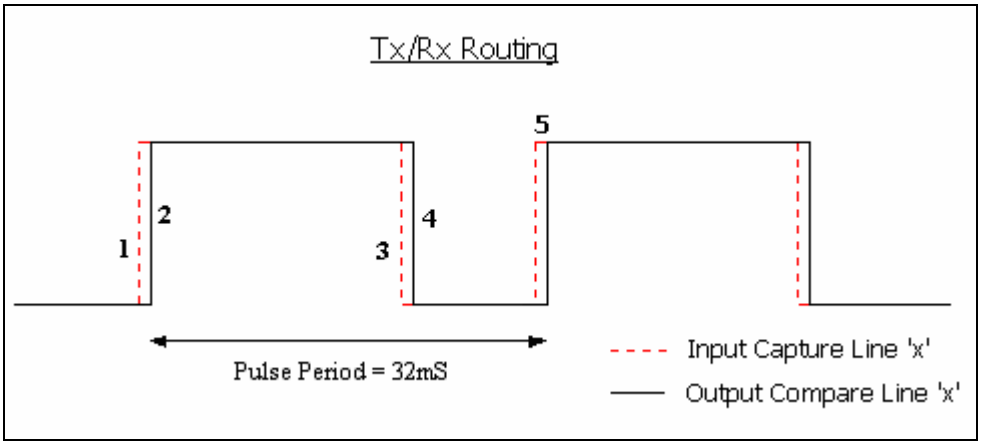

Figure 6.1: Tx/Rx Routing Through the HC12

The steps to instigate the transitions numbered one to five in figure 6.1 are detailed below.

(1) The Tx/Rx signal transition '0' – '1' is detected using the input capture feature of the HC12.

(2) The '0' – '1' transition identified is immediately mirrored by the output compare line designated to control a servo.

(3) The Tx/Rx signal transition '1' – '0' is detected.

(4) The '1' – '0' transition identified is again immediately mirrored by the output compare line designated to control a servo.

(5) Process repeats.

The time lag between the identification of the transitions by the input capture channel and the conveying of the transition to the output compare line will be in the order of tenths of microseconds and therefore will not be a significant problem.

6.2.2 Servo Motor Control

One of the primary control applications related to the aircraft itself is the need to communicate with the servo motors. Servo motors are small DC motors that essentially provide the interface between the user and the control surfaces of the model aircraft (elevator, rudder, ailerons etc). These motors operate via a PWM signal, with the duty cycle of this signal determining the angular position of the

servo. The angular range of the servo spans 180^o (90^o either direction from centre).

Because the control system detailed in chapter three essentially bypasses all original manual remote controls through software, it was necessary to develop a program to generate the required PWM signal for servo control. This program, shown in appendix D(b), was developed in assembly language and utilises the real time interrupt (RTI) and output compare (OC) features of the HC12. Essentially the program creates a pulse every 32mS (a desirable value for servo control), with the pulse width controlled as shown in figure 6.2 below.

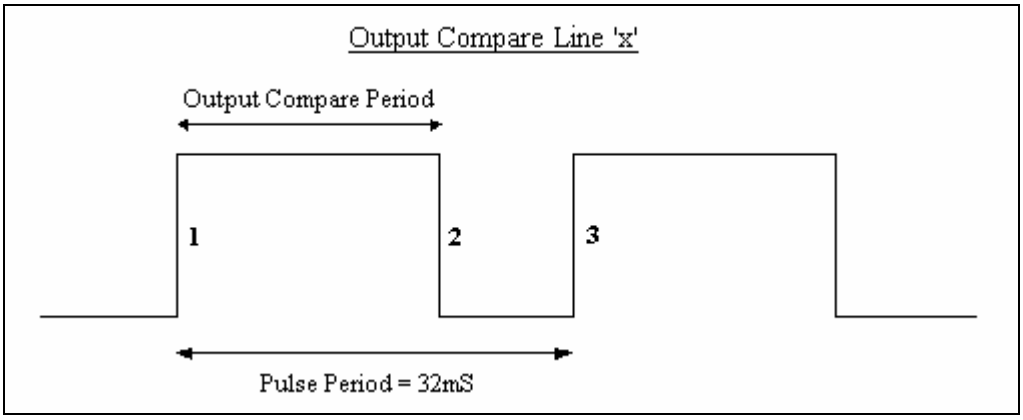

Figure 6.2: Servo Control Theory

The steps to instigate the transitions numbered one to three in figure 6.2 are detailed below.

(1) At the beginning of each RTI service routine (after an RTI has been registered) the OC line is forced ‘high’.

(2) The OC line remains ‘high’ until the Enhanced Capture Timer (ECT) value is reached (ultimately defined by the user and ultimately controls the duty cycle). When a successful compare occurs (the ECT reaches the user defined value) the OC line is forced ‘low’.

(3) Another RTI is recorded after 32mS and the pulse generation begins again.

For the servo to be centred (essentially 0^o rotation), a pulse width of approximately 1.5mS was needed. Figure 6.3 summarises the finer details regarding pulse width and level of angular control.

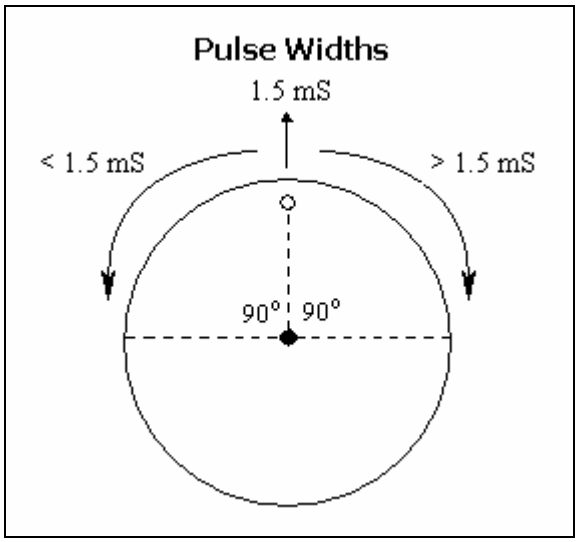

Figure 6.3: Servo Limitations

From practical testing by inputting an arbitrary pulse time delay, it was found that for a servo movement of 1^o, a pulse width variation of approximately 9.55 µS was required. Using this information it becomes possible to completely control the servo motor, within its 180^o range, to an accuracy of approximately 1^o.

6.3 Sensors

Attitude sensors are arguably the most important part of any motion control system, whether it be terrestrial, aquatic or air based. Without such sensors autonomy would be impossible. The primary function of any sensor is to provide information relating to the attitude of the object (in this case the aircraft). In a flight control system these attitudes can include pitch, roll, yaw, velocity, altitude and position in space. Table 6.3 provides a summary of the sensors that will be incorporated in this project and their function (note that the compass module and the GPS system are beyond the scope of this project and are discussed in "Navigation and User Interface" (Knox, 2005).

Sensor	*Type*	*Function*	*Specifications*
Analog Devices ADXL213	2-axis Accelerometer	Provides 2-axis tilt sensing for pitch and roll	Static acceleration measurement range of ± 1.2g
Vector 2x Electronic Compass Module	Compass Module	Provides heading information	• Accuracy = 2^{o} • Low power • 3-wire serial output format (SPI)
Garmin GPS 35LP	Global Positioning Unit	Provides position, altitude and velocity information	• Compact Design • Low power • RS-232 Serial connectivity

Table 6.3: Sensor Information Summary

6.3.1 Accelerometer

The accelerometer unit is fundamental to the control of the aircraft as it provides information relating to roll and/or pitch and/or yaw attitudes (with the number of measurement axes depending on whether the unit is capable of dual or tri axis measurement). The ADXL213 accelerometer that has been chosen for this project is a simple dual axis sensor and is therefore restricted to two axes of measurement (in this case pitch and roll attitudes). This unit has been chosen essentially due to cost and availability. The determination of yaw information is carried out using an electronic compass module (Knox, 2005).

The operation of the ADXL213 accelerometer module relies on a micro machined polysilicon structure suspended with polysilicon springs over a silicon wafer. Deformations in the polysilicon structure modulate a pulse width modulation (PWM) oscillator which produces either a duty cycle axis output or analogue outputs from filtered demodulation channels. The deformation of the structure may come from a physical acceleration of the IC, or from gravity when angularly displaced from a horizontal position (MacQueen, 2002).

For this project it was decided that the duty cycle output of the accelerometer would be most useful and most accurate. To decode these signals using the HC12, the input capture feature of the microcontroller was utilised. Input capture operates by essentially capturing the value of a 16 bit free running timer module

in the event of a successful transition event. The transition event can be either high-low or low-high, as determined and set by the user. The decoding of the pulse width modulated signal is summarised by figure 6.4, with the actual algorithm shown in appendix D(c).

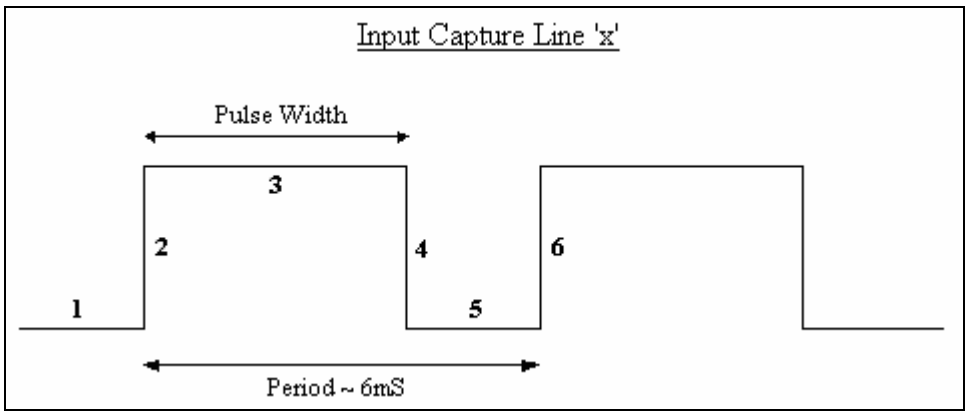

Figure 6.4: PWM Decoding Theory

The steps that occur at the instants numbered one to six in figure 6.4 are detailed below.

(1) Input capture channel is set to capture on rising edge.

(2) Timer is captured with the occurrence of a rising edge and the timer value is stored to memory.

(3) Input capture channel is set to capture on falling edge.

(4) Timer is captured with the occurrence of a falling edge and calculation of pulse width is conducted immediately with the result stored to memory. (ie "Time 2" – "Time 1").

(5) Input capture channel is set to capture on rising edge.

(6) Timer is captured with the occurrence of a rising edge and calculation of period is conducted immediately (using value from first capture) with the result stored to memory. (ie "Time 3" – "Time 1").

The immediate calculation of required fields is achievable due to the timing characteristics of the process. The period of the PWM pulse (as determined by the accelerometer configuration) is far large enough to allow for this calculation. The actual capture timer of the microcontroller increments at a rate of 8MHz, which indicates that one full 16 bit timer cycle (0000 – FFFF) will take

approximately 8.19 ms. It was a concern that rollovers from FFFF – 0000 by the main timer counter would affect the calculations, however the HC12 accesses each timer value as a single 16 bit word, hence signs are not an issue.

The decoding of the accelerometer signals results in an error value that is proportional to the amount by which the aircraft's pitch and roll are away from zero (where zero error indicates level flight). These figures (one each for pitch and roll) will be used as comparison values to an ideal state, where the ideal state depends on whether or not the aircraft is required to be turning or simply flying straight and level. To determine these allowable constraints, it is necessary to analyse the output data from the accelerometer decoding to determine maximum and minimum error values. Obviously it is not desirable to allow the aircraft a full 180^{o} of roll or pitch freedom about its level flight condition; therefore constraints need to be decided upon. Figure 6.5 summarises the results of this constraint analysis for both axes. Note that whilst pitch and roll are measured on separate accelerometer channels, the results are identical as the measurement range is identical in each axial plane ($\pm 1.2g$).

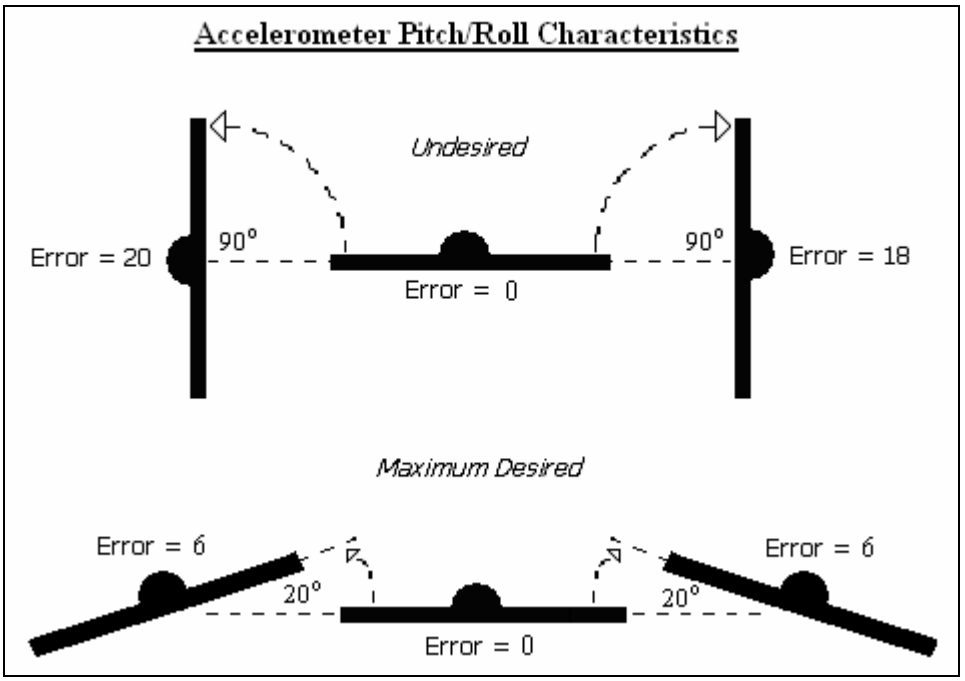

Figure 6.5: Accelerometer Pitch and Roll Error Measurement Characteristics

When tested to obtain the above readings, the accelerometer was mounted on slight angles to ensure that an error of zero was recorded for 0^{o} roll (and pitch). It

will also become necessary to mount the accelerometer in this manner when installing the sensor into any prototyping aircraft to ensure that level flight is indeed acknowledged by the control system as being "level flight". From figure 6.5 it appears that the mounting angle does not tend to affect the error value over small angular ranges (ie within the desired roll/pitch constraints). A discrepancy does appear however for larger angular values as denoted by the maximum achievable roll of 90^{o}. This calibration issue could possibly be due to an internal IC calibration error, a PCB mounting error, or perhaps even a software rounding error (more likely a combination of the three). This problem should not be significant as it appears that up to the designated roll constraints of approximately 20^{o}, the errors in either direction appear identical. Hopefully in the process of constraining the roll and pitch of the aircraft, large angular errors will not be experienced and therefore the problem will be minimised.

6.4 Manual Handover/System Monitoring

System monitoring is a built in device aimed at allowing automatic handover from pilot to controller and vice versa. System monitoring will also include circuitry to monitor the status of the HC12 to ensure that the controller is functioning. If the controller were to fail in any way, the system monitoring circuit would automatically revert to manual pilot control. This is an important added safety feature and is not in essence critical to the project. Manual/autonomous transition and autonomous/manual transition is however an important feature that must be incorporated into any prototype.

As a prototype will not be developed for this project, a manual handover circuit will not be constructed; however a proposed layout and design will be included for future reference. Figure 6.6 shows a general block diagram of the proposed manual handover/system monitoring hardware.

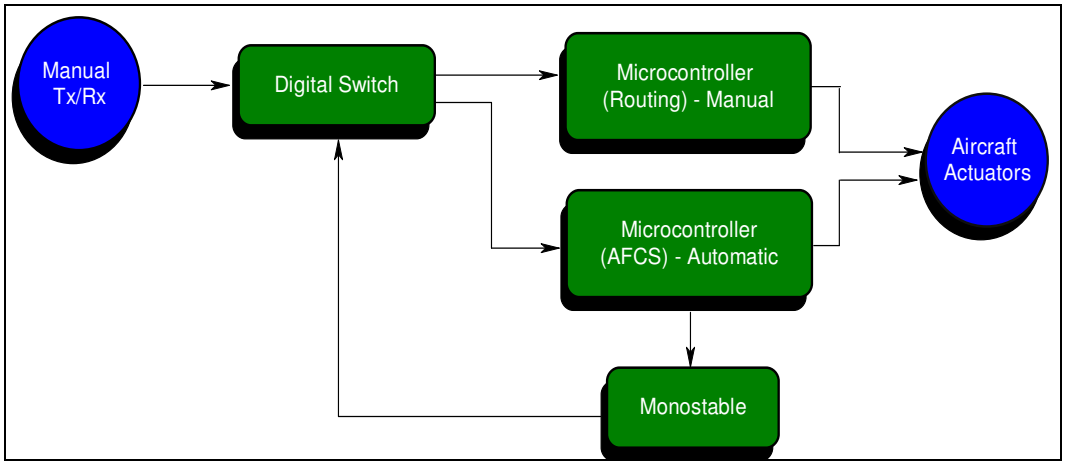

Figure 6.6: Block Diagram of Proposed Hardware

Basically, the digital switch allows for selection of either manual or automatic control of the aircraft through the microcontroller. The system monitoring circuit consists of a simple monostable arrangement where a periodic pulse is sent to the monostable by the AFCS to indicate that automatic systems are operational. The monostable will continue to generate an output pulse as long as it is receiving the periodic input from the AFCS. This output pulse will be used by the switch to maintain its "automatic control" setting. If the AFCS were to become corrupted or fail in any way, the periodic output pulse would cease, thus halting the monostable output and reverting the switch automatically back to manual control (with appropriate warning generation to the user interface).

The monostable can simply be a general purpose 555 timer configuration such as that shown in figure 6.7, or a similar arrangement such as a 74LS123 Retriggerable Monostable Multivibrator.

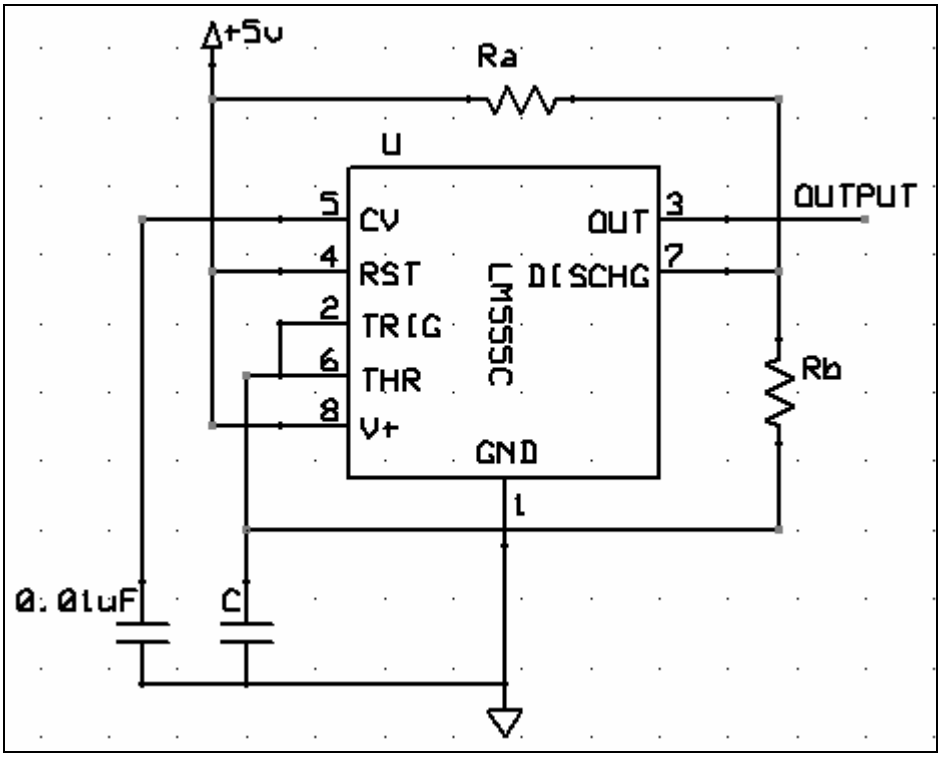

Figure 6.7: 555 Timer Monostable Circuit Arrangement

Similarly, the digital switch shown in figure 6.6 could basically be a "trigger unit" where either a logic '0' or logic '1' is generated depending on an input signal received. The output from this switch can be used to control a hardware interrupt whereby the service routine would most likely be set to manual control (simply calling on the Tx/Rx routing algorithm). Due to the critical nature of this handover feature, the Non-Maskable Interrupt Request ($\overline{XIRQ}$) pin on the HC12 microcontroller is recommended. The $\overline{XIRQ}$ is an updated version of the non-maskable interrupt ($\overline{NMI}$) input of similar MCUs (Motorola, 2002), and will allow for the necessary priority to handle the critical task of automatic/manual in-flight transitions.

Whilst this hardware has not and will not be constructed for this project it utilises only simple electronics and should not be difficult to develop for future work.

Chapter 7 Intuitive Control and Pre-Flight Testing

7.1 Intuitive Control versus Conventional Control

As touched upon in chapter three, an intuitive "observe-and-correct" control system will be implemented based on simple inner loop and outer loop control principles. This method was chosen primarily due to the simplicity of the model aircraft system, but more importantly the lack of available data relating to the stability analysis of a model aircraft. Some limited model aircraft stability derivatives were available for the longitudinal system, however no similar derivatives could be found for the lateral system. If this data could be discovered or derived (through wind tunnel testing of a model aircraft) it is recommended that a more conventional approach be taken towards the design of the AFCS. All system plant data is available in chapters two and three of this dissertation, and will not vary significantly between aeroplane types. With more accurate stability derivatives, PID control techniques or a suitable alternative are recommended.

7.2 The Intuitive Approach

Figure 7.1 shows a block diagram representation of the control method being employed as the AFCS for this project.

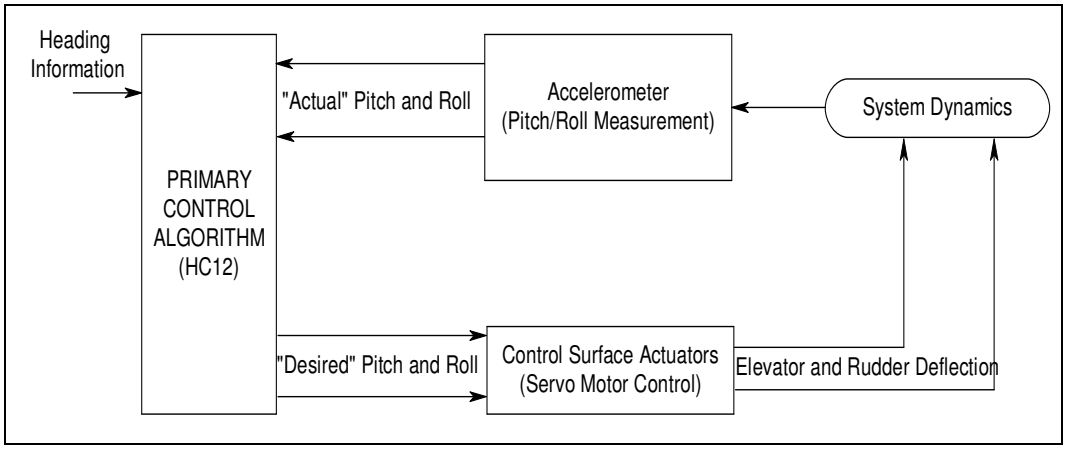

Figure 7.1: Primary closed loop system

Outer loop information (or heading and navigation information) will essentially be passed straight through to the control surface actuator controlling the heading of the aircraft (rudder servo motor). The outer loop's main function is to retrieve heading updates approximately four times per second, and provide the necessary control signal to the rudder to attempt to minimise the heading error. In between these updates, it is the inner loop's task to monitor and maintain the desired pitch and roll based on allocated allowable constraints.

Figure 7.2 shows a process flow diagram detailing the functional aspects of the primary control algorithm.

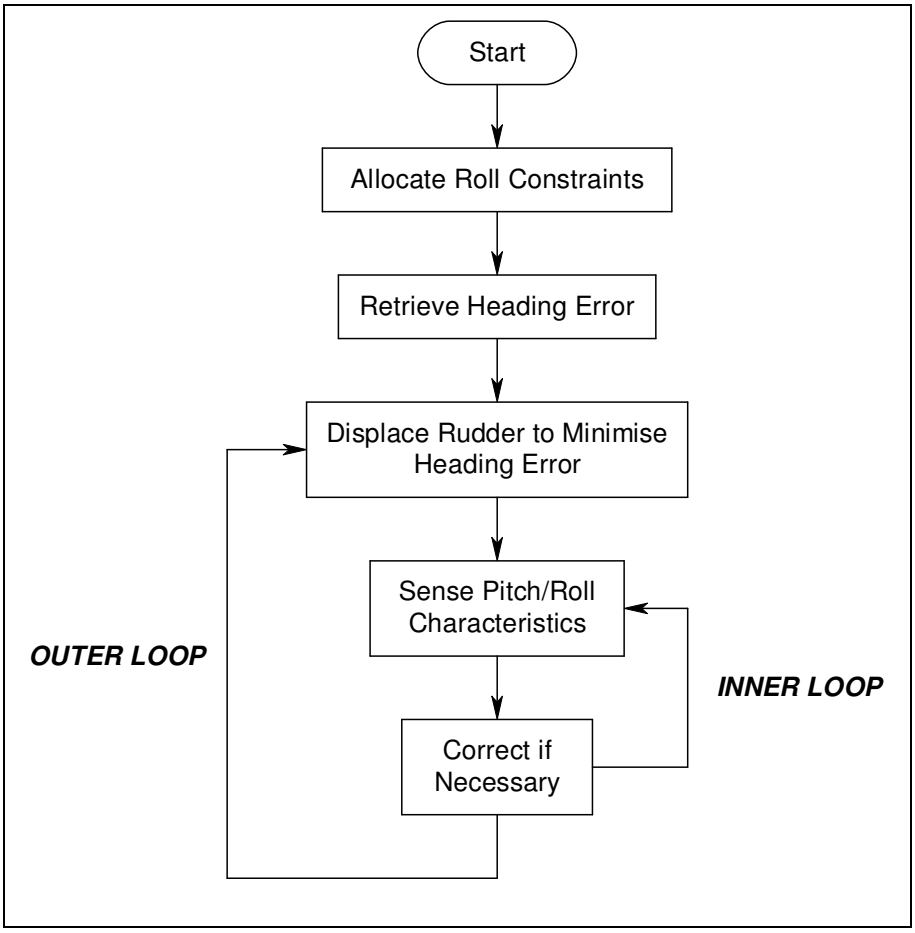

Figure 7.2: Process Flow of Primary Control Algorithm

The heading information is in the form of a scaled integer so as to provide a scaled timing value fed directly to the rudder servo control algorithm. The raw heading information is essentially in the form of $\pm 180^{o}$. This raw information is scaled according to equation 7.1.

$$Scaled\ Heading \quad = \quad 12000 + \left(\frac{1146}{180} * raw\ error \right)$$

Where : $12000 \rightarrow$ Output compare time for centred servo

$1146 \rightarrow$ Maximum allowable rudder deflection (15^{o})

$180 \rightarrow$ Maximum angular range (either side of centre)

Equation 7.1: Heading Scaling

Table 7.1 indicates a range of rudder deflections expected from various raw heading errors. Note that the information in table 7.1 was calculated using equation 7.1.

Raw Heading Error	***Servo Deflection (Output Compare Timer Value)***	***Servo Deflection (Degrees)***
180^o	13146	15^o
150^o	12955	12.5^o
120^o	12764	10^o
90^o	12573	7.5^o
60^o	12382	5^o
30^o	12191	2.5^o
0^o	12000	0^o
-30^o	11809	-2.5^o
-60^o	11618	-5^o
-90^o	11427	-7.5
-120^o	11236	-10
-150^o	11045	-12.5
-180^o	10854	-15

Table 7.1: Scaled Heading Examples

7.3 Roll Constraints

The allocation of roll constraints is used to prevent the AFCS from essentially "fighting" itself during a turn. As mentioned in the aim of the project, the autonomous UAV system is required to fly a specific flight path, and therefore level flight is not the sole requirement of the control system. To navigate a path over a set of defined waypoints, the aircraft will be required to engage in turns in order complete its mission. Turning an aircraft essentially involves some amount of roll. If straight and level flight were the only flight conditions considered, turning would dynamically be quite challenging. Therefore it has been decided that roll constraints will be used and will be determined directly from the magnitude of the heading error. Essentially a large heading error will result in the allowance of the largest amount of roll (20^o in either direction (Byrne 2005)), with a small heading error representing the level flight condition or minimum amount of roll (ideally 0^o).

Table 7.2 summarises the five constraints that have been chosen and the requirements for enforcement of each constraint.

Heading Error	***Servo Rotation Induced (Degrees)***	***Output Compare Timer Count (for Servo Rotation)***	***Maximum Allowable Roll Angle (Roll Constraints)***
0^o - 10^o	0^o – 0.83^o	12000 (centred) – 12000 ± 64.67	0^o
10^o - 30^o	0.83^o – 2.5^o	12000 ± 64.67 – 12000 ± 194	5^o
30^o - 80^o	2.5^o – 6.77^o	12000 ± 194 – 12000 ± 517.3	10^o
80^o - 120^o	6.77^o – 10.16^o	12000 ± 517.3 – 12000 ± 776	15^o
120^o - 180^o	10.16^o – 15.23^o	12000 ± 776 – 12000 ± 1164	20^o

Table 7.2: Roll Constraint Guide

Table 7.2 was developed by basically adapting the five roll constraints to correspond to servo rotation angular limits. In the event that a roll constraint is exceeded, the system will correct by simply reducing the angle of deflection applied to the rudder.

The information shown in table 7.3 was also used within the inner loop function to compare the "actual" tilt errors to the designated constraints. This table shows the expected error for each constraint limit.

Constraint Limit	***Error***
20^o	6
15^o	4
10^o	3
5^o	1
0^o	0

Table 7.3: Expected Errors for Constraint Limits

7.4 Primary Control Algorithm Testing

Because an aircraft was unavailable for testing purposes, an alternate method was required to verify the functionality of the control algorithm. Obviously, the ideal case would be to physically implement the entire system into a prototype UAV, where the system is subject to atmospheric disturbances and dynamics of flight. In this ideal case, issues such as the magnitudes of servo rotation, as well as the

magnitudes of the allowable roll constraints could be tested and "fine-tuning" of the algorithm could be conducted. However, this will be recommended as future work, and for the testing stage of this project, the algorithm will simply be tested without subjecting the system to the dynamics of aircraft flight.

As mentioned earlier, the system is required to control both the pitch and roll of the aircraft. Essentially, the pitch can simply be a "set" level, whereby the aircraft attempts to fly at the same altitude throughout its entire mission. The roll however, as previously stated, essentially results from changes in yaw angle required by the aircraft to complete its mission. This yaw angle, and hence the level of roll required, will be continually changing depending on the current path of the aircraft and its proximity in relation to the waypoint path selected. From this information it can be concluded that the roll axis is essentially the most important axis to consider, and therefore for testing purposes this axis will be the focus. It should be noted here that, the algorithm derived for control of the roll axis (shown in appendix D(d)) can be easily adapted to pitch axis control.

7.4.1 Hardware Setup

The control algorithm, shown in appendix D(d) was developed in assembly language, and is essentially a combination of the applications listed in chapter six, namely accelerometer decoding and servo motor control. The testing was carried out using the accelerometer module and a single servo motor. For angular measurements, a jig (constructed by Terry Byrne from the Faculty of Engineering and Surveying) was used to mount the accelerometer in conjunction with a protractor so that accurate angles of tilt could be measured. The jig used for this testing is shown in figure 7.3.

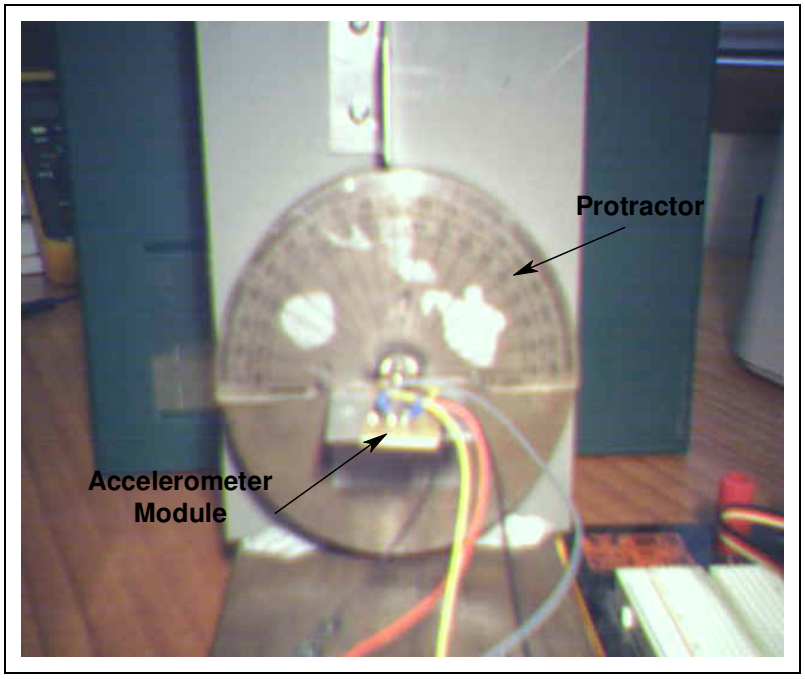

Figure 7.3: Accelerometer Testing Setup

This jig allowed for angular measurements up to $\pm 180^{o}$. When operated in tandem with the accelerometer decoding program shown in appendix D(c), error values for varying tilt angles could be identified.

For servo motor angular rotation testing, a similar setup was used. The servo motor was placed within another jig with a 360^{o} protractor for angular measurement placed above. This particular setup is shown in figure 7.4.

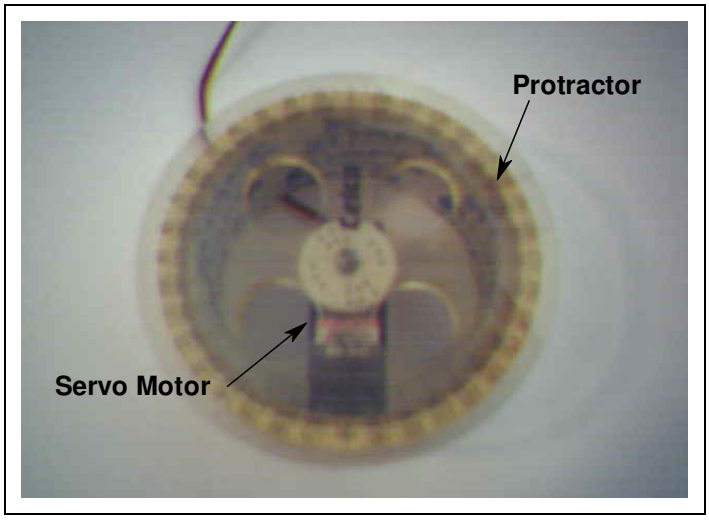

Figure 7.4: Servo Motor Testing Setup

For the final testing of the control algorithm itself, the entire system setup is shown in figure 7.5.

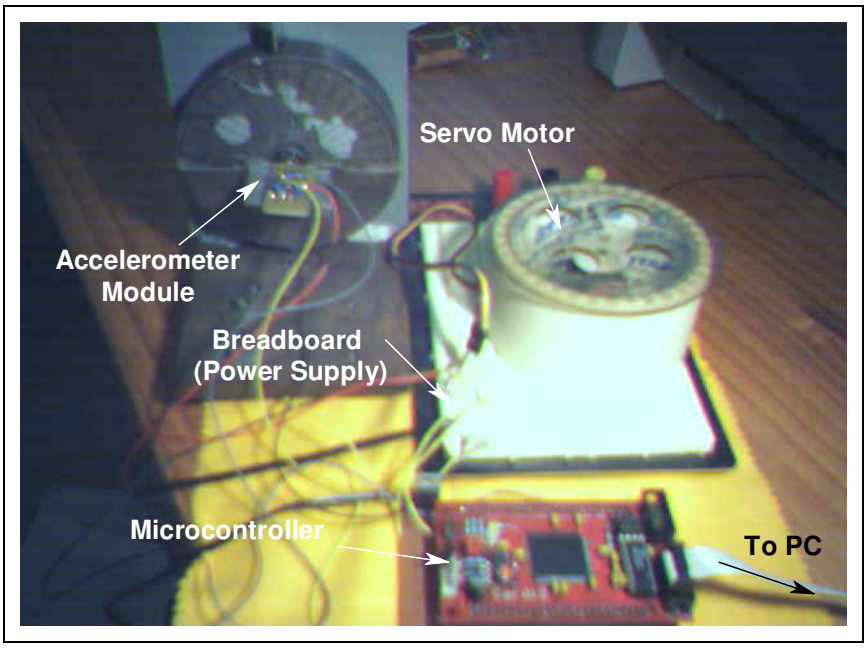

Figure 7.5: Overall Test Setup

The breadboard was used in the testing stage as an intermediate step to remove the need to extensively solder signal and power supply lines to the microcontroller itself. It also allowed for greater flexibility and easy removal or substitution of signal lines for analysis. The microcontroller itself was connected via a serial port to a PC where the TwinPEEKs monitor program was used for programming and monitoring of the unit. This monitor program, together with the code shown in appendix D(e), (written by Terry Byrne of the Faculty of Engineering and Surveying) allowed for easy monitoring of register contents via a hexadecimal to decimal conversion. A screen shot of the output of the accelerometer decoding algorithm is shown in figure 7.6. It shows the two important goals of the accelerometer measurement, which is the relative error between actual tilt and zero tilt, and the direction of that tilt (indicated by either a '1' or a '0' in the MSB of a designated memory location, hence shown as either 000 or 128 when converted to decimal notation).

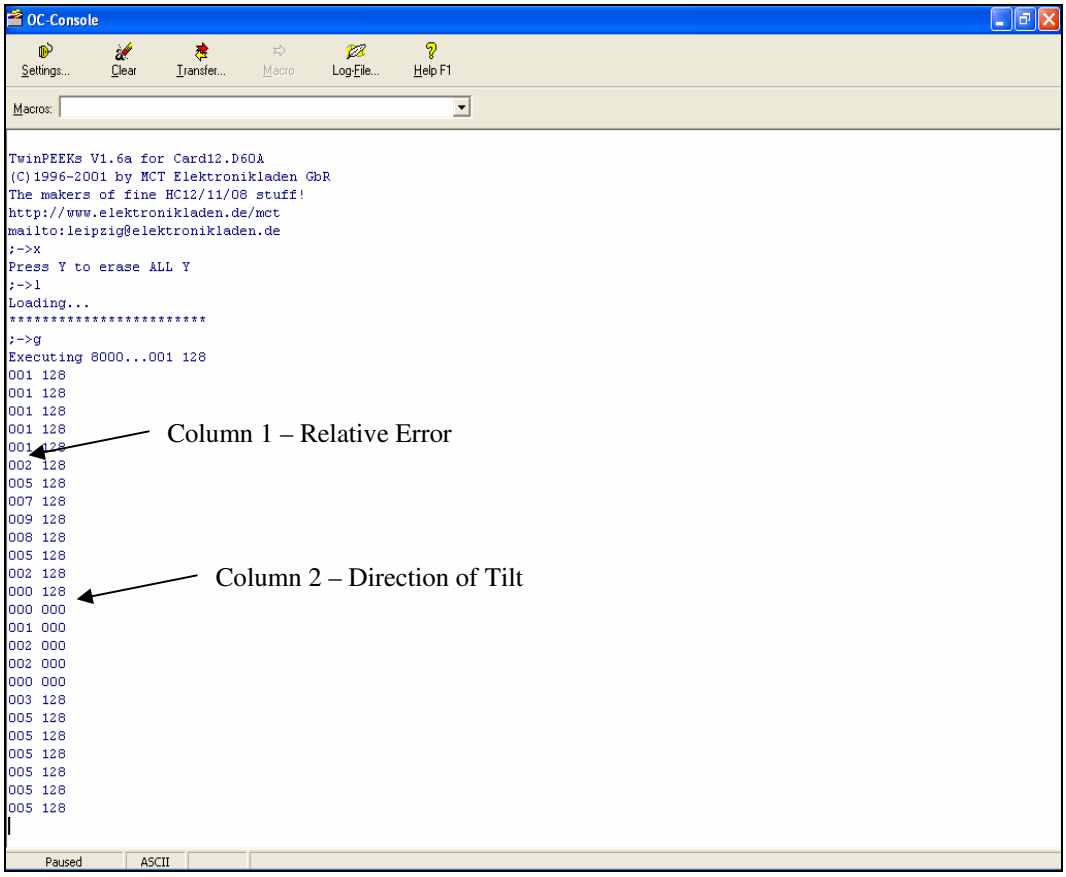

Figure 7.6: Screen Shot of TwinPEEKs Monitor Program

7.4.2 Software Setup

Figure 7.7 shows a software flow chart of the sub-routines that are called upon to provide the necessary control of aircraft roll. The actual coded program is shown in appendix D(d). Note that the outer loop control (heading information) is simply inputted manually for testing purposes. In a realistic flight situation, this value would be updated approximately every 0.25 seconds.

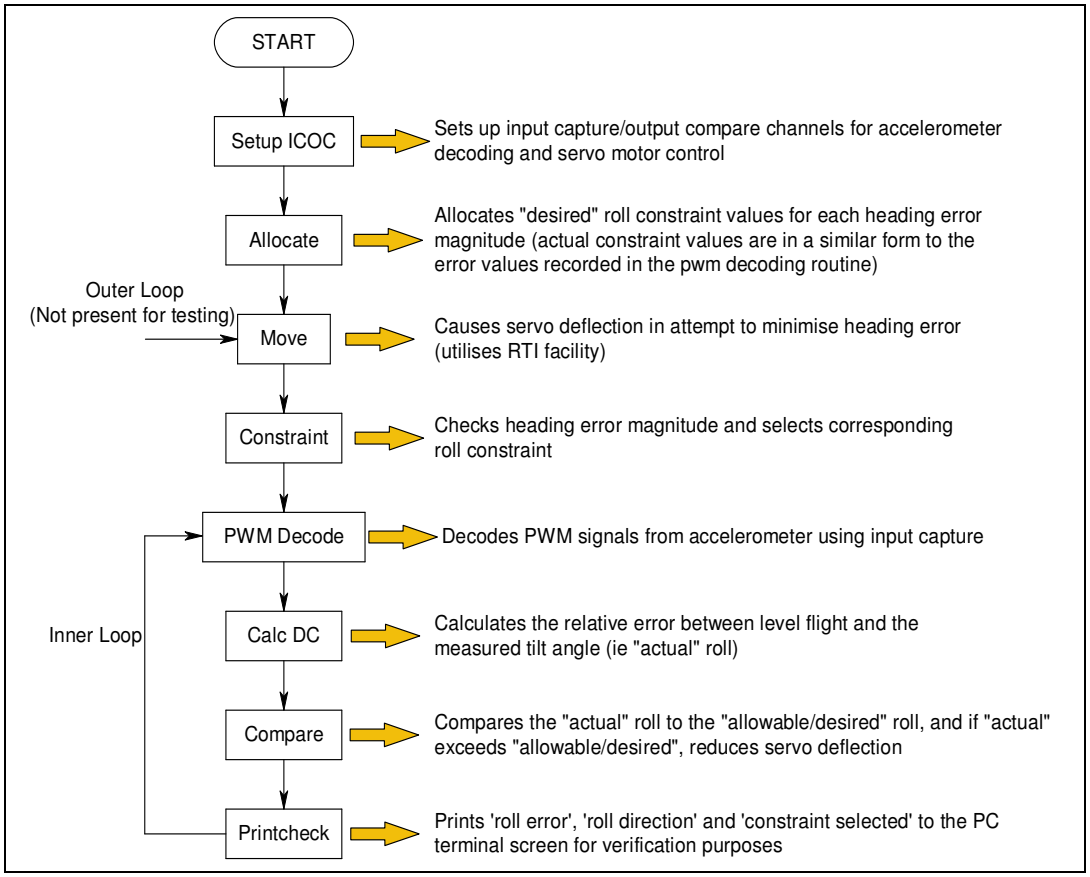

Figure 7.7: Software Flow Chart of Primary Control Algorithm

To test this primary algorithm, a heading value was manually inserted into the required memory location. In a prototype situation this value would be retrieved from communications with the navigation system, at a rate of approximately four times per second. To test all possible situations, the manual input of the heading information was made a number of times with varying magnitudes. With this manual input, the inner loop function will basically just monitor the roll characteristics until process is halted, acting only when the measured roll is outside of the selected constraint.

7.4.3 Test Results

Manually inserted values of heading were chosen carefully so as to ensure all cases of roll constraint were tested. The tests showed that the initial heading information produced the required angular deflection of the servo motor. From this point the accelerometer module was manually rotated using the jig shown above in figure 7.3. The tests concluded that for each constraint value, the servo

motor would remain unchanged from its initial deflection until the constraint angle of roll was reached. Beyond this angular limit, the deflection of the servo motor was reduced by approximately 1^{o} until the roll angle was again brought below the allowable constraint. Overall all values tested appeared to have the desired result.

7.5 Remote Tx/Rx Signal Routing Algorithm Testing

As detailed in chapter six, a requirement of the prototype is to allow for manual control for the take-off and landing sequences. This feature required the routing of remote Tx and Rx PWM signals through the microcontroller. Without an aircraft it was decided that the testing method to be used for this algorithm would be to generate a PWM signal with a function generator and to simply compare the output from the designated output compare channel (used to route the signal) to the PWM input using a dual channel CRO. A screenshot of the test result is shown in figure 7.8.

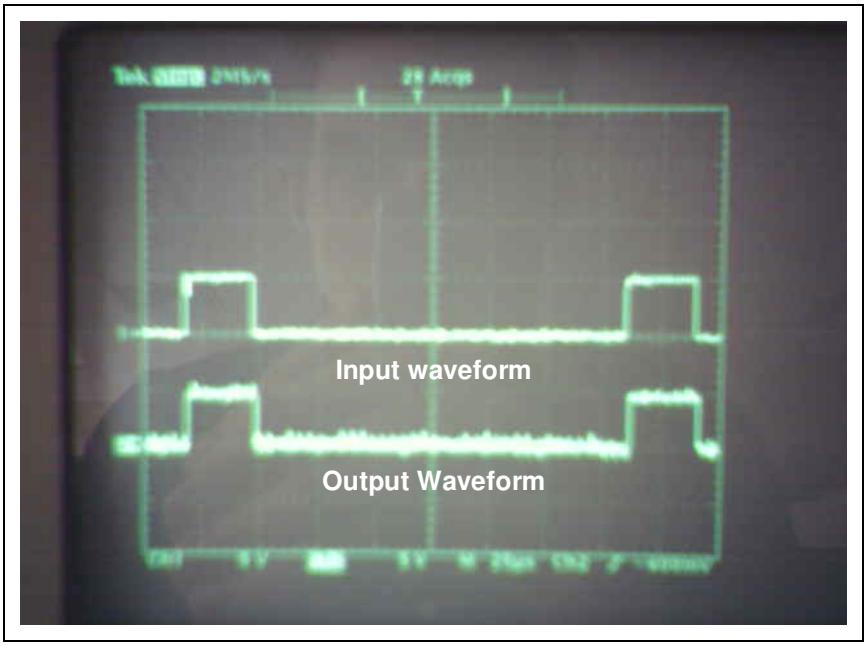

Figure 7.8: CRO Screenshot of Tx/Rx Algorithm Testing

Figure 7.8 indicates that, as expected, the output simply follows the input. The input wave that was generated was made to appear as similar as possible to the actual remote control Tx/Rx signal; that is a voltage level of approximately 0V –

5V and a pulse width of approximately 30ms. As indicated by figure 7.8, the expected output waveform is almost identical to the constructed input.

One difference to note however is the presence of a slight phase offset in the output waveform. As touched upon in chapter six, this phase offset is caused by the time delay in executing the Tx/Rx routing algorithm. To quantify this delay, the horizontal scale on the CRO was changed from its original 25ms per division (as shown in figure 7.8) to 5µs per division (as shown in figure 7.9).

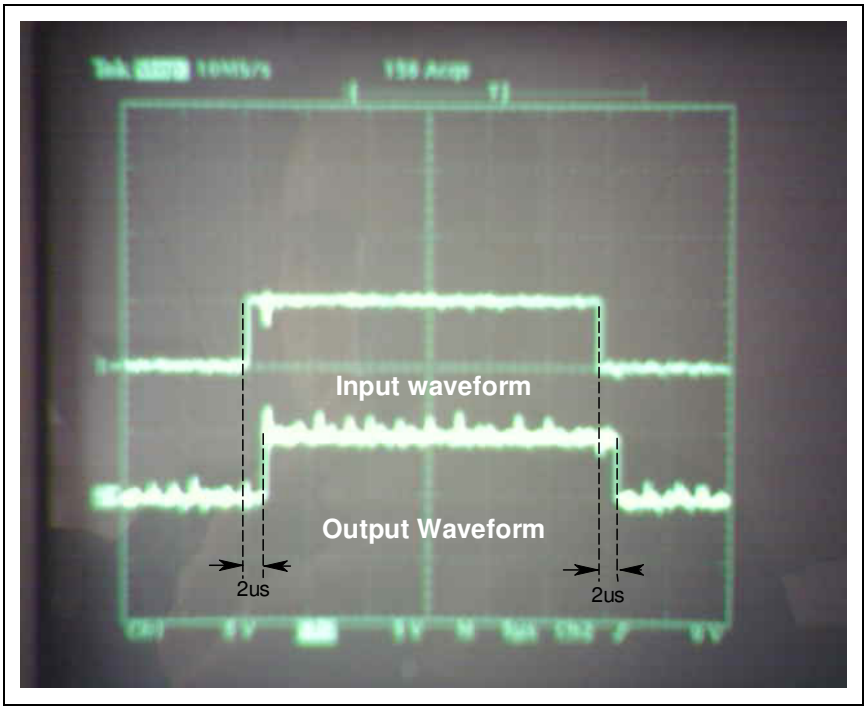

Figure 7.9: CRO Screenshot with Shortened Time Scale

This figure highlights the slight phase shift that is present between the input and the output. This delay is approximately 2µs in length and is not significant enough to produce any error in the desired application of the Rx/Tx routing system. Overall, testing of this algorithm appears to be conclusive that the remote Rx/Tx routing system will operate as required.

7.6 Future Testing

7.6.1 Primary Control Algorithm

The "fine-tuning" of this algorithm as mentioned above is necessary for future progress with this control method. The figures used as limits for servo deflection and maximum allowable roll angle are realistically just guesses based on flight experience with manual control of a remote controlled aircraft. For example the maximum servo motor deflection of 15^{o} chosen as the limit for this project may well be too large, and as such may cause the aircraft to become unstable very quickly. Alternatively, this figure may be too small, and hence result in an excessively large turning radius, thus making navigation difficult. Either way, more analysis needs to be conducted into the dynamics of model aircraft flight. This again reinforces the need for more accurate model aircraft stability data. If this data was known, the analysis of maximum rudder (servo) deflections, as well as maximum allowable roll angles, could be conducted via the MATLAB simulation process detailed earlier in this dissertation. Other "fine-tuning" could also be applied to the servo angle reduction phase of the control algorithm, once outside of the allowable roll range. As mentioned, once the roll becomes too excessive, the servo deflection is currently being reduced by approximately 1^{o}. Again, this may be too low or indeed too high for practical purposes.

7.6.2 Manual Handover and System Monitoring

Whilst this feature has not yet been constructed and can therefore not be physically tested, it is obviously recommended that for future work the designs outlined in section 6.4 of this dissertation should be adequately tested before any physical implementation. This testing should ideally be conducted with the remote controlled unit chosen for a prototype aircraft. However if this is again unavailable, the circuit can also be tested by generating a similar 'handover' signal to what is expected from the remote unit itself. Whilst the algorithm for manual control of the aircraft has been written, the primary control algorithm needs to be added to incorporate this manual feature. As mentioned, the use of

the $\overline{XIRQ}$ non-maskable interrupt feature of the HC12 is recommended as the basis for the incorporation of the manual/automatic handover system. Also, for system monitoring purposes, a periodic pulse generator needs to be incorporated into the primary control algorithm, possibly after each inner loop measurement of the pitch and roll characteristics of the aircraft. The periodicity of this pulse should be such that, if a failure occurs within the primary control system, reaction time in reverting to manual control is minimised.

Chapter 8 Discussion and Conclusions

8.1 Overall System Analysis

The development of a prototype autonomous vehicle system is a significantly complex task no matter what platform is desired (aquatic, air or terrestrial). Extensive theoretical research, combined with software, hardware and suitable system testing has allowed this project to give an insight into these complexities across all fields. To analyse the achievements and progress of the autonomous UAV system as a whole, it is necessary to revisit the aims and objectives of this project as outlined in chapter 1.

Research has indicated that the field of autonomous robotics is a fast changing and dynamic field of science and engineering. With technological advances rapidly becoming commercially available, low cost UAV systems are becoming more attractive for an ever increasing list of applications. Aside from hardware advances themselves, control techniques used for autonomous capability are also a fast changing, dynamic field of research within the scientific and engineering sectors. Control techniques range from simple “observe-and-correct” type systems, to more conventional approaches such as state feedback and PID based control. Recent shifts have also seen the evolution adaptive control techniques utilising almost “artificial intelligence” like systems.

The control technique utilised for this project was a simple “observe-and-correct”, heading error minimisation system. It was observed that this is not the ideal approach to be taken in regards to control system design, primarily due to stability concerns. By utilising this approach, the stability analysis of the AFCS is essentially just a “guess and check” method, requiring extensive manual flight tests of an actual model aircraft to determine various timing constraints and system responses. The best form of control for this type of simple UAV platform would be a conventional control system design approach, utilising state feedback, PID control and possibly an observer system. Before a method such as this can be developed however, more research needs to be carried out into the dynamics of the chosen model aircraft. These physical characteristics can be directly applied to the theory outlined in chapters 2 – 5, and it was the lack of this physical dynamics data that restricted the use of a conventional control approach for this project. It is hoped that much of the theory outlined in this dissertation will provide the necessary starting point for further work.

The hardware selection for this project was governed primarily by the need to minimise costs. The HC12 microcontroller unit that was chosen to be the heart of the AFCS, proved to be adequate in achieving all required tasks. The ADXL213 accelerometer module gave the desired accuracy of roll and pitch measurement, however it was noted that care must be taken in the calibration and mounting of the unit as it appears that ‘level’ to the human eye may not necessarily be ‘level’ to the electronics of the accelerometer. Further hardware does need to be developed for successful prototyping of a similar UAV system. Manual handover is a critical part of the current system configuration, and a system monitoring feature is important in meeting relevant legal and ethical requirements. Designs have been outlined in chapter 6, and can be used as a starting point for the development of this final hardware.

The intuitive control approach itself appears in theory to be able to provide the necessary path navigation that it is intended. Despite this confidence in the system, it is still largely untested in a real flight situation. With the eventual acquirement of an aircraft, fine tuning of this AFCS algorithm could be conducted, with the end result being a viable (but controlled) test flight. Probably

more significant to this project was the testing of individual control areas within the primary AFCS itself. Requirements such as accelerometer decoding and interpreting, servo motor control, and remote Rx/Tx routing are critical to any similar UAV system. These assembly language codes have been tested and do operate as expected, and can be incorporated into any future system with confidence.

Overall, without any actual flight testing having been conducted, the AFCS system developed appears to be able to provide the necessary autonomy. More importantly the lead-up stages to this design (dynamics analysis and simulation methods) can be utilised as a starting point for a more conventional control approach. The hardware selected for autonomy is adequate for either control approach, and coding has been developed specifically for control and interpretation of these hardware components.

8.2 Limitations Encountered

A summary of the limitations encountered throughout the course of this project is important for the future development and expansion possibilities of this autonomous UAV topic. The primary limitation that was encountered essentially shaped the course of this project by limiting the development of a more conventional control approach. As previously mentioned, the dynamics analysis conducted in chapter 2 is common for all aeroplane types (with some simplification or expansion depending on the type of plane). The eventual result of this analysis should have been the derivation of a state space plant matrix system describing the dynamic characteristics of the model aircraft to be used as the platform for the UAV. This plant matrix forms the initial start point for the design of a conventional state feedback, PID control system as shown in figure 8.1.

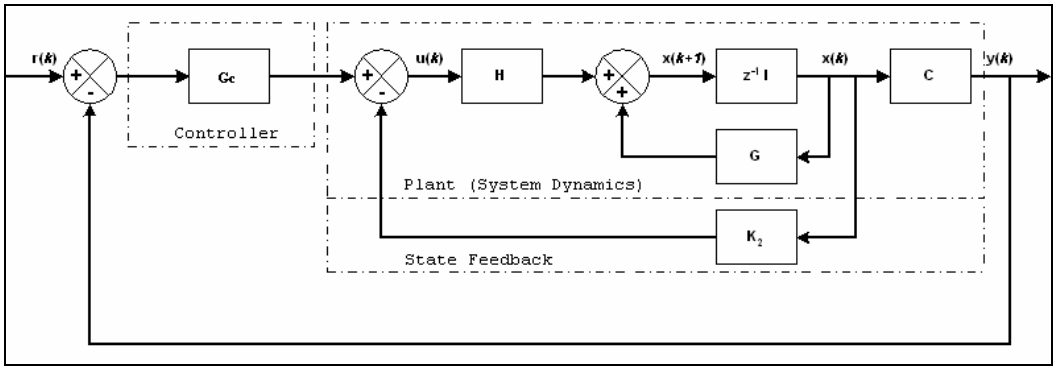

Figure 8.1: Conventional Control Approach

As indicated by figure 8.1, the 'plant' is essentially a representation of the dynamics of the system. This information relating to the dynamics of a model aircraft (most model aircraft of a similar size would have similar dynamic characteristics) was not readily available for use in developing the 'plant' system. Data such as this is available for larger scale aircraft (as was used for the simulations for this project), however extensive research uncovered very little relating to model aircraft platform. The data itself is generally obtained through wind tunnel testing of the aircraft, where control surface deflections are applied to the aircraft and system responses are observed in a controlled environment. Many hours of research were put into attempts to locate relevant data however due to time constraints; the possibility of implementing a form of conventional control was abandoned. In the end this lack of the dynamics data was the determining factor for the adoption of the "observe-and-correct" control method.

Aside from this major limitation, the only other influential limitation encountered was the unavailability of a testing aircraft. Due to funding constraints the University was unable to purchase an aircraft for prototyping and testing purposes. In terms of system testing, suitable alternatives were sought and all aspects were tested to an adequate level without any actual physical prototyping. For example the servo motor control algorithms were simply tested on a single servo motor similar to which is found in any commercially available model aircraft. The one limitation of the unavailability of the aircraft itself was in regards to testing the primary AFCS control algorithm. As mentioned previously, "fine tuning" of this aspect of the project could not be conducted due to the unavailability of a suitable aircraft. It is hoped that for future project work in this

field of autonomous UAV systems, that a suitable aircraft is available to complete this final testing phase.

8.3 Recommendations for Future Work

As mentioned on several occasions, with the unavailability of an aircraft the perceived focus of this project has shifted slightly from the actual construction of a working prototype UAV system, to providing the building blocks and necessary background information for a future continuing project. Obviously, before even mentioning any future recommendations, the primary aim for any future research work in this field would be to address the limitations that have been detailed above. So for simplicity, recommendations have been summarised in point form below:

1) *Obtain stability and dynamics data for a model aircraft.*

This data may be already accessible from aerospace research groups or university research divisions. As mentioned, extensive research attempted to find this information to no avail. Aside from accessing pre-existing data, it is a possibility (with access to suitable facilities and equipment) that a separate project topic may be to physically conduct wind tunnel testing of a model aircraft to determine the dynamics data from first principles. This is not recommended as a sub-part of an autonomous UAV research project as the level of detail in just these tests would most likely be significant enough to constitute an entire project. Either way it is a strong recommendation that this information (or similar) be gathered for any future attempts at AFCS design.

2) *Design of a more conventional AFCS.*

Assuming the model aircraft data has been found it is recommended that a more conventional control approach be taken to the AFCS design process (as touched upon in figure 8.1). The information detailed in chapters 2 – 5 should provide a useful starting point for this redevelopment. Conventional control theory takes a more mathematical approach to control problems such as the autonomous UAV system. A conventional system (provided it is designed correctly) should prove

to be more accurate than the intuitive approach detailed in this dissertation. Also, this new approach allows for greater flexibility in simulation and therefore greater certainty in the functioning of the AFCS prior to any flight testing. So whilst the intuitive approach taken for this project appears to be adequate for an initial attempt, it is recommended that with the availability of the required data a more traditional approach be taken towards AFCS design.

3) Obtain suitable model aircraft for prototyping

Obviously to accomplish the ultimate aim of this project (see chapter 1) a model aircraft is needed to develop a fully functional prototype autonomous UAV system. When choosing an aeroplane care must be taken so as to ensure that the payload capacity of the chosen vehicle is sufficient to handle the complete UAV system hardware. Aside from payload, the aircraft must also have adequate physical dimensions so as to allow for fixation of these hardware components. The last issue of significance that requires further investigation is the legal requirements of the chosen UAV platform. Parameters such as classification, weight, noise and safety are outlined by the CASA and are explored in chapter 1 and appendix B.

8.4 Autonomous Take-off and Landing Feasibility

The feasibility of developing autonomous take-off and landing sequences was identified as an extra possible objective for this project in chapter 1. This is in essence the final step towards full autonomy, and removes the need for manual pilot control for take-off and landing sequences as dealt with in this project. For safety purposes, circuits such as the manual handover configuration described in chapter 6 would still need to be present in a fully autonomous system, however the ability to fully program a UAV mission from take-off to landing would be a significant development for this system. In October 2004, the Saab company conducted its first ever test flight with its fully autonomous UAV system, the SHARC. According to the company, SHARC took off, flew and landed completely according to plan and completely autonomously. A spokesperson from Saab stated that: “There are many advantages of being able to conduct

autonomous take-offs and landings, as these are the points where a large proportion of UAV failures occur. Automating these parts of a flight therefore represents a dramatic risk reduction, while also bringing about tactical and operational benefits such as landing at dusk or in darkness" (UAVWorld News, 2004). The SHARC project represents just one of many similar research and development platforms throughout the world, all aimed at developing a fully autonomous system.

For the purposes of this project, autonomous take-off and landing does seem feasible for future investigation. The primary feature that would need to differ from the system described in this dissertation is the accuracy of altitude sensing. Currently altitude is measured by non-differential GPS, and whilst this provides the necessary accuracy to essentially maintain a suitable aircraft height, this form of measurement would not prove suitable for take-off and landing applications. Non-differential GPS resolves information to an accuracy of approximately five metres in most cases. If this technique were to be used for take-off and landing, the aircraft would essentially be unaware of the current ground position to a degree whereby almost certain destruction of equipment would result. Figures 8.2 and 8.3 show the basic information required by the aircraft if it were to autonomously attempt take-off and landing.

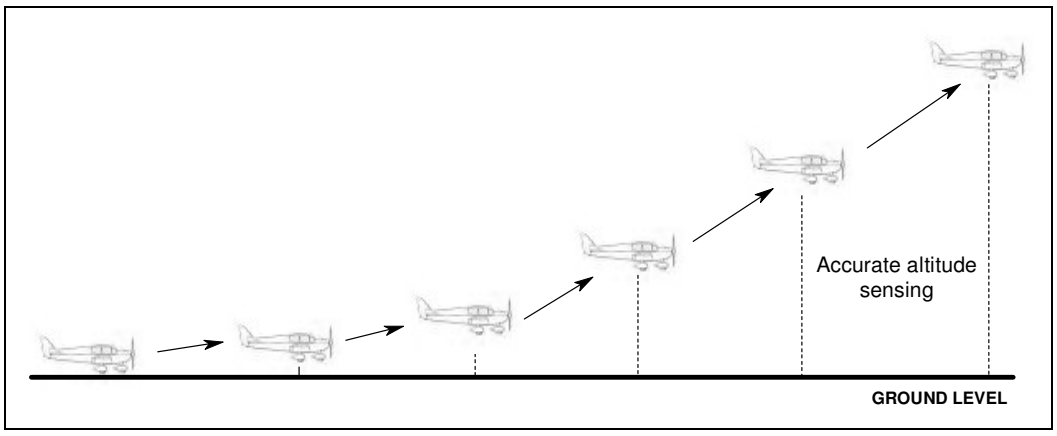

Figure 8.2: Take-off Sequence

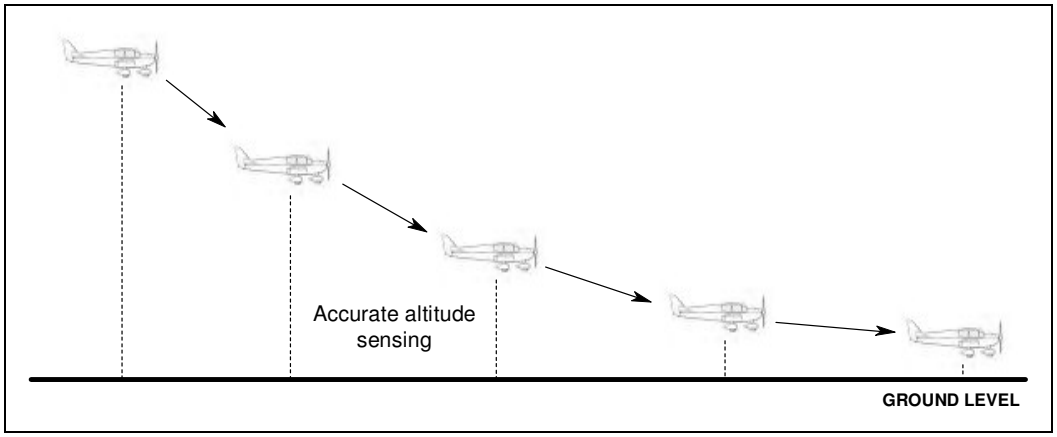

Figure 8.3: Landing Sequence

So the fundamental component of autonomous take-off and landing is the need for accurate altitude sensing so that the aircraft knows precisely where the ground is during take-off and landing sequences. To achieve this accuracy, a relatively low cost sensor unit has been identified. The SensComp 6500 Series Ranging Module (previously manufactured by Polaroid) is an economical sonar based ranging module that accurately measures altitudes from 6 inches to 35 feet (SensComp Inc, 2004). This module was initially investigated as a sensor for the actual altitude information for the purposes of this project; however for this purpose its maximum range of 35 feet was inadequate. However for the purposes of take-off and landing sequences the module would be more suited. Further specifications for the 6500 Ranging Module are shown in appendix E.

Whilst the details mentioned in this section in regards to autonomous take-off and landing are simply a very small representation of the level of research and further investigation required, it does appear that the development of a fully autonomous system may well be possible in future projects. Software details have not yet been explored and it can be expected that the addition of this extra autonomy feature will increase the complexities of the control platform. The need for accuracy becomes fundamental in the design of autonomous take-off and landing sequences and therefore it is recommended that if such a system is to be implemented, then extensive testing should be carried out before any flight tests are conducted. Overall it does appear that fully autonomous flight could be an interesting and indeed a feasible future addition to this project.

8.5 Final Word

The field of autonomous UAV research is a rapidly growing area, particularly at the low budget university level. Future prospects and applications for these forms of autonomous systems are continuing to increase, with continued emphasis on the development of low cost systems for non-military applications. This project has provided the initial building blocks for further research in this area at an undergraduate level. The opportunity to combine theoretical research with practical software and hardware development significantly adds to the attractiveness of pursuing a future project in this topic. Expansion and development opportunities for this project are significant and it is hoped that students will continue take up this challenge for many years to come with the hope of developing the optimal low cost autonomous UAV system.

References

Analog Devices Inc. 1999, 'Low Cost 2g/10g Dual Axis iMEMS Accelerometers with Digital Output', Norwood, MA.

Beard, R, Kingston, D, Quigley 2003, M, *Autonomous Vehicle Technologies for Small Fixed Wing UAVS*, Available [http://www.ee.byu.edu], (21 March 2005)

Byrne, T. 2005, 'Model Aircraft Specifications', ed. C Littleton, USQ, Toowoomba

Byrne, T. 2005, 'M68HC12 Assembly Language Programming', ed. C Littleton, USQ, Toowoomba

Civil Aviation Safety Authority 1998, *Civil Aviation Safety Regulations 1998 (CASR 1998)*, Available [http://casa.gov.au/rules/index.htm], (21 May 2005)

Dallas Personal Robotics Group (DPRG) 2003, *Low Cost Gyro-Accelerometer Combo Sensor*, Available [http://www.dprg.org/projects/2003-01a/], (18 March 2005)

Electronic Circuits Study Book, 2002, Distance Education Centre, USQ, Toowoomba, Australia

Elektronikladen 2005, 'Card 12; HC12 Controller Module with MC912D60A/MC912DG128A', Detmold, Germany

Franklin, G, Powell, J. 1994, *Feedback Control of Dynamic Systems*, Addison-Wesley, USA

Gabrynowicz, Prof. J.I 2003, *Legal Issues Using Satellite, Aerial and UAV Platforms*, National Remote Sensing and Space Law Centre, University of Mississippi School of Law, MI

Garmin 2004, *GPS 35 Specifications*, Available [http://www.garmin.com/products/gps35/spec.html], (1 March 2005)

Goebel, G 2005, *Greg Goebel / In the Public Domain*, Available [http://www.vectorsite.net/index.html], (14 April 2005)

Institution of Engineers Australia 1997, *Towards Sustainable Engineering Practice: Engineering Frameworks for Sustainability*, IEAUST, Australia

Institution of Engineers Australia 2000, *2000 Code of Ethics*, IEAUST, Australia

Keeffe, M 2003, *The Autonomous Scale Model Surveillance Aircraft*, Undergraduate, University of Southern Queensland, Toowoomba

Lazarski, Lt. Col. A.J 2002, 'Legal implications of the uninhabited combat aerial vehicle - Focus: Unmanned Aerial Vehicles', *Aerospace Power Journal,* Summer 2002, Available [http://www.findarticles.com]

MacQueen A.S 2002, *Autonomous Scale Yacht*, Undergraduate, University of Southern Queensland, Toowoomba

McLean, D 1990, *Automatic Flight Control Systems*, Prentice Hall, United Kingdom

Motorola 2002, *M68HC12 & HCS12 Microcontrollers; CPU 12 Reference Manual*, Rev. 3 5/2002, Motorola Inc, Colorado

Motorola 2000, *68HC912D60 68HC12D60 Advance Information*, Rev 2, Motorola Inc, Colorado

Nise, N.S 2000, *Control Systems Engineering 3rd Edition*, John Wiley and Sons, Inc, New York

Ogata, K 1995, *Discrete-Time Control Systems 2nd Edition*, Prentice Hall, New Jersey

Phythian, M. 2003, *Embedded Systems Design Study Book*, Distance Education Centre, USQ, Toowoomba, Australia

Precision Navigation Inc (n.d), *Vector 2X and 2XG Electronic Compass Modules; Complete Application Notes*, Available [https://www.pnicorp.com/], (1 March 2005)

Senscomp Inc. 2004, *'6500 Series Ranging Modules'*, Livonia, MI.

Sindahl, L 2004, *'SHARC completes autonomous take-off/landing'*, *UAVWorld News,* 26 October 2004, Available [http://www.uavworld.com/_disc4/0000007c.htm]

APPENDIX A

Project Specification

University of Southern Queensland
FACULTY OF ENGINEERING AND SURVEYING

ENG4111/4112 Research Project

PROJECT SPECIFICATION

NAME: Craig Andrew LITTLETON

DEGREE: Bachelor of Engineering – Electrical and Electronic
Bachelor of Business – Operations and Logistics Management

TITLE: Autonomous Unmanned Aerial Surveillance Vehicle – Autonomous Control and Flight Dynamics

SUPERVISORS: Mr. Mark Phythian

ENROLMENT: ENG4111 – S1, 2005 (ONC)
ENG4112 – S2, 2005 (ONC)

PROJECT AIM: The ultimate goal of this project, (when integrated with "Navigation and User Interface" (Soz Knox), is to develop a fully functional prototype autonomous unmanned aerial vehicle (UAV) to conduct specific flight path surveillance. This particular project focuses on the autonomous flight control aspect of the UAV system based on the dynamics of flight.

PROGRAMME: Issue A, 21 March 2003

1. Research into various control methods currently employed in similar UAV systems including relevant components.
2. Select, interface and test hardware components required for autonomous capability.
3. Design and simulate control system algorithms required for autonomous flight.
4. Construct prototype UAV (using a model aircraft) and integrate flight control system with "Navigation and User Interface" being carried out by Soz Knox.

As time permits:

1. Examine the viability of developing control algorithms for autonomous take-off and landing sequences.

AGREED:

_____ (Student) _____ (Supervisor)
__ / __ /2005 __ / __ /2005

APPENDIX B

Exert from Civil Aviation Safety Regulations act of 1998
(CASA, 2004)

Subpart 101.A Preliminary

101.025 Meaning of *populous area*

For this Part, an area is a ***populous area*** in relation to the operation of an unmanned aircraft or rocket if the area has a sufficient density of population for some aspect of the operation, or some event that might happen during the operation (in particular, a fault in, or failure of, the aircraft or rocket) to pose an unreasonable risk to the life, safety or property of somebody who is in the area but is not connected with the operation.

101.030 Approval of areas for operation of unmanned aircraft or rockets

(1) A person may apply to CASA for the approval of an area as an area for the operation of:

(a) unmanned aircraft generally, or a particular class of unmanned aircraft; or

(b) rockets.

(2) For paragraph (1) (a), the classes of unmanned aircraft are the following:

(a) tethered balloons and kites;

(b) unmanned free balloons;

(c) UAVs;

(d) model aircraft.

(3) In considering whether to approve an area for any of those purposes, CASA must take into account the likely effect on the safety of air navigation of the operation of unmanned aircraft in, or the launching of rockets in or over, the area.

(4) An approval has effect from the time written notice of it is given to the applicant, or a later day or day and time stated in the approval.

(5) An approval may be expressed to have effect for a particular period (including a period of less than 1 day), or indefinitely.

(6) CASA may impose conditions on the approval in the interests of the safety of air navigation.

(7) If CASA approves an area under subregulation (1), it must publish details of the approval (including any condition) in NOTAM or on an aeronautical chart.

(8) CASA may revoke the approval of an area, or change the conditions that apply to such an approval, in the interests of the safety of air navigation, but must publish details of any revocation or change in NOTAM or on an aeronautical chart.

(9) CASA must also give written notice of the revocation or change:

(a) to the person who applied for the approval of the area; or

(b) if that person applied for that approval as an officer of an organisation concerned with unmanned aircraft or rockets, and no longer holds that office — to the person who now holds the office.

Subpart 101.C Provisions applicable to unmanned aircraft Generally

101.060 Applicability of this Subpart

This Subpart applies to the operation of unmanned aircraft of all kinds, except operation mentioned in subregulation 101.005 (3).

Note Rockets that are not aircraft are dealt with separately in Subpart 101.H.

101.065 Operation in prohibited or restricted area

(1) A person may operate an unmanned aircraft in or over a prohibited area, or in or over a restricted area, only with the permission of, and in accordance with any conditions imposed by, the authority controlling the area.

Penalty: 25 penalty units.

Note For ***prohibited area*** and ***restricted area***, see regulation 2.07 of the Air Services Regulations. Details of prohibited or restricted areas are published in AIP or NOTAM.

(1A) An offence against subregulation (1) is an offence of strict liability.

Note For ***strict liability***, see section 6.1 of the *Criminal Code*.

(2) In subregulation (1):

authority controlling the area means:

(a) in the case of a prohibited area — the Secretary to the Department of Defence; and

(b) in the case of a restricted area — the authority mentioned in AIP (as issued from time to time) as the controlling authority for the area.

(3) For subregulation (1):

(a) the authority controlling the area must give a written statement of any condition so imposed to the person who applied for the permission; and

(b) unless the authority gives the statement to the person, the person is not bound by the condition.

101.070 Operation in controlled airspace

(1) A person may operate an unmanned aircraft above 400 feet AGL in controlled airspace only:

(a) in an area approved under regulation 101.030 as an area for the operation of unmanned aircraft of the same kind as the aircraft, and in accordance with any conditions of the approval; and

(b) in accordance with an air traffic control clearance.

Penalty: 50 penalty units.

Note AGL = above ground level (see the Dictionary).

(2) An offence against subregulation (1) is an offence of strict liability.

Note For ***strict liability***, see section 6.1 of the *Criminal Code*.

101.075 Operation near aerodromes

(1) A person may operate an unmanned aircraft at an altitude above 400 feet AGL within 3 nautical miles of an aerodrome only if:

(a) the operation is permitted by another provision of this Part; or

(b) permission has been given for the operation under regulation 101.080.

Penalty: 25 penalty units.

Note AGL = above ground level (see the Dictionary).

(2) A person may operate an unmanned aircraft over an area mentioned in paragraph (3) (a) or (b) only if:

(a) the operation is permitted by another provision of this Part; or

(b) permission has been given for the operation under regulation 101.080.

Penalty: 25 penalty units.

(3) The areas for subregulation (2) are:

(a) a movement area or runway of an aerodrome; and

(b) the approach or departure path of a runway of an aerodrome.

(4) A person must not operate an unmanned aircraft in such a manner as to create an obstruction to an aircraft taking off from, or approaching for landing at, a landing area or a runway of an aerodrome.

Penalty: 25 penalty units.

(5) An offence against subregulation (1), (2) or (4) is an offence of strict liability.

Note For ***strict liability***, see section 6.1 of the *Criminal Code*.

101.080 Permission for operation of unmanned aircraft near aerodrome

(1) The authority from which permission must be obtained for the purposes of regulation 101.075 is:

(a) if the aerodrome concerned is a controlled aerodrome — the air traffic control service for the aerodrome; or

(b) in the case of any other aerodrome — CASA.

(2) A person applies for permission under this regulation by giving to the relevant authority mentioned in subregulation (1) the information required by table 101.080, so far as relevant to the proposed operation.

Table 101.080 Details of operation of unmanned aircraft to be given to CASA or ATC

Item Information to be provided

1 In all cases:

(a) the name, address and telephone number of the person who will operate the aircraft or (if the aircraft concerned is an unmanned free balloon) release the balloon (or, if several people will be involved, the name, address and telephone number of the person who will coordinate the operation); and

(b) the date and time the operation or release is to begin and how long it is to last; and

(c) where it is to be carried out; and

(d) if more than 1 unmanned aircraft is to be operated at a time, how many unmanned aircraft are to be operated at that time

2 In the case of the operation of a tethered balloon or a kite:

(a) a brief description of the balloon or kite, including its predominant colour; and

(b) the height to which it is to be operated; and

(c) its mass

3 In the case of the release of a free balloon:

(a) how many balloons are to be released; and

(b) the estimated size and mass of the balloon's payload

4 In the case of the release of a medium or heavy balloon:

(a) the balloon's flight identification or its project code name; and

(b) the balloon's classification, or a description of the balloon; and

(c) the balloon's SSR code or NDB frequency, and its Morse identification; and

(d) the expected horizontal direction of the balloon's ascent, and the balloon's expected rate of climb; and

(e) the balloon's float level (given as pressure altitude); and

(f) when the balloon is expected to reach 60 000 feet pressure altitude, and the location over which it is expected to do so; and

(g) when the flight is expected to end, and where the balloon and its payload are expected to fall

Note For ***free balloon*** and ***heavy balloon***, see regulation 101.145. For ***tethered balloon***, see regulation 101.105.

(3) If more than 1 aircraft is to be operated at a time, such a requirement is a requirement to give the information about each such aircraft.

(4) Regulation 101.035 does not authorise a person who or that applies for permission under this regulation to make the application to a body mentioned in paragraph 101.035 (1) (a) or (b).

(5) If the authority grants the permission, it may impose conditions on the permission in the interests of the safety of air navigation.

(6) A person must not contravene a condition imposed under subregulation (5).

Penalty: 50 penalty units.

(7) An offence against subregulation (6) is an offence of strict liability.

Note For ***strict liability***, see section 6.1 of the *Criminal Code*.

101.085 Maximum operating height

(1) A person may operate an unmanned aircraft at above 400 feet AGL only:

(a) in an area approved under regulation 101.030 as an area for the operation of unmanned aircraft of the same class as the aircraft concerned, and in accordance with any conditions of the approval;

(b) as otherwise permitted by this Part.

Penalty: 50 penalty units.

Note AGL = above ground level (see the Dictionary).

(2) An offence against subregulation (1) is an offence of strict liability.

Note For ***strict liability***, see section 6.1 of the *Criminal Code*.

101.090 Dropping or discharging of things

(1) A person must not cause a thing to be dropped or discharged from an unmanned aircraft in a way that creates a hazard to another aircraft, a person, or property.

Penalty: 25 penalty units.

(2) An offence against subregulation (1) is an offence of strict liability.

Note For ***strict liability***, see section 6.1 of the *Criminal Code*.

101.095 Weather and day limitations

(1) A person may operate an unmanned aircraft:

(a) in or into cloud; or

(b) at night; or

(c) in conditions other than VMC; only if permitted by another provision of this Part, or in accordance with an air traffic control direction.

Penalty: 25 penalty units.

(2) An offence against subregulation (1) is an offence of strict liability.

Subpart 101.F UAVs

Division 101.F.1 General

101.235 Applicability of this Subpart

(1) This Subpart applies to:

(a) the operation of a large UAV; and

(b) the operation of a small UAV for purposes other than sport or recreation.

Note 1 There is no practicable distinction between a small UAV and a model aircraft except that of use — model aircraft are flown only for the sport of flying them.

Note 2 For ***large UAV*** and ***small UAV***, see regulation 101.240. For ***model aircraft*** see the Dictionary.

(2) Nothing in this Subpart applies to the operation of a UAV if:

(a) while it is being operated, the person operating it keeps it in sight; and

(b) it is operated in a way that complies with Subpart 101.G.

(3) This Subpart does not apply to the operation of a micro UAV.

Note 1 See subregulation 101.005 (3).

Note 2 For ***micro UAV***, see regulation 101.240.

101.240 Definitions for Subpart

In this Subpart:

approved area means an area approved under regulation 101.030 as an area for the operation of UAVs.

Note CASA must publish details of the approval of an area (including any conditions) in NOTAM or on an aeronautical chart — see subregulation 101.030 (5).

certified UAV controller means a person certified under Division 3 as a controller of UAVs.

controller of a UAV means a person who performs a function that would be, if the UAV were a manned aircraft, a function of its flight crew.

large UAV means any of the following:

(a) an unmanned airship with an envelope capacity greater than 100 cubic metres;

(b) an unmanned powered parachute with a launch mass greater than 150 kilograms;

(c) an unmanned aeroplane with a launch mass greater than 150 kilograms;

(d) an unmanned rotorcraft with a launch mass greater than 100 kilograms;

(e) an unmanned powered lift device with a launch mass greater than 100 kilograms.

micro UAV means a UAV with a gross weight of 100 grams or less.

small UAV means a UAV that is not a large UAV nor a micro UAV.

UAV means unmanned aircraft, other than a balloon or a kite.

Division 101.F.2 Operation of UAVs generally

101.245 Operation near people

(1) Subject to subregulations (2) and (3), a person must not operate a UAV within 30 metres of a person who is not directly associated with the operation of the UAV.

Penalty: 10 penalty units.

(1A) An offence against subregulation (1) is an offence of strict liability.

Note For ***strict liability***, see section 6.1 of the *Criminal Code*.

(2) Subregulation (1) does not apply in relation to a person who stands behind the UAV while it is taking off.

(3) Subregulation (1) also does not prevent the operation of a UAV airship within 30 metres of a person if the airship approaches no closer to the person than 10 metres horizontally and 30 feet vertically.

101.250 Where small UAVs may be operated

(1) A person may operate a small UAV outside an approved area only if:

(a) where the UAV is operated above 400 feet AGL, the operator has CASA's approval to do so; and

(b) the UAV stays clear of populous areas.

Penalty: 10 penalty units.

Note 1 ***AGL*** = above ground level (see the Dictionary). For ***populous area***, see regulation 101.025. For ***small UAV***, see regulation 101.240.

Note 2 CASA must publish details of the approval of an area (including any conditions) in NOTAM or on an aeronautical chart — see subregulation 101.030 (5).

Note 3 For the kinds of UAV operation to which this Subpart does not apply, see regulation 101.235.

(2) An offence against subregulation (1) is an offence of strict liability.

Note For ***strict liability***, see section 6.1 of the *Criminal Code*.

101.280 UAVs not to be operated over populous areas

(1) In this regulation:

certificated UAV means a UAV for which a certificate of airworthiness has been issued.

(2) A person must not operate a UAV that is not a certificated UAV over a populous area at a height less than the height from which, if any of its components fails, it would be able to clear the area.

Penalty: 50 penalty units.

Note 1 For ***populous area***, see regulation 101.025. For ***UAV***, see regulation 101.240.

Note 2 For the kinds of UAV operation to which this Subpart does not apply, see regulation 101.235.

(3) Without the approval of CASA, a person must not operate a certificated UAV over a populous area at a height less than the height from which, if any of its components fails, it would be able to clear the area.

Penalty: 50 penalty units.

(3A) An offence against subregulation (2) or (3) is an offence of strict liability.

Note For ***strict liability***, see section 6.1 of the *Criminal Code*.

(4) In considering whether to give an approval under subregulation (3), CASA must take into account:

(a) the degree of redundancy in the UAV's critical systems; and

(b) any fail-safe design characteristics of the UAV; and

(c) the security of its communications and navigation systems.

(5) Before giving an approval under subregulation (3), CASA must be satisfied that the person who intends to operate the UAV will take proper precautions to prevent the proposed flight being dangerous to people and property.

Subpart 101.G Model aircraft

101.375 Applicability of this Subpart

This Subpart applies to the operation of model aircraft weighing 100 grams or more (except operation mentioned in paragraph 101.005 (3) (a) or (b)).

101.385 Visibility for operation of model aircraft

(1) A person may operate a model aircraft only if the visibility at the time is good enough for the person operating the model to be able to see it continuously.

Penalty: 25 penalty units.

(2) An offence against subregulation (1) is an offence of strict liability.

Note For ***strict liability***, see section 6.1 of the *Criminal Code*.

101.390 Operating model aircraft at night

(1) A person may operate a model aircraft at night only in accordance with the written procedures of an approved aviation administration organisation.

Penalty: 25 penalty units.

(2) An offence against subregulation (1) is an offence of strict liability.

Note For ***strict liability***, see section 6.1 of the *Criminal Code*.

101.395 Keeping model aircraft away from people

(1) A person must not operate a model aircraft over a populous area at a height less than the height from which, if any of its components fails, it would be able to clear the area.

Penalty: 50 penalty units.

Note For ***populous area***, see regulation 101.025.

(2) Subject to subregulations (3) and (4), somebody who is operating a powered model aircraft must ensure that, while the model aircraft is in flight, or is landing or taking off, it stays at least 30 metres away from anyone not directly associated with the operation of model aircraft.

Penalty: 50 penalty units.

(3) Subregulation (2) is not contravened if somebody stands behind the model aircraft while it is taking off.

(4) Subregulation (2) is also not contravened if, as part of a model flying competition, a model aircraft is flown within 30 metres of somebody who is judging the competition.

(5) An offence against subregulation (1) or (2) is an offence of strict liability.

Note For ***strict liability***, see section 6.1 of the *Criminal Code*.

APPENDIX C

MATLAB Simulation Files

Appendix C(a)

Longitudinal.m

```
%%%%%%%%%%%%%%%%%%%%%%%%%%%%%%%%%%%%%%%%%%%%%%%%%%%%%%%%%%%%%%%%%%%%%%%%
%File written to determine pole locations, compute transfer
%function, determine controllability and observability, and
%plot responses of continuous and discrete LONGITUDINAL SYSTEM
% Written By Craig Littleton - 16/4/05
%%%%%%%%%%%%%%%%%%%%%%%%%%%%%%%%%%%%%%%%%%%%%%%%%%%%%%%%%%%%%%%%%%%%%%%%
clear all
close all
clc
%Generic Constants
g = 9.81;
U0 = 16;
gamma0 = 0;
%Longitudinal Stability derivatives
Xu = -0.6284;
Xw = -2.6762;
XsigE = -0.061;
Zu = -0.2232;
Zw = -2.6764;
ZsigE = 0.1543;
Mu = 0.01019;
Mw = -0.1384;
Mq = -0.1575;
MsigE = 0.9686;
Mtheta = 0;
%Longtitudinal State Space Matrices
A_long = [Xu, Xw, 0, -g*cos(gamma0), 0;
    Zu, Zw, U0, -g*sin(gamma0), 0;
    Mu, Mw, Mq, Mtheta, 0;
    0, 0, 1, 0, 0;
    0, -1, 0, U0, 0];
B_long = [XsigE, ZsigE, MsigE, 0, 0]';
C_long = [0 0 0 0 1/U0];
D_long = [0];
%Find Eigenvalues (pole locations) of longitudinal system
eig(A_long)
%Determine controllability of system
control = ctrb(A_long,B_long);
uncontrol = length(A_long)-rank(control)
%Define systems as State Space in MATLAB
long_system = ss(A_long,B_long,C_long,D_long)
%Convert Systems to Transfer Function form
long_tf = tf(long_system)
%%%%%%%%%%%%%%%%%%%%%%%%%%%%%%%%%%%%%%%%%%%%%%%%%%%%%%%%%%%%%%%%%%%%%%%%
%CONTINUOUS-TIME RESPONSES
%Plot step response of longitudinal system
long_system = long_system*0.008;
figure(1)
step(long_system)
grid
%Plot Root Locus of System
figure(2)
rlocus(long_system)
%Bode Plot of System
figure(3)
```

```
margin(long_system)
figure(4)
bode(long_system)
%Impulse Response of System
figure(5)
impulse(long_system)
grid
damp(long_system)
pause
close all
%%%%%%%%%%%%%%%%%%%%%%%%%%%%%%%%%%%%%%%%%%%%%%%%%%%%%%%%%%%%%%%%%%%%%%%%%%%%
%SYSTEM DISCRETIZATION AND DISCRETE RESPONSES
Ts = 0.625;
[phi,gamma] = c2d(A_long,B_long,Ts);
gamma = gamma*0.008;
%Plot step response of longitudinal system
figure(1)
dstep(phi,gamma,C_long,D_long)
grid
%Plot Root Locus of System
figure(2)
rlocus(phi,gamma,C_long,D_long)
%Bode Plot of System
figure(3)
bode(phi,gamma,C_long,D_long)
%Impulse Response of System
figure(4)
dimpulse(phi,gamma,C_long,D_long)
grid
pause
close all
%EOF
```

Appendix C(b)

Lateral.m

```
%%%%%%%%%%%%%%%%%%%%%%%%%%%%%%%%%%%%%%%%%%%%%%%%%%%%%%%%%%%%%%%%%%%%%%%
%File written to determine pole locations, compute transfer
%function, determine controllability and observability, and
%plot responses of continuous and discrete LATERAL SYSTEM
% Written By Craig Littleton - 21/4/05
%%%%%%%%%%%%%%%%%%%%%%%%%%%%%%%%%%%%%%%%%%%%%%%%%%%%%%%%%%%%%%%%%%%%%%%
clear all
close all
clc
%Generic Constants
g = 9.81;
U0 = 1000;
gamma0 = 0;
%Lateral Stability Derivatives (for general aviation aircraft)
Yv = -0.174;
Lv = -3.71;
Lp = -2.43;
Lr = 0.36;
Nv = 3.71;
Np = -0.27;
Nr = -0.325;
LsigA = 2.62;
LsigR = 1.02;
NsigA = -0.061;
NsigR = -2.1;
YsigR = 0.049;
%Lateral State Space Matrices
A_lat = [Yv, 0, -1, -g/U0, 0;
    Lv, Lp, Lr, 0, 0;
    Nv, Np, Nr, 0, 0;
    0, 1, tan(gamma0), 0, 0;
    0, 0, sec(gamma0), 0, 0];
B_lat = [0, LsigA, NsigA, 0, 0;
    YsigR, LsigR, NsigR, 0, 0]';
C_lat = [0 0 0 1 0; 0 0 0 0 1];
D_lat = [0 0; 0 0];
%Define states as strings
states = {'V' 'P' 'R' 'Phi' 'Psi'};
inputs = {'aileron' 'rudder'};
outputs = {'roll' 'yaw'};
lat_system = ss(A_lat,B_lat,C_lat,D_lat,'statename',states,...
                    'inputname',inputs,...
                    'outputname',outputs);
%Find Eigenvalues (pole locations) of longitudinal system
eig(A_lat)
%Determine controllability of system
control = ctrb(A_lat,B_lat);
uncontrol = length(A_lat)-rank(control)
%Define systems as State Space in MATLAB
lat_ss = ss(A_lat,B_lat,C_lat,0)
%Convert Systems to Transfer Function form
lat_tf = tf(lat_system)
%Apply gain value for scaling
lat_system = 0.008*lat_system;
%%%%%%%%%%%%%%%%%%%%%%%%%%%%%%%%%%%%%%%%%%%%%%%%%%%%%%%%%%%%%%%%%%%%%%%
%CONTINUOUS-TIME RESPONSES
```

```
%Plot step response of lateral system
figure(1)
step(lat_system)
%Bode Plot of System
figure(2)
bode(lat_system)
%Impulse Response of System
figure(3)
impulse(lat_system)
pause
close all
%%%%%%%%%%%%%%%%%%%%%%%%%%%%%%%%%%%%%%%%%%%%%%%%%%%%%%%%%%%%%%%%%%%%%%%
%SYSTEM DISCRETIZATION AND DISCRETE RESPONSES
Ts = 0.564;
[phi,gamma] = c2d(A_lat,B_lat,Ts);
%Plot step response of discrete lateral system
figure(1)
dstep(phi,gamma,C_lat,D_lat)
%Bode Plot of discrete system
figure(2)
bode(phi,gamma,C_lat,D_lat)
%Impulse Response of discrete system
figure(3)
dimpulse(phi,gamma,C_lat,D_lat)
pause
close
%EOF
```

APPENDIX D

MC912D60A HC12 Microcontroller Assembly Language Control Algorithms

Appendix D(a)

Remote.a

```
            CPU 68HC12
            PADDING OFF

COPCTL    equ $16     ;COP Control
TIOS      equ $80     ;Timer Input Capture/Output Compare Select
CFORC     equ $81     ;Timer Compare Force
TSCR      equ $86     ;Timer System Control
TCTL2     equ $89     ;Timer Control  2
TCTL3     equ $8A     ;Timer Control  3
TFLG1     equ $8E     ;Timer Interrupt Flag  1
TC4       equ $98     ;TIC/TOC 4
SC0BDH    equ $C0     ;SCI 0 Baud Rate
SC0CR2    equ $C3     ;SCI 0 Control 2

RAMTOP      equ   $0600       ;Top of usable RAM
RAMTOPMON   equ   $07FF       ;Top of RAM used by monitor
CODE        equ   $8000

            ORG $0200

HIVAL       RMB 3
HEXVAL      RMB 1

;=============================================================
; START OF MAIN PROGRAMME
      ORG   CODE
main  lds   #RAMTOP     ;Stack Pointer
      clr   COPCTL      ;Disable COP Watchdog
      jsr   serial_init ;Setup serial port
      jsr   SETUP_ICOC  ;Setup i/p capture and o/p compare
loop1 jsr   PWM_REC     ;Decodes pulse width from remote
                        ;transmitter
      bra   loop1

;*************************************************************
;Setup input capture and output compare
SETUP_ICOC
      ldaa  #%10010000  ;Timer to operate normally (p188) and
      staa  TSCR        ;enable fast clear of TC flag
      ldaa  #%00001100  ;1->Output  0->Input (p185)
      staa  TIOS        ;Channel 0/1 - accel i/p; Channel 2/3 -
                        ;servo o/p; Channel 4/5 - remote i/
      RTS

;*************************************************************
;Decode PWM signal from accelerometer and control enable servo
pulses
PWM_REC
      ldaa  #%00000001  ;i/p capture on line 4 on rising edge
      staa  TCTL3
      ldd   TC4         ;clears flag
      ldaa  #%00110000  ;Sets up to set o/p compare line 2 to
                        ;'high' on successful compare (p190)
      staa  TCTL2
```

```
WAIT1 ldaa  TFLG1       ;Waits for input capture to occur on line
                        ;4 (rising edge capture)
      anda  #%00010000
      BEQ   WAIT1
      ldaa  #%00000100  ;Forces o/p compare line 2 to 'high'
                        ;immediately
      staa  CFORC
      ldaa  #%00000010  ;i/p capture on line 4 on falling edge
      staa  TCTL3
      ldaa  #%00100000  ;Sets up to set o/p compare line 7 to
                        ;'low' on successful compare (p190)
      staa  TCTL2
      ldd   TC4         ;Clears flag
WAIT2 ldaa  TFLG1       ;Waits for input capture to occur on line
                        ;4 (falling edge capture)
      ANDA  #%00010000
      BEQ   WAIT2
      ldaa  #%00000100  ;Forces o/p compare line 2 to 'low'
                        ;immediately
      staa  CFORC

      RTS

;***************************************************************
;To use the serial port, one must set the baud rate. Set it to
;19200 baud. The value here is a 16 bit divisor.
serial_init
      ldd   #26   ; Value from Baud Rate Generation Table
        std SC0BDH
      ldaa  #$0C  ; Enable transceiver
      staa  SC0CR2
      rts

;***************************************************************
      end   main
```

Appendix D(b)

Servo.a

```
            CPU 68HC12
            PADDING OFF
RTICTL      equ $14     ;Real Time Interrupt Control
RTIFLG      equ $15     ;Real Time Interrupt Flag
COPCTL      equ $16     ;COP Control
TIOS        equ $80   ;Timer Input Capture/Output Compare Select
CFORC       equ $81     ;Timer Compare Force
TCNT        equ $84     ;Timer Counter
TSCR        equ $86     ;Timer System Control
TCTL1       equ $88     ;Timer Control  1
TC7         equ $9E     ;TIC/TOC 7
SC0BDH      equ $C0     ;SCI 0 Baud Rate
SC0CR2      equ $C3     ;SCI 0 Control 2

RAMTOP      equ   $0600       ;Top of usable RAM
RAMTOPMON   equ   $07FF ;Top of RAM used by monitor
CODE        equ   $8000

            ORG $0200

SERVO1            RMB 2

;=================================================================
; START OF MAIN PROGRAMME

      ORG   CODE

main  lds   #RAMTOP     ;Stack Pointer
      clr   COPCTL      ;Disable COP Watchdog
      jsr   serial_init       ; Setup serial port
      jsr   SET_RTI
loop  nop
      bra   loop

;*****************************************************************
; To use the serial port, one must set the baud rate. Set it to
;19200 baud. The value here is a 16 bit divisor.

serial_init
      ldd   #26         ; Value from Baud Rate Generation Table
      std   SC0BDH
      ldaa  #$0C        ; Enable transceiver
      staa  SC0CR2

      RTS

;*****************************************************************
; SETUP RTI for servos

SET_RTI
      jsr   RTI_SETUP
      jsr   SETUP_OUTCOM
      ldd #12000        ;Pulse Width for Servo-> 1 count  = 125nS
      std servo1        ;12000 = 1.5mS = centre servo

      RTS
```

```
;*****************************************************************
;Setup Pseudo Interrupt Vectors as per Page 11-12 in Card12 User
;Manual

RTI_SETUP
      ldaa #$06         ;JMP Command Opcode
      staa $07EB        ;RTI Pseudo Vector
      ldd #RTI_SERVICE  ;Address to jump, RTI Service
      std $07EC
      cli               ;Clear interupt mask
      ldaa #%10000110   ;Value to Setup RTI for an INT every 32mS
      staa RTICTL       ;Store Value in RTI Control Registe
      ldaa #%10000000   ;Clear RTI Flag
      staa RTIFLG

      RTS

;*****************************************************************
SETUP_OUTCOM
      ldaa #%10000000
      staa TSCR              ;Timer to operate normally (p188)
      ldaa #%10000000        ;1->Output  0->Input (p185)
      staa TIOS              ;Channel 7 as o/p --> 1-6 as i/p

      RTS

;*****************************************************************
;Real Time Interrupt Service Routine
;Manually sets output line, sets up automatic clearing of bit
;then loads required delay into Output Compare register
;When Main timer "TCNT" equals compare register bit is cleared
;automatically

RTI_SERVICE
      ldaa #%10000000   ;Clear RTI Flag as time-out period is met
      staa RTIFLG
      ldaa #%11000000   ;Sets up to set o/p compare line 7 to
                        'high' on successful compare (p190)
      staa TCTL1
      ldaa #%10000000   ;Forces o/p compare line 7 to 'high'
                        immediately
      staa CFORC
      ldaa #%10000000   ;Sets up to set o/p compare line 7 to
                        'low' on successful compare (p190)
      staa TCTL1
      ldd TCNT          ;Get value from Main Timer Counter
      addd SERVO1       ;add required delay
      std TC7           ;Store in Output Compare Register
                        ;--> When main timer counts up to this
                        ;value you get a successful compare which
                        ;clears output pin (sets o/p compare line
                        ;7 to 'low')

      RTI               ;Return from Interrupt

;*****************************************************************
      end   main
```

Appendix D(c)

Pwm.a

```
            CPU 68HC12
            PADDING OFF
COPCTL     equ $16   ;COP Control
TIOS       equ $80   ;Timer Input Capture/Output Compare Select
TSCR       equ $86   ;Timer System Control
TCTL4      equ $8B   ;Timer Control  4
TFLG1      equ $8E   ;Timer Interrupt Flag  1
TC0        equ $90   ;TIC/TOC 0
SC0BDH     equ $C0   ;SCI 0 Baud Rate
SC0BDL     equ $C1   ;SCI 0 Baud Rate Low Byte
SC0CR1     equ $C2   ;SCI 0 Control 1
SC0CR2     equ $C3   ;SCI 0 Control 2
SC0SR1     equ $C4   ;SCI 0 Status 1
SC0SR2     equ $C5   ;SCI 0 Status 2
SC0DRH     equ $C6   ;SCI 0 Data
SC0DRL     equ $C7   ;SCI 0 Data Low Byte

RAMTOP     equ      $0600       ;Top of usable RAM
RAMTOPMON  equ      $07FF       ;Top of RAM used by monitor
CODE       equ      $8000

            ORG $0200

TIME_1              RMB 2
TIME_2              RMB 2
TIME_3              RMB 2
PULSE_WIDTH         RMB 2
PERIOD              RMB 2
LEVEL_CYCLE         RMB 2
ERROR               RMB 2
DIRECTION           RMB 1
HIVAL               RMB 3
HEXVAL              RMB 1

;=================================================================
; START OF MAIN PROGRAMME

            ORG   CODE
main        lds   #RAMTOP           ;Stack Pointer
            clr   COPCTL            ;Disable COP Watchdog
            jsr   serial_init       ;Setup serial port
            jsr   SETUP_INCAP

decode      jsr   PWM_DECODE  ;Jump to decode routine
            jsr   CALC_DC     ;Jump to error calculation routine

            ldd   ERROR       ;Prints error results to terminal
                              ;for verification
            jsr   PRINT_CHECK ;Jumps to terminal print routine

;*****************************************************************
;Setup input capture
SETUP_INCAP
      ldaa  #%10010000  ;Timer to operate normally (p188) and
      staa  TSCR        ;enable fast clear of TC flag
      ldaa  #%00001100  ;1->Output  0->Input (p185)
```

```
      staa  TIOS        ;Channel 0/1 - accel i/p; Channel 2/3 -
                        ;servo o/p; Channel 4/5 - remote i/p
      RTS

;*****************************************************************
;Decode PWM signal from accelerometer
PWM_DECODE
      ldaa  #%00000001  ;i/p capture on line 0 on rising edge
      staa  TCTL4
      ldd   TC0         ;clears flag

WAIT1 ldaa  TFLG1       ;Waits for input capture to occur on line
                        ;0 (rising edge capture)
      anda  #%00000001
      BEQ   WAIT1
      ldaa  #%00000010  ;i/p capture on line 0 on falling edge
      staa  TCTL4
      ldd   TC0         ;Retrieves timer value of rising edge (16
      std   TIME_1      ;bit) from IC register and stores to
                        ;time_1, also clears TC flag
WAIT2 ldaa  TFLG1       ;Waits for input capture to occur on line
                        ;0 (falling edge capture)
      ANDA  #%00000001
      BEQ   WAIT2
      ldaa  #%00000001  ;i/p capture on line 0 on rising edge
      staa  TCTL4
      ldd   TC0         ;Retrieve timer value from falling
      std   TIME_2      ;trigger and store to time_2
      subd  TIME_1      ;also clears TC flag
      std   PULSE_WIDTH
WAIT3 ldaa  TFLG1       ;Waits for input capture to occur on line
                        ;0 (rising edge capture)
      ANDA  #%00000001
      BEQ   WAIT3
      ldd   TC0         ;Retrieve timer value from next rising
      std   TIME_3      ;trigger and store to time_3 also clears
                        ;TC flag
      subd  TIME_1
      std   PERIOD

      RTS

;*****************************************************************
;Calculate duty cycle from recorded timer values
CALC_DC
            ldd   PERIOD
            lsrd              ;Divide period by 2 to get duty-
                              ;cycle 50% (level flight)
            std   LEVEL_CYCLE
            cpd   PULSE_WIDTH
            bls   greater     ;If result is negative, actual d/c
                              ;is greater than desired d/c
            subd  PULSE_WIDTH ;Find difference between desired
                              ;and actual duty cycle
            std   ERROR       ;Store difference in d/c's (ie
                              ;error) in ERROR
            ldaa  #%10000000  ;If actual d/c less than desired
                              ;d/c then store 1 in MSB of
            staa  DIRECTION
            bra   difference
greater     ldd   PULSE_WIDTH ;Compute difference between pulse
```

```
                              ;width and 50%
            subd  LEVEL_CYCLE
            std   ERROR
            clra
            staa  DIRECTION   ;If actual d/c greater than
                              ;50% then store 0 in DIRECTION
difference  RTS

;***************************************************************
; To use the serial port, one must set the baud rate. Set it to
19200
; baud. The value here is a 16 bit divisor.

serial_init
      ldd   #26   ; Value from Baud Rate Generation Table
        std SC0BDH
      ldaa  #$0C  ; Enable transceiver
      staa  SC0CR2
      rts

;***************************************************************
      end   main
```

Appendix D(d)

Control.a

```
            CPU 68HC12
            PADDING OFF
RTICTL      equ $14    ;Real Time Interrupt Control
RTIFLG      equ $15    ;Real Time Interrupt Flag
COPCTL      equ $16    ;COP Control
TIOS        equ $80    ;Timer Input Capture/Output Compare Select
CFORC       equ $81    ;Timer Compare Force
TCNT        equ $84    ;Timer Counter
TSCR        equ $86    ;Timer System Control
TCTL1       equ $88    ;Timer Control  1
TCTL4       equ $8B    ;Timer Control  4
TFLG1       equ $8E    ;Timer Interrupt Flag  1
TC0         equ $90    ;TIC/TOC 0
TC7         equ $9E    ;TIC/TOC 7
SC0BDH      equ $C0    ;SCI 0 Baud Rate
SC0CR2      equ $C3    ;SCI 0 Control 2
SC0SR1      equ $C4    ;SCI 0 Status 1
SC0DRL      equ $C7    ;SCI 0 Data Low Byte

RAMTOP      equ   $0600       ;Top of usable RAM
RAMTOPMON   equ   $07FF       ;Top of RAM used by monitor
CODE        equ   $5000

;*****************************************************************
            ORG $0200

TIME_1            RMB 2
TIME_2            RMB 2
TIME_3            RMB 2
PULSE_WIDTH       RMB 2
PERIOD            RMB 2
LEVEL_CYCLE       RMB 2
ERROR_X           RMB 2
DIRECTION_X       RMB 2
head_error        RMB 2
servo1            RMB 2
constraint1       RMB 2
constraint2       RMB 2
constraint3       RMB 2
constraint4       RMB 2
constraint5       RMB 2
con_select        RMB 1
reduction         RMB 2
temp              RMB 2
roll1             RMB 1
roll2             RMB 1
roll3             RMB 1
roll4             RMB 1
roll5             RMB 1
difference        RMB 2
HIVAL             RMB 3
HEXVAL            RMB 1

;===============================================================
; START OF MAIN PROGRAMME
```

```
      ORG   CODE
main  lds   #RAMTOP           ;Stack Pointer
      clr   COPCTL            ;Disable COP Watchdog
      jsr   serial_init       ;Setup serial port
      jsr   SETUP_ICOC        ;Setup input capture/output compare
      jsr   ALLOCATE          ;Allocate roll constraint values
      ldd   #12800            ;FOR MANUAL TESTING ONLY
      std   head_error
      jsr   MOVE              ;Read initial heading error and act
                              ;accordingly
      jsr   CONSTRAINT        ;Select constraint based on
                              ;magnitude of error
decodejsr   PWM_DECODE_X      ;Accelerometer pwm decoding
      jsr   CALC_DC_X         ;and calculation of roll error
      jsr   COMPARE
      jsr   PRINTCHECK        ;FOR VERIFICATION ONLY
      bra   decode

;*****************************************************************
;Setup input capture/output compare channels
SETUP_ICOC
      ldaa  #%10010000  ;Timer to operate normally (p188) and
      staa  TSCR        ;enable fast clear of TC flag
      ldaa  #%10110000  ;1->Output  0->Input (p185)
      staa  TIOS        ;Channel 0/1-accel i/p;Channel 2/3-remote
                        ;i/p;Channel 4/5-servo o/p
      RTS

;*****************************************************************
;Allocate roll constraints
ALLOCATE
      ldd   #776
      std   constraint1       ;Error for 20 degrees
      ldaa  #6
      staa  roll1
      ldd   #519
      std   constraint2       ;Error for 15 degrees
      ldaa  #4
      staa  roll2
      ldd   #194
      std   constraint3       ;Error for 10 degrees
      ldaa  #3
      staa  roll3
      ldd   #65
      std   constraint4       ;Error for 5 degrees
      ldaa  #1
      staa  roll4
      ldaa  #0                ;Error for 0 degrees
      staa  roll5

      RTS

;*****************************************************************
;Use heading error as input to servo (outer loop control)
MOVE
      jsr   RTI_SETUP   ;Setup and enable Real Time Interrupt
      ldd   head_error  ;Use heading error as OC timer count
      std   servo1
      ldaa  #$10
meme1 ldx   #$FFFF      ;Delay for approx 60 ms to allow for
loop1 dex               ;servo rotation
```

```
      bne   loop1
      deca
      bne   meme1
      clra                    ;After delay, disable RTI
      staa  RTICTL

      RTS

;***************************************************************
;Decode PWM signal from accelerometer for channel X (Roll)
PWM_DECODE_X
      ldaa  #%00000001  ;i/p capture on line 0 on rising edge
      staa  TCTL4
      ldd   TC0         ;clears flag
WAIT1 ldaa  TFLG1       ;Waits for input capture to occur on line
                        ;0 (rising edge capture)
      anda  #%00000001
      BEQ   WAIT1
      ldaa  #%00000010  ;i/p capture on line 0 on falling edge
      staa  TCTL4
      ldd   TC0         ;Retrieves timer value of rising edge (16
      std   TIME_1      ;bit) from IC register and stores to
                        ;time_1, also clears TC flag
WAIT2 ldaa  TFLG1       ;Waits for input capture to occur on line
                        ;0 (falling edge capture)
      ANDA  #%00000001
      BEQ   WAIT2
      ldaa  #%00000001  ;i/p capture on line 0 on rising edge
      staa  TCTL4
      ldd   TC0         ;Retrieve timer value from falling
                        ;trigger and store to time_2
      std   TIME_2      ;also clears TC flag
      subd  TIME_1
      std   PULSE_WIDTH
WAIT3 ldaa  TFLG1       ;Waits for input capture to occur on line
                        ;0 (rising edge capture)
      ANDA  #%00000001
      BEQ   WAIT3
      ldd   TC0         ;Retrieve timer value from next rising
      std   TIME_3      ;trigger and store to time_3 also clears
      subd  TIME_1      ;TC flag
      std   PERIOD

      RTS

;***************************************************************
;Calculate duty cycle from recorded timer values (for X - roll)
CALC_DC_X
            ldd   PERIOD
            lsrd              ;Divide period by 2 to get duty-
                              ;cycle 50% (level flight)
            std   LEVEL_CYCLE
            cpd   PULSE_WIDTH
            bls   greater1    ;If result is negative, actual d/c
                              ;is greater than desired d/c
            subd  PULSE_WIDTH ;Find difference between desired
                              ;and actual duty cycle
            std   ERROR_X     ;Store difference in d/c's (ie
                              ;error) in ERROR

            ldaa  #%10000000  ;If actual d/c less than desired
```

```
                              ;d/c then store 1 in MSB
            staa  DIRECTION_X
            bra   difference1
greater1    ldd   PULSE_WIDTH
            subd  LEVEL_CYCLE
            std   ERROR_X
            clra
            staa  DIRECTION_X ;If actual d/c greater than 50%
                              ;then store 0 in DIRECTION
difference1 RTS

;***************************************************************
;Allocate pitch/roll constraints depending on heading error
CONSTRAINT
            ldd   head_error  ;Puts heading information in form
                              ;of 'error' for comparison with
                              ;constraints
            cpd   #12000
            bpl   now         ;Determination of magnitudes
            std   temp
            ldd   #12000
            subd  temp
            bra   now2
now         ldd   head_error
            subd  #12000
            std   difference
now2        cpd   constraint1 ;Compares error with constraint 20
                              ;degrees
            bpl   select1
            cpd   constraint2 ;Compares error with constraint 15
                              ;degrees
            bpl   select2
            cpd   constraint3 ;Compares error with constraint 10
                              ;degrees
            bpl   select3
            cpd   constraint4 ;Compares error with constraint 5
                              ;degrees
            bpl   select4
            bra   select5
select1     ldaa  #%00000001        ;Selects 20 degree constraint
            staa  con_select
            bra   selected
select2     ldaa  #%00000010        ;Selects 15 degree constraint
            staa  con_select
            bra   selected
select3     ldaa  #%00000100        ;Selects 10 degree constraint
            staa  con_select
            bra   selected
select4     ldaa  #%00001000        ;Selects 5 degree constraint
            staa  con_select
            bra   selected
select5     ldaa  #%00010000        ;Selects 0 degree constraint
            staa  con_select

selected    RTS

;***************************************************************
;Decrease rudder deflection (decrease roll) depending on
;constraints identified
COMPARE
      ldaa  con_select  ;Checks if constraint 1 is selected
```

```
      anda  #%00000001
      beq   next1
      ldd   ERROR_X     ;Checks if actual error is outside/inside
      cpd   roll1       ;constraint
      bpl   reduce
      bra   done
next1 ldaa  con_select  ;Checks if constraint 2 is selected
      anda  #%00000010
      beq   next2
      ldd   ERROR_X     ;Checks if actual error is outside/inside
      cpd   roll2       ;constraint
      bpl   reduce
      bra   done
next2 ldaa  con_select  ;Checks if constraint 3 is selected
      anda  #%00000100
      beq   next3
      ldd   ERROR_X     ;Checks if actual error is outside/inside
      cpd   roll3       ;constraint
      bpl   reduce
      bra   done
next3 ldaa  con_select  ;Checks if constraint 4 is selected
      anda  #%00001000
      beq   next4
      ldd   ERROR_X     ;Checks if actual error is outside/inside
      cpd   roll4       ;constraint
      bpl   reduce
      bra   done
next4 ldd   ERROR_X     ;Checks if constraint 5 is selected
      cpd   roll5
      bpl   reduce
      bra   done
reduceldd   #90         ;If actual level of roll is exceeding the
      std   reduction   ;desired constraint, then reduce the
      ldaa  DIRECTION_X ;deflection of the servo motor by
      anda  #%10000000  ;altering time-out period of output
      beq   left        ;compare (ie changing servo pulse width)
      ldd   servo1
      subd  reduction
      std   servo1
      bra   delay
left  ldd   servo1
      addd  reduction
      std   servo1
delay jsr   RTI_SETUP   ;Setup and enable Real Time Interrupt
      ldx   #$02        ;Delay for approx 0.2 seconds to allow
loop5 ldy   #$FFFF      ;for servo rotation of 2 degrees
loop4 dey
      bne   loop4
      dex
      bne   loop5
      clra              ;After delay, disable RTI
      staa  RTICTL

done  RTS

;*****************************************************************
;Setup Pseudo Interrupt Vectors as per Page 11-12 in Card12 User
Manual
RTI_SETUP
      ldaa #$06         ;JMP Command Opcode
      staa $07EB        ;RTI Pseudo Vector
```

```
      ldd #RTI_SERVICE  ;Address to jump to, RTI Service Routine
      std $07EC
      cli               ;Clear interupt mask
      ldaa #%10000110   ;Value to Setup RTI for an INT every 32mS
      staa RTICTL       ;Store Value in RTI Control Register
      ldaa #%10000000   ;Clear RTI Flag
      staa RTIFLG

      RTS

;***************************************************************
;Real Time Interrupt Service Routine
;Manually sets output line, sets up automatic clearing of bit
;then loads required delay into Output Compare register
;When Main timer "TCNT" equals compare register bit is cleared
;automatically
RTI_SERVICE
      ldaa #%10000000   ;Clear RTI Flag as time-out period met
      staa RTIFLG
      ldaa #%11000000   ;Sets up to set o/p compare line 7 to
                        ;'high' on successful compare (p190)
      staa TCTL1
      ldaa #%10000000   ;Forces o/p compare line 7 to 'high'
                        ;immediately
      staa CFORC
      ldaa #%10000000   ;Sets up to set o/p compare line 7 to
                        ;'low' on successful compare (p190)
      staa TCTL1
      ldd TCNT          ;Get value from Main Timer Counter
      addd SERVO1       ;add required delay
      std TC7           ;Store in Output Compare Register
                        ;--> When main timer counts up to this
                        ;value you get a sucessful compare which
                        ;clears output pin (sets o/p compare line
                        ;7 to 'low')
      RTI               ;Return from Interrupt

;***************************************************************
;To use the serial port, one must set the baud rate. Set it to
;19200 baud. The value here is a 16 bit divisor.
serial_init
      ldd   #26         ; Value from Baud Rate Generation Table
      std   SC0BDH
      ldaa  #$0C        ; Enable transceiver
      staa  SC0CR2
      rts

;***************************************************************
      end main
```

Appendix D(e)

'Print_Check' Routine

```
;***************************************************************
;Prints to screen for verification
PRINTCHECK
      ldd   ERROR_X
      staa  HEXVAL
      jsr   HEX2DEC
      jsr   PRINT_SPACE
      ldaa  DIRECTION_X
      staa  HEXVAL
      jsr   HEX2DEC
      jsr   PRINT_SPACE
      ldaa  con_select
      staa  HEXVAL
      jsr   HEX2DEC
      jsr   write_newline
      ldaa  #$06;
loop3 ldx   #$FFFF            ;Delay to slow print

loop2 dex
      bne   loop2
      deca
      bne   loop3

;***************************************************************
;Transmits the HEX value that has bee placed in HEXVAL in Decimal
;(Byrne 2005)
HEX2DEC     LDX     #HIVAL
            CLR     HIVAL
            CLRA
            LDAB    HEXVAL
            LSLB
            BCC     LESS128
            LDAA    #$01
            STAA    HIVAL
            LDAA    #$28
LESS128     LSLB
            BCC     BIT6
            ADDA    #$64
            DAA
            BCC     BIT6
            INC     HIVAL
BIT6        LSLB
            BCC     BIT5
            ADDA    #$32
            DAA
            BCC     BIT5
            INC     HIVAL
BIT5        LSLB
            BCC     BIT4
            ADDA    #$16
            DAA
            BCC     BIT4
            INC     HIVAL
BIT4        LSLB
            BCC     BIT3
            ADDA    #$8
```

```
            DAA
            BCC     BIT3
            INC     HIVAL
BIT3        LSLB
            BCC     BIT2
            ADDA    #$4
            DAA
            BCC     BIT2
            INC     HIVAL
BIT2        LSLB
            BCC     BIT1
            ADDA    #$2
            DAA
            BCC     BIT1
            INC     HIVAL
BIT1        LSLB
            BCC     ALLDONE
            ADDA    #$1
            DAA
            BCC     ALLDONE
            INC     HIVAL
ALLDONE     LDAB    #$30
            ADDB    HIVAL
            STAB    HIVAL
            TAB
            ANDA    #%11110000
            LSRA
            LSRA
            LSRA
            LSRA
            STAA    1,X
            LDAA    #$30
            ADDA    1,X
            STAA    1,X
            ANDB    #%00001111
            STAB    2,X
            LDAA    #$30
            ADDA    2,X
            STAA    2,X
            LDAA    0,X
            JSR     TXBYTE
            LDAA    1,X
            JSR     TXBYTE
            LDAA    2,X
            JSR     TXBYTE
            RTS

;***************************************************************
;Transmit a character which is in A
txbyte
      brclr SC0SR1, #$80 txbyte
      staa  SC0DRL
      rts

;***************************************************************
;Send a carriage return and line feed to screen
write_newline
      ldaa #$0D   ;Load Carriage return ASCII
      jsr  txbyte
      ldaa #$0A   ;Load Line Feed ASCII
      jsr  txbyte
```

```
      rts

;*****************************************************************
;Print a space

PRINT_SPACE
      ldaa #' '
      jsr  txbyte
      rts
```

APPENDIX E

Technical Specifications of SensComp 6500 Series Ranging Module
(SensComp, 2004)

SensComp, Inc.
36704 Commerce Rd.
Livonia, MI 48150
Telephone: (734) 953-4783
Fax: (734) 953-4518
www.senscomp.com

6500 Series Ranging Modules

SensComp's Ranging Modules provide the drive electronics for SensComp Electrostatic Transducers

Features

Accurate Sonar Ranging from 6 inches to 35 feet
Drives a 50 kHz Electrostatic Transducer Without an Additional Interface
Operates from a Single Power Supply Source
Accurate Clock Output Provided for External Use
Selective Echo Exclusion
TTL Compatible
Multiple Measurement Capability
Integrated Transducer Cable
Variable Gain Control Potentiometer

Part No.

PID# 615078 -- 6500 Series Sonar Ranging Module
PID# 615079 -- 6500 Series Enhanced Sonar Ranging Module; Includes Pull-up Resistors and an Internal Oscillator for Repetitive Operation
PID# 615080 -- 6500 Series Sonar Ranging Module Without the Connector

Specifications

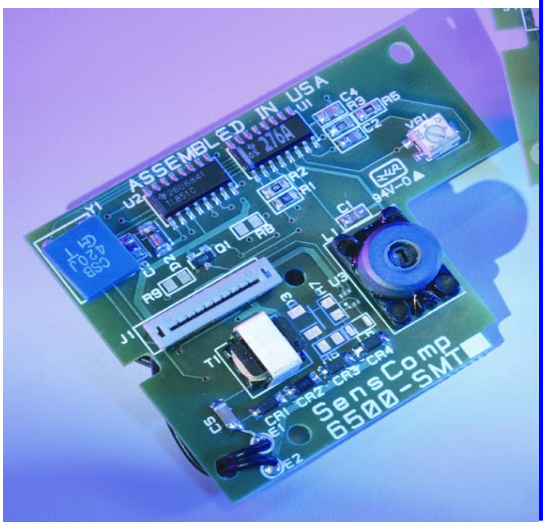

Description

The 6500 Series is an economical sonar ranging module that can drive all SensComp electrostatic transducers. This module, with a simple interface, is able to measure distances from 6 inches to 35 feet. The typical accuracy is +/- 1% of the reading over the entire range.

This module has an external blanking input that allows selective echo exclusion for operation on a multiple-echo mode. The module is able to differentiate echos from objects that are only three inches apart. The digitally controlled gain, variable bandwidth amplifier minimizes noise and side-lobe detection in sonar applications.

The module has an accurate ceramic resonator controlled 420 kHz time base generator. An output based on the 420 kHz time base is provided for external use. The sonar transmit output is 16 cycles at a frequency of 49.4 kHz.

The 6500 Series module operates over a DC power supply range from 4.5 volts to 6.8 volts (5 volts nominal) and is characterized for operation from 0° C to 40° C.

For more information, visit our website: www.senscomp.com

Absolute Maximum Ratings over Operating Free-air temperature range

Voltage from any pin to ground (see Note 1) ..... 7 VDC
Voltage from any pin except XDCR to V_{CC} (see Note 1) .....-7 VDC to 0.5 VDC
Operating free-air temperature range.....0° C to 40° C
Storage temperature range .....-40° C to 85° C

NOTE 1: The XDCR pin may be driven from -1 volt to 400 volts typical with respect to ground.

Recommended Operating Conditions

		MIN	MAX	UNIT
Supply Voltage, Vcc		4.5	6.8	V
High-level Input Voltage, VIH	BLNK, BINH, INIT	2.1		V
Low-level Input Voltage, VIL	BLNK, BINH, INIT		0.6	V
ECHO and OSC Output Voltage			6.8	V
Delay Time, Power Up to INIT High		5		ms
Recycle Period		80		ms
Operating Free-air Temperature, T_A		0	40	°C

Electrical Characteristics over Recommended Ranges of Supply Voltage and Operating Free-Air Temperature

PARAMETER		TEST COND.	MIN	TYP	MAX	UNIT
Imput Current	BLNK, BINH, INIT	V_I = 2.1 V			1	mA
High-level Output Current, I_{OH}	ECHO, OSC	V_{OH} = 5.5V			100	µA
Low-level Output Voltage, V_{OL},	ECHO, OSC	I_{OL}= 1.6 mA			0.4	V
Transducer Bias Voltage		T_A = 25° C		200		V
Transducer Output Voltage (peak to peak)		T_A = 25° C		400		V
No. of Cycles for XDCR Output to Reach 400V		C = 500 pF			7	
Internal Blanking Interval				2.38†		ms
XMIT Drive Signal Duration				1.1†		ms
Frequency During 16-pulse	OSC output			49.4†		kHz
Transmit Period	XMIT output			49.4†		kHz
Frequency After 16-pulse	OSC output			93.3†		kHz
Transmit Period	XMIT output			0		kHz
Supply Current, Icc	During transmit period				2000	mA
	After transmit period				100	mA

† These typical values apply for a 420 kHz ceramic resonator

Operation With SensComp Electrostatic Transducers

There are two basic modes of operation for the 6500 Series Sonar Ranging Modules: Single-echo mode and multiple-echo mode. The application of power (V_{CC}), the application of the initiate (INIT) input, and the resulting transmit output, and the use of the Blanking Inhibit (BINH) input are basically the same for either mode of operation. After applying power (V_{CC}) a minimum of 5 milliseconds must elapse before the INIT signal can be taken high. During this time, all internal circuitry is reset and the internal oscillator stabilizes. When INIT is raised to a high level, drive to the transducer (XDCR) output occurs. Sixteen pulses at 49.4 kHz with an amplitude of 0 volts to 400 volts peak to peak will excite the transducer as transmission occurs. At the end of the 16 transmitted pulses, a 200 VDC bias remains on the transducer (as recommended) for optimum receiving operation.

In order to eliminate ringing of the transducer from being detected as a return signal, the Receive (REC) input of the ranging control IC is inhibited by internal blanking for 2.38 milliseconds after the initiate signal. If a reduced blanking time is desired, then the BINH input can be taken high to end the blanking of the Receive input any time prior to internal blanking. This may be desirable to detect objects closer than 1.33 feet (corresponding to 2.38 milliseconds) and may be done of transducer damping is sufficient so that ringing is not detected as a return signal.

In the single-echo mode of operation (Figure 1), all that must be done next is to wait for the return of the transmitted signal, traveling at approximately 0.9 milliseconds per foot out and back. The returning signal is amplified and appears as a high logic level echo output. The time between INIT going high and the Echo (ECHO) output going high is proportional to the distance of the target from the transducer. If desired, the cycle can now be repeated by returning INIT to a low logic level and then taking it high when the next transmission is desired.

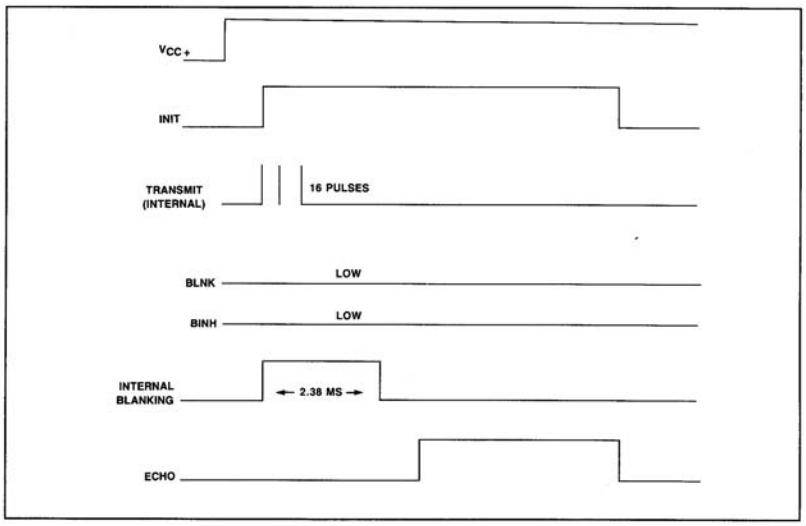

FIGURE 1: EXAMPLE OF A SINGLE-ECHO-MODE CYCLE WITHOUT BLANKING INPUT

If there is more than one target and a single transmission detects multiple echos, then the cycle is slightly different (Figure 2). After receiving the first return signal which causes the ECHO output to go high, the Blanking (BLNK) input must be taken high then back low to reset the ECHO output for the next return signal. The blanking signal must be at least 0.44 milliseconds in duration to account for all 16 returning pulses from the first target and allow for internal delay times. This corresponds to the two targets being 3 inches apart.

During a cycle starting with INIT going high, the receiver amplifier gain is increased at discrete times (Figure 3) since the transmitted signal is attenuated with distance. At approximately 38 milliseconds, the maximum gain is attained. Although gain can be increased by varying R1 (see Component Layout), there is a limit to which the gain can be increased for reliable module operation. This will vary from application to application. The modules are “kitted” prior to their final test during manufacture. This is necessary because the desired gain distribution is much narrower than the module gain distribution if all were kitted with one value resistor. As kitted, these modules will perform satisfactorily in most applications. As a rule of thumb, the gain can be increased up to a factor of 4, if required, by increasing R1 correspondingly. Gain is directly proportional to R1.

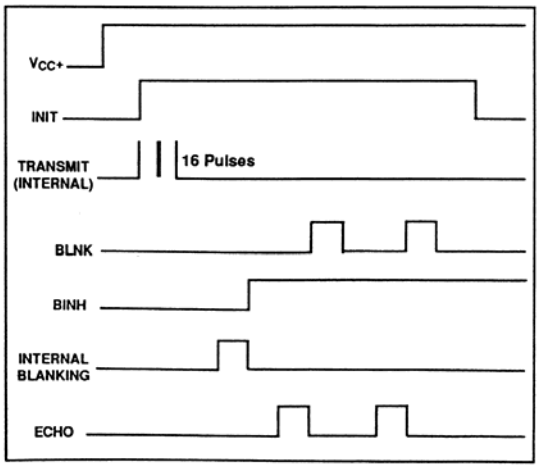

FIGURE 2: EXAMPLE OF A MULTIPLE-ECHO-MODE CYCLE WITH BLANKING INPUT

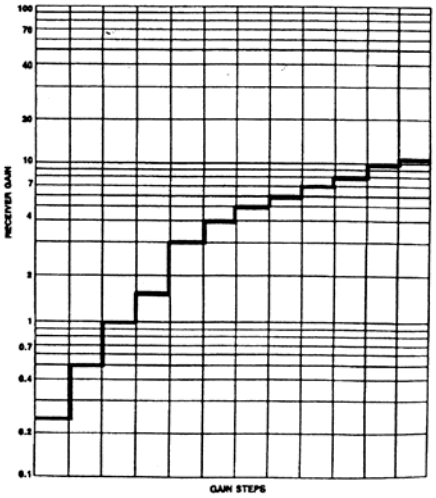

FIGURE 3: RECEIVER GAIN VS GAINSTEP NUMBERS

Input/Output Schematic Notes:

The ECHO and OSC outputs are open collector NPN transistor outputs (Figure 4) requiring 4.7 Kohm pull-up resistors between V_{CC} and the output.

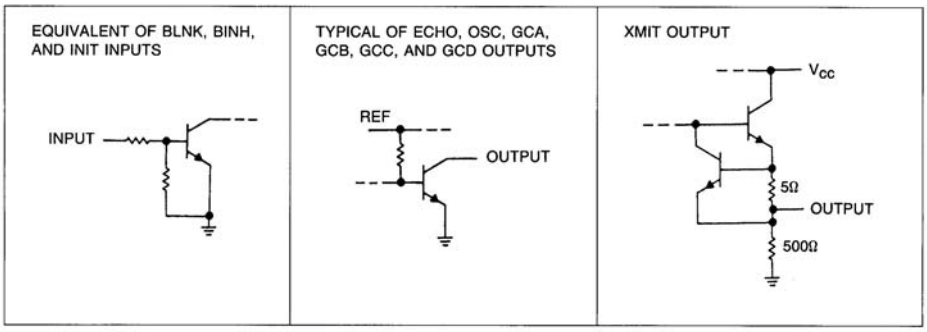

FIGURE 4: SCHEMATIC EQUIVALENT CIRCUITS OF BOARD INPUTS/OUTPUTS

Component Layouts

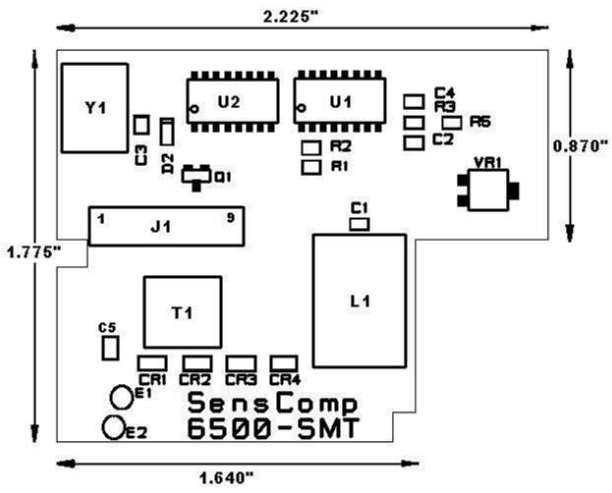

6500 SMT Ranging Module

PID#615078

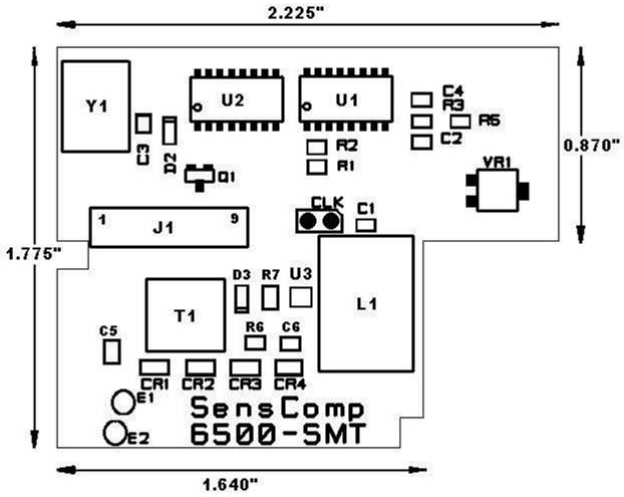

6500E Enhanced SMT Ranging Module

PID#615079

Schematic – 6500 SMT Ranging Module--PID#615078

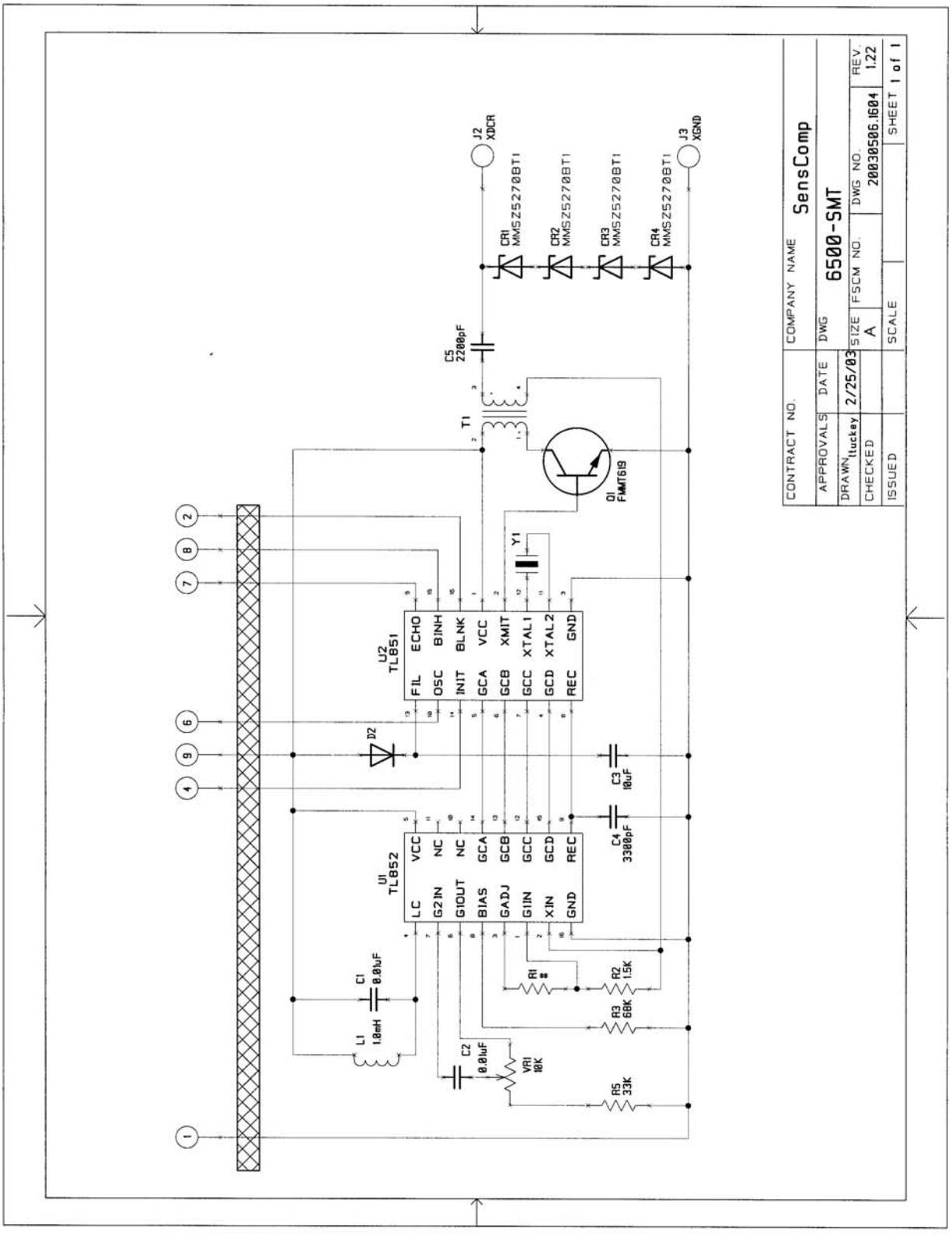

Schematic – 6500E Enhanced SMT Ranging Module --PID#615079